NUMERICAL STUDY OF PILED RAFT FOUNDATION UNDER VERTICAL STATIC AND SEISMIC LOADS

By

GETASEW MARE YIRSAW

A Thesis Submitted to Department of Civil Engineering

School of Civil Engineering and Architecture

Office of Graduate Studies

Adama Science and Technology University

August, 2020

Adama, Ethiopia

NUMERICAL STUDY OF PILED RAFT FOUNDATION UNDER VERTICAL STATIC AND SEISMIC LOADS

By

GETASEW MARE YIRSAW

Advisor: Argaw Asha (PhD)

A Thesis Submitted to Department of Civil Engineering

School of Civil Engineering and Architecture

Office of Graduate Studies

Adama Science and Technology University

August, 2020

Adama, Ethiopia

APPROVAL PAGE

We, the undersigned, members of the Board of Examiners of the final open defense by Getasew Mare Yirsaw have read and evaluated his thesis entitled "Numerical Study of Piled Raft Foundation Under Vertical Static and Seismic Loads" and examined the candidate. This is, therefore, to certify that the thesis has been accepted in partial fulfillment of the requirement of the Degree of Master's in Civil Engineering with Specialization in Geotechnical Engineering.

Name	Signature	Date
Getasew Mare *Name of the Student*		
Dr. Argaw Asha *Advisor*		
Dr. -Ing. Tensay Gebremedhin *External Examiner*		
Dr. Afzal Khan *Internal Examiner*	Afzal Khan.	06/08/2020
Chair Person		
Head of Department		
School Dean		
Post Graduate Dean		

DECLARATION

I hereby declare that this MSc Thesis is my original work and has not been presented for a degree in any other university, and all sources of material used for this thesis have been duly acknowledged.

Name: Getasew Mare

Signature: ___________

This MSc Thesis has been submitted for examination with my approval as thesis advisor.

Name: Dr. Argaw Asha

Signature: __________________

Date of submission: - _____________

ACKNOWELEDGEMENT

In this thesis project many peoples are involved from the beginning and it could not have been possible without their advice, guidance, support and encouragement. The author would like to express his greatest thanks from the depth of his heart to this thesis advisor Dr. Argaw Asha for his limitless advice and guidance throughout the project. Next, the author would like to express his appreciation to Dr. Eleyas Assefa for his advice and providing FLAC3D V6 software package. Furthermore, the author would like to thank the staff members of Commercial Bank Headquarter building, Nib Bank and United Bank for extensive assistance in providing geological, geotechnical and structural data which are input of thesis project. Warm thanks to ASTU for providing full scholarship. Finally, the author would like to appreciate all staff of civil engineering department, librarians and administrative workers of the faculty. At the end the author would like to dedicate this thesis project to families and friends who's moral and material support kept through the ups and downs of his academic life.

TABLE OF CONTENTS

Contents *Page No.*

LIST OF TABLES

Tables *Page No.*

LIST OF FIGURES

Figures *Page No.*

LIST OF ACRONYMS

A_G	Area of pile group,
A_R	Area of the raft,
A_{loop}	Area of the hysteresis loop,
A_s	Effective pile surface area,
A1	constant (20),
B1	Constant (72),
CN	Correction factor for overburden,
C_h	Horizontal direction damping,
C_θ	Rotational direction damping,
Dp	Diameter of pile,
E	Young's modulus,
G	Shear modulus,
G_{max}	Maximum shear modulus,
G_{sec}	Secant moduli,
H	Height of building,
K	shear modulus,
K_{Pr}	Stiffness of piled raft,
K_n	Normal spring stiffness,
K_o	At rest earth pressure coefficient,
K_h	Horizontal direction stiffness,
K_θ	Rotational direction stiffness,
K_r	Stiffness of the raft,
K_s	Shear spring stiffness,
L	Length of the pile,
$(N_1)_{60}$	Normalized and standardized corrected blow count,
N_{60}	N-value corrected for energy efficiency,
P	Load from the superstructure,
Q_b	End resistance of pile,
Q_s	Skin resistance of the pile,
S_s	Shear bond strengths,

T_s	Tensile bond strengths,
U_g	Amplitude of free-field motion,
U_0	Amplitude of the base relative to the free-field motion,
Vs	Shear wave velocity,
W_D	Dissipated energy in one loop,
W_S	Maximum strain energy,
c'_n	Normal direction cohesion,
c'_s	Shear direction cohesion,
f_s	Shear stress capacity along the pile shaft,
k_P	Pile group stiffness,
r_c	Average radius of raft,
r_o	Radius of pile,
$2a$	Width of the foundation,
b	Body force per unit mass,
d[v]/dt	Material derivative of the velocity,
f	Frequency of wave,
h	Height of the structure,
m	Mass of the structure,
n	Number of piles,
tr	Thickness of the raft,
$\tilde{u}_g$	Equivalent input motion,
$\emptyset'_n$	Normal direction friction angle,
$\emptyset'_s$	Shear direction friction angle,
ΔZ_{min}	Minimum grid size,
α_{rP}	Raft pile interaction factor,
σ_{ij}	Stress tensor,
σ'_v	Vertical effective stress
$\tilde{c}$	Equivalent damping value,
$\tilde{k}$	Equivalent soil structure stiffness,
$\tilde{\xi}$	Equivalent damping ratio,

$\tilde{\omega}$	Equivalent natural frequency,
γ	Unit weight of the soil,
λ	Wave length,
ν	Poisson's ratio of the soil,
ξs	Total settlement reduction factor,
$\xi \Delta s$	Differential settlement reduction factor,
ρ	Density of soil,
Υ	Shear strain,
ϕ'	Effective friction angle of the soil, and
ψ	Dilation angle.

LIST OF ABBREVIATIONS

ATH	Acceleration time history,
BEM	Boundary element method,
EARS	The East African Rift system,
FDM	Finite difference method,
FEM	Finite element method,
FLM	Finite Layer Method,
FLAC3D	Fast Lagrangian analysis in continua in three dimensions,
FVM	Finite volume method,
IST	International system of time,
MH	Mohr coulomb,
PGA	peak ground acceleration,
PRF	piled raft foundation,
SSI	Soil structure interaction, and
TH	Time history.
PEER	Pacific Earthquake Engineering Research Center

ABSTRACT

Piled raft foundation (PRF) is a combination of pile and raft working together to provide adequate bearing capacity under the allowable settlement. A uniform pile positioning has been used in PRF, however, there is a wide room for optimization through parametric study to provide a lesser number of piles within the required design criteria under vertical load. Addis Ababa is found in seismic zone 3 with a peak ground acceleration (PGA) above the threshold of damage that makes investigating the performance of PRF under seismic load considering the dynamic kinematic soil-structure interaction (SSI) vital. The study area is located in Addis Ababa around Mexico (commercial bank) and Kirkos (Nib, Zemen and United Bank) in which input parameters (pile length, pile diameter, pile spacing, raft area, raft thickness and load) are taken. A finite difference based numerical software, FLAC3D V6 is used for the analysis. The 1940 El Centro earthquake is selected, scaled to the required PGA and deconvolution analysis was done. The static analysis showed that increasing spacing results rise of load sharing of the raft by 11.5% while settlement has reduced non uniformly. A close load sharing between pile and raft was achieved at a spacing of 7D with different pile lengths and diameters. The maximum settlement reduction achieved is 9% for a pile of 2 m diameter by increasing length from 10 m to 20 m, which show pile length is not effective in reducing settlement. The installation of piles results increases of negative bending moment of the raft compared with unpiled raft. Hence, the optimized design depends on pile spacing and the raft edge length from the outermost pile, while pile length and diameter are not significant parameters. An optimized piled raft configuration proposed has reduced pile number by 40% and differential settlement by 95%. The dynamic analysis shows the acceleration plot at the top of the friction piled raft has PGA of $1.5\, m/sec^2$ *and* $3\, m/sec^2$ *under El Centro earthquake respectively due to amplification of seismic waves. There was no observed residual pile head displacement and resonance by the El Centro earthquake. Compared with friction PRF, an end bearing PRF has lower amplification, pile head displacement and vertical settlement under the 1940 El Centro earthquake with different peak ground acceleration, hence, PRF perform very well under seismic load.*

KEY WORDS: - FLAC3D V6; Earthquakes; Optimized piled raft foundation; Pile Head Displacement; Soil structure interaction;

CHAPTER – 1: INTRODUCTION

1.1 Background of the Study

To build civil structure, it is necessary to use a foundation that can transfer any type of load to the underlying soil strata. Foundations are used mainly to anchor or connect the superstructure with the ground. The subsoil condition, the magnitude of load, load type, the importance of the structure and other conditions determine the foundation type to be employed. Foundation types can be shallow or deep. Ordinary and medium-size buildings are built usually on shallow foundations. While deep foundation is used for high rise buildings, heavy structures and poor subsoil conditions to meet the design requirement. In Addis Ababa, the need for the construction of high-rise buildings is increasing. The scarcity of land in urban areas, intention for future purpose, advancement in technology, to use as a landmark and other are reasons for construction of high-rise buildings.

In a settlement sensitive soils, the construction of high-rise buildings leads to the settlement of the structure itself and other adjacent structures. This initiates engineers to use the piled raft foundation (PRF) which is a combination of pile and raft foundation to tackle settlement related problems. If the subsoil condition is not enough to provide the required bearing capacity, piled raft foundation, is used to transfer load of super structure to competent soil layer. This foundation is an economical option for heavy and high-rise buildings found on poor soil deposits. In addition to being economical, the PRF foundation type reduces the total and differential settlement to acceptable limit.

Famous high-rise buildings have been constructed around the world using the piled raft foundation system. Among those Burj Dubai is the one, which is over 800 m height and 160 stories. Twin Petronas Towers in Kuala Lumpur is another building, which has 450 m height and above 88 stories. In Germany also, the MesseTurm tower, 256 m in height and Deutsche bank, 162 m height are noticeable. In Ethiopia, many high-rise buildings have been built using PRF among these Commercial Bank, Nib Bank, Zemen Bank and United Bank headquarter buildings can be specified. The best and economical way of designing to withstand distortion, differential and total settlement design is still under study. Numerous investigations have been understudy using both instrumentally monitored and numerical investigations. Numerical study is coming the common first hand and simple investigation method from simple to complex structural models covering numerous fields of study. Optimized design is providing as much small number of piles, small pile length, small pile diameter and raft size with satisfying the design requirement. This can be easily done using numerically parametric study under different pile length, pile diameter, pile spacing and raft size with fulfilling the design requirement.

Addis Ababa, the capital of Ethiopia has located at 9° 1′ 48″ N and 38° 44′ 24″ E. This city is very close to Main Ethiopian Rift Valley about 75- 100 kilometers away (Gouin, 1979; Yoseph and Ramana, 2008). According to the newly revised code (CES-160-2015, 2015), the country is divided in to five zones of approximately equal seismic risks depending on the known distribution of earthquake. These zones are no damaging zone (0 zone), less damaging zone (zone 1 and 2) and zones of major damaging (zone 3 and 4). Based on this code, the study area is labeled under zone 3. Different studies also indicate the capital city had experienced different devastating earthquakes. For instance, in 1906 Addis Ababa was shocked by a 6.75 magnitude earthquake at an epicentral distance of 100 km south (Gouin, 1979; Yoseph and Ramana, 2008). This earthquake destroyed many buildings and structures that were built in the time. Gouin (1979) also writes major earthquake events starting from the 14th century up to the 1970s and this book shows Addis Ababa is an earthquake-prone area. Investigating performance of PRF under seismic load is critical. This can be alleviated through experimental study (centrifuge test) or numerical study which can reproduce the true physical and response replica.

At any time, the earth itself may induce a tectonic force called seismic force, which is devastating even in small magnitude. This requires the foundation to resist and adequately transfer any lateral load to the underlying soil without significant harm and disturbance to the superstructure. In this study, an attempt has made to investigate the influence of complex interaction from the soil, raft and pile to the dynamic response of piled raft foundations. Different loading conditions and analysis techniques including static and dynamic loadings from the representative earthquake history of Addis Ababa will be used.

1.2 Statement of the Problem

In recent years many but not adequate investigations using numerical and experimental have been done by numerous researchers and scholars to study the behavior of piled raft foundation under gravity and seismic loads. These investigations involve the load sharing between the pile and raft, the settlement and bearing capacity. Each foundation systems can yield its maximum contribution if it is properly designed and provided. Provision of uniform piles under the raft, which is uneconomical, has been used as a settlement reducer and increase bearing capacity. However, this method is very costly in pile installation and need to be designed cost effectively. A small number of piles, small diameter and length of pile with a relatively thin raft should be provided in order to achieve higher economy with fulfilling design requirements and overall safety of the structure. This optimized piled raft foundation can be achieved by detailed study of the geometric nature of PRF system through deep parametric study under various pile number, pile length, pile diameter, pile spacing and raft thickness. This helps to identify the role played by each PRF components to achieve the design requirement while fulfilling maximum economy of the solution.

Addis Ababa, the capital city of Ethiopia and Africa, is found in major damaging zone (zone 3) according to the newly revised code CES-160-2015 (2015), which regulate structures to be designed to withstand seismic action. The historic earthquake magnitude of Addis Ababa is beyond the threshold of damage. PRF is an ideal choice to reduce the differential and total settlement of itself and adjacent structures. Even though PRF is being used widely in Addis Ababa, till now piled raft foundation subjected to lateral, vertical and seismic loads needs additional study. This initiates in an investigation and evaluation the performance of PRF under seismic load considering the effect of soil structure interaction (SSI) on layered soil of Addis Ababa.

This study will be useful to identify the main significant piled raft geometric component and provide and optimized configuration that safe huge economy under allowable design requirement. Furthermore, it will help to the understand response and performance of the pile raft foundation under static and seismic loads.

1.3 Objectives of the Study

1.3.1 General Objective

The general objective of this thesis is a detailed investigation and evaluating performance of piled raft foundation under vertical static and seismic loads via a numerical method.

1.3.2 Specific Objectives

The specific objectives of this thesis are: -

- Identify major geometric parameters which influence the performance of piled raft foundation under vertical static load through parametric study.
- Provide an optimized piled raft configuration based on the result of parametric study without compromising the safety of the structure.
- Investigate the influence of seismic waves on the response of piled raft foundation with consideration of kinematic dynamic soil structure interaction (SSI).
- Evaluate the performance of piled raft foundation under seismic loading.

1.4 Methodology

In order to achieve the main objective of the study a method is used which involves from analyzing and interpreting raw geotechnical data to writing a command on FLAC3D V6 in order to model the three-dimensional piled raft foundation. Hence, the method adopted involves numerous steps and detailed analysis prior to the main numerical investigation, chapter three described it in detail. However, major steps in the method will be outlined here.

1. Collection of raw geotechnical data on building found on PRF around Kirkos and Mexico sub city.
2. Determining initial PRF size from codes and practices, and deconvolution analysis on SHAKE2000
3. Writing command (code) on FLAC3D V6 to model and analysis PRF under static and seismic loads.

1.5 Significance of the Study

Geotechnical Engineers have a responsibility to design safe and most economical structures. These structures can be subjected to both static and dynamic loads. Hence the safety and economy are dependent on detailed assessment and study of possible forces that may pose on the intended structure. Addis Ababa is a seismic area in its location and soil type due to the amplification of dynamic loads. Seismic analysis and parametric study of PRF in different loading conditions by changing parameters will be conducted. In the previous years, the effect of seismic loads on pile foundations standing on sandy soils had studied extensively in countries like Japan and other Far East countries. The behavior of a PRF built on layered soils (ranges from soft soils to hard rock) subjected to vertical static and seismic load is less known and studied. This study will be useful for: -

- Identify the main determinant geometric nature of PRF for optimized design of such foundation. Hence, optimization can be made through it to reduce construction expense.
- The actual analysis and evaluation of a similar foundation on similar soil types for seismically active regions like Addis Ababa, Dire Da'wa, Adama and other cities.

1.6 Scope of the Study

In this study, a piled raft foundation under static and seismic loads using a finite difference method FLAC3D V6. will be studied in detail. The optimized design of PRF will be done through a detailed parametric study involving variation of pile length diameter and spacing while keeping raft thickness and size constant. Through parametric study an optimized design pile raft configuration will be provided in accordance with the acceptable design criteria. Equivalent dynamic analysis methods with a representative earthquake history of Addis Ababa will be used to evaluate the performance of piled raft foundation with taking in to account the dynamic kinematic soil structure interaction (SSI). In this study, layered soil data from the construction of the Commercial Bank of Ethiopia headquarter building will be used. Twenty-seven (27) different piled raft combinations for static loading and two different PRF (consisting of the floating pile and end-bearing pile) for dynamic study under two different earthquakes will be analyzed.

1.7 Thesis Organization

The thesis is divided into five chapters. The background of the study, statement of problem, objectives and scope of the study are included in chapter one. A comprehensive literature review on the history of piled raft, analysis and design of PRF, earthquake history of Addis Ababa, soil behavior under dynamic load, dynamic soil-structure interaction and related studies on the static and seismic analysis of PRF are reviewed in detail in chapter two. Chapter three covers the general procedure and methodology used involving selecting a constitutive model, simulation of single pile capacity, selection of strong ground motion, estimation of dynamic ground motion and finally deconvolution analysis. Chapter four is devoted to sensitivity study, interpretation of results and comparisons of the parametric static and seismic analyses results. Finally, conclusions are drawn and recommendations for future works are presented in Chapter five.

CHAPTER – 2: REVIEW OF LITERATURES

2.1 Introduction

In this chapter different relevant studies will be reviewed in detail. Analysis technique, methodology and procedure adopted for analysis are derived from the detailed literature reviews. Vertical static and seismic loads are the main concerns of the study. Hence, literatures selected and reviewed in the following section relies on achieving the main objectives of the study.

2.2 History of Piled Raft Foundation

In traditional foundation design, it was customary to consider first the use of shallow foundations such as strip, combined or raft. If it is not adequate, a deep foundation which is a fully piled foundation is used instead. In the shallow foundations, it is assumed that a load of the superstructure is transmitted to the underlying ground directly by the raft or isolated footings. In the deep foundations, the entire design loads are assumed to be carried by the piles (Poulos, 2001). Beginning from the 1970s an intermediate foundation between shallow and deep (specially raft and pile) emerged as one good alternative foundation system that can enhance the settlement and bearing capacity requirement by the civil engineers. Piled raft foundation has been used extensively in Europe, Asia and now in Ethiopia beginning from the 2000s. A piled raft is intended to be used for reducing excessive settlement or increasing the bearing capacity. In the former, the raft should have adequate bearing capacity but the overall settlement is beyond the permissible limit, then a small number of piles will be placed strategically below the raft. In the later, the raft has suffered from excessive shearing or bending moment that it will fail the whole structure, then a larger number of piles from the settlement reducing pile should be used. This results in saving of economy from piling practice by a huge number of piles in the pile group foundation. In the following topics, case history of the piled raft foundation across the world including Africa, Europe and Asia will be described in detail.

In Ethiopia, Addis Ababa, beginning from 2000 E.C PRF has begun used extensively for buildings ranging from 4B+G+30 to 4B+G+50 stories. Nib Bank, Zemen Bank and United Bank headquarter building around Mexico and Commercial Bank headquarter building in Kirkos have built on this foundation system. The main reason was the high vertical load from the superstructure that leads to excessive shearing and settlements (Fisseha, 2019; Mahider, 2018). Some buildings that used the piled raft foundation system is attached in Table 2.1.

1. Commercial Bank Headquarter, Addis Ababa, Ethiopia

The Commercial Bank Headquarter building located in Kirkos sub-city built at depth of 22 m below the normal ground level. It has 4 basements, 46 floors above the ground level having an overall height of 186.4 m making it the tallest in Ethiopia. The expected load on the foundation is about 960 MN and foundation type of piled raft. 46 bored piles having a different pile length and diameter were used. Among those 36 piles have a diameter of 2.2 m and the rest have 1.8 m diameter. The raft has a thickness of 3 m and connected to the pile heads rigidly for effective load transfer. The geological condition of the site includes in the range of soil to rock. The groundwater table was located at 6.5 m below the normal ground level.

Table 2.1: Buildings in Addis Ababa found in PRF

Building	H(m)	P(MN)	A_R (m2)	tr (m)	n (-)	Lp (m)	Dp (m)	Pile Spacing(m)
Commercial Bank	186.4	1426	1380	3	46	5-10	1.8-2.2	-
Zemen bank	112.2	1699	1378	2.8	130	20-28	0.6-0.8	3Dp&6Dp
United bank	131.0	1253	1469	3.9	175	28	0.8	3Dp
Nib bank	131.0	1260	1763	2	161	24	0.8	3Dp

2. Hisckocks House, London, United Kingdom

Hisckocks House located in London is a 16-story, plan size of $44 \times 20.8\ m$ building having a total permanent load of 156 MN. The raft has 0.9 m thickness and has an expected bearing capacity of 700 MN. A total of 351 bored piles having 0.45 m diameter with a spacing of 1.6 m and length of 13 m were used and each pile has 1.6 MN expected bearing capacity. This foundation is built on homogenous overconsolidated clay and it was highly instrumented. A total settlement of 18mm was measured at the end of the construction. Besides, 75% of the total load was taken by the piles. Later on, numerical study 144 piles having a uniform distribution under the raft result only a very small increase in settlement. Further reduction of the pile to 36 leads to an increase of 20% settlement and a 28% load shared by the raft. The above study indicates that there is wide room for the economical design of this foundation system (Viggiani, 2001).

3. Messe Torhaus, Frankfurt, Germany

A case history, where piles are utilized as “settlement reducers”, is the Messe Torhaus, a 130 m high building in Frankfurt (Reul and Randolph, 2004). The Messe Torhaus was constructed between 1983 and 1986, and it is the first building in Germany with a piled raft foundation. A uniform distribution of piles over the raft area is employed. The design of the foundations was based on the experience from piled raft foundations in London and therefore a pile enhanced raft was applied to reduce excessive settlement. Heavy instrumentation was employed, since it was the first structure in Germany built on such foundations, which allows the assessment of its performance in terms of average settlement, settlement profile, pile load distribution and load share between piles and raft (Giannopoulos, 2011).

4. Messe Turm, Frankfurt, Germany

MesseTurm is a high-rise building of 256 m height with 60 story’s and it is ranked among the tallest buildings in Europe. Its importance is highlighted by the fact that it was one of the first high-rise buildings which were founded on a piled raft foundation and, therefore, significant instrumentation was installed in order to monitor the foundation performance. Settlements were estimated to be around 40 cm, if the building was designed on a mat foundation. This was able to reduce using piles below the mat to transfer some portion of the load to the underlying soil below the mat (Katzenbach *et al.*, 2005).

5. Burj Dubai, Dubai, UAE

Burj Dubai is the world’s tallest building that stands on a piled raft foundation system, founded on deep deposits of carbonate soils and rocks. It is founded on a 3.7 m thick raft supported on bored piles, 1.5 m in diameter, extending approximately 50 m below the base of the raft. The foundation system including 3.7 m thick raft and 926 piles subjected to both live and dead load was assessed for settlement using (pile group analysis) PIGS software. The predicted settlements of the tower range from 45 mm to 62 mm. These results were considered to be within an acceptable range (Poulos, 2008).

2.3 Design of Piled Raft Foundation

The collected experimental evidence for pile groups with piles at small spacing ratio s/d (3-4) and covering the entire raft area AR ($A_G/A_R \sim 1$), indicate that the percentage of load carried by the raft is not less than 20%. This increase up to 60–70% for increasing s/d or decreasing $A_G/A_{R.}$ This is a traditional design approach (Capacity Based Design approach, CBD) and it conflict with the observed experimental result (Mandolini *et al*., 2013). This method of design approach usually used to design a pile group foundation where the raft contribution is neglected or limited to very small.

Piled Raft Foundations consists of three bearing elements piles, raft and subsoil. The stiffness of raft and pile, the soil properties, the dimension and strategy of pile location, play the significant role in the design of a pile raft foundation system. Hence, the design of piled raft foundation relies on the consideration of all bearing element with the anticipated vertical, lateral or the earthquake loads. The main considerations that should be taken to account while designing a piled raft foundation are the following:

- Ultimate geotechnical capacity under vertical, lateral and moment loadings
- Maximum and total settlements.
- Differential settlement and angular rotation
- Lateral movement and stiffness
- Load shearing between the piles and raft
- Raft moment and shear for the structural design of raft and its stiffness
- Pile loads and moments for the structural design of the piles and its stiffness

Considering the above factor, there are preliminary and detailed design stages for this foundation system. Assessing the feasibility, rough estimation of number of pile and overall bearing capacity without the use of detailed computer analysis is done under preliminary design. While in the detailed design stage it is expected to determine optimum number of piles, location and configuration of piles, compute the detailed distribution of settlement, bending moment and shear force in the raft and piles. This stage requires physical prototype modeling, numerical modeling and reliability analysis of the provided piled raft geometric configuration. In the last decades specialist focused in this field with a different geotechnical purpose of the pile under the raft. Three practical design approaches for piled raft foundation are described below with a main purpose of enhancing the overall stiffness or reduce the total and differential settlement. These are described below (Poulos, 2001).

1. Conventional Approach

In this method the foundation is designed as pile group foundation in which major part of the load (usually 60-75%) is taken by the piles while some allowance is made for the raft to directly transfer load to the underlaying soil. A uniformly spaced pile loaded below the shaft capacity distributed over the whole area of the raft is provided. The allowance for the raft is not well defined and left for engineering judgment.

2. Creep Piling Approach

In this approach piles are loaded up until creep start to occur which is usually about 70 – 80% of its ultimate load bearing capacity of the pile. Piles are provided under the raft to reduce the net contact pressure between the raft under the soil. This prohibit a direct load transfer from the raft to the under-laying soil.

3. Differential Settlement Control Approach

Piles are provided strategically in order to reduce the differential settlement. Differential settlement usually occurs after full utilization of ultimate bearing capacity of each of the single individual pile in the group. In comparison with the above two design approach this design approach will require a smaller number of piles that make it more economical approach.

2.4 Analysis Method

Piled raft foundation is designed after assessing the ultimate load capacity for vertical, lateral and moment loadings, maximum settlement, differential settlement, raft moments and shears, pile loads and moments. After detailed analysis of piled raft foundation, the geotechnical engineer is required to decide the key geometry of the piled raft. These are (Poulos, 2002):

a) The required raft thickness,
b) The type of piles to be used, and
c) The required locations of the piles, and the pile diameter and length, to support a structure.

The analysis method for PRF is generally categorized in to three (Sinha, 2013; Fisseha, 2019). These are:

1. Simplified calculation methods
2. Approximate computer-based methods
3. More rigorous numerical methods

4.1.1 Simplified Analysis Method

This involves the development of mathematical model, based on established theory and principles, which can be performed by simple hand calculation without extensive use of computer. A good example is the Poulos-Davis-Randolph (PDR) method, which is a combination of the Poulos and Davis (1980) and Randolph (1994) methods.

i. Butterfield and Banerjee Approach

This were the first method to estimate the load sharing between the pile and cap, and the corresponding settlement behavior for various pile configuration (pile number, size and space) and a rigid raft (Sinha, 2013). The total vertical displacement *S(P)* due to the load P in an elastic soil medium of semi-infinite depth can be expressed as:

$$S\,(P)= \int_{c} \varphi C\, K(P, QC\,)dC \;+ \int_{s} \varphi_{s} K(P, Q\,)dS \qquad (2.1)$$

Where φC is shear stress on the cap, dC is element size in the cap occupied by the pile, φs is shear stress in the pile and dS is pile shaft element and base area. This elastic calculation is used mainly to get the total settlement. It does not include the interaction of different parameters like pile and mat interaction, pile and soil interaction and so on (Sinha, 2013).

ii. Davis and Poulos Approach

Davis and Poulos performed an elastic analysis of pile-raft interaction, considering a rigid floating pile connected with a rigid cap subjected to a vertical point load. This method cannot be used to explicitly calculate the load sharing between the pile and raft. In this analysis, pile length is divided into 'n' cylindrical element and pile cap is also divided into 'v' annuli each is subjected to a uniform shear stress p_b acting p_c respectively. The soil displacement at a typical element *i* is calculated from elastic stress-strain relationship as follows:

$$\rho_i = \frac{d}{E_s}(\textstyle\sum_{j=1}^{n}(1I_{ij}+ 21I_{ij})P_j \text{ + Pb } (1I_{ib}+ 21I_{ib}) + (\sum_{j=k}^{n} P_{ck}(1I_{ik}+ 21I_{ik})) \qquad (2.2)$$

where ρ_i is soil displacement at a typical element i, P is the uniform stress, Pb uniform stress on the pile tip, Pc uniform load on the pile cap, $1I_{ij}$ is the influence factor for vertical displacement at *i* due to shear stress on element *j* of pile, $1I_{ib}$ is the influence factor for vertical displacement at i due to vertical stress on base of pile j and $1I_{ik}$ is the influence factor for vertical displacement at *i* due to uniform stress on annular *k* of pile.

iii. Poulos- Devis –Randolph (PDR) method

This method is used for assessing the overall bearing capacity and load settlement behavior of piled raft in the preliminary design stage. The analysis was on a unit of rigid floating pile, which is attached to a rigid circular cap and the soil was considered as elastic semi-infinite mass. The required numbers of piles which satisfy the overall bearing capacity and the allowable average settlement of the foundation can be estimated by developing load settlement curve of the foundation. The curve depends on the stiffness of individual foundation component.

$$K_{Pr} = \frac{k_P + (1 \cdot 2\alpha_{rP})K_r}{1 - a_{rP}^2 (k_r / K_P)} \tag{2.3}$$

Where K_{Pr} is the stiffness of piled raft, k_P is the pile group stiffness, K_r is the stiffness of the raft and α_{rP} is raft pile interaction factor.

$$\alpha_{r_P} = 1 - \frac{\ln(r_c/r_o)}{\zeta} \tag{2.4}$$

Where r_c = average radius of raft (corresponding to an area equal to the raft area divided by number of piles); r_o= radius of pile

$$\zeta = \ln\left(\frac{r_m}{r_o}\right) \tag{2.5}$$

Where r_m is the maximum radius of influence of pile, which is related to the pile length as $r_m = 2.5p(1 - \upsilon)$and to the degree of homogeneity (ρ) of the soil. Consequently, the load shared by the raft and pile are calculated using the Equation 2.6 and 2.7 below.

$$\frac{p_r}{P_r + p_P} = \frac{(1 - \alpha_{rp})k_r}{kp + (1 - 2\alpha_{rp})kr} \tag{2.6}$$

$$\frac{p_P}{P_r + p_P} = 1 - \frac{(1 - \alpha_{rp})k_r}{kp + (1 - 2\alpha_{rp})kr} \tag{2.7}$$

4.1.2 Approximate Computer-Based Methods

Approximate computer-based methods the ones employing a “strip on springs” or a “plate on springs” approach. In both methods, the piles are represented by springs of appropriate stiffness and the raft by a series of strip footings for the “strip on springs” approach or by a plate for the “plate on springs” approach (Giannopoulos, 2011).

i. Strip on Spring Approach

This method considers rafts as a number of beams having equal length and piles as springs of equivalent stiffness in an elastic continuum of soil mass. This method utilized the boundary element method for strip, together with some results from simplified analysis (RDP approach above) for axial pile response, in order to simulate the piles behavior.

ii. Plate on Spring Approach

In this method raft is modelled as a thin plate, the piles as interacting springs of appropriate stiffness and the soil as an equivalent elastic continuum. Several idealizations and assumptions are made on this method regarding:

(a) The raft-soil contact pressure: it is specified for both compression and tension on the basis of bearing capacity theory, allowing for local bearing failure or lift-off of the raft from the soil.

(b) The raft: it is modelled as a thin elastic plate

(c) The piles: they are modelled as springs whose stiffness is pre-determined from elastic theory and whose ultimate axial capacity in compression and tension is specified;

(d) The soil: it is assumed to be an isotropic elastic continuum consisting of horizontal layers

4.1.3 More Rigorous Numerical Methods

The numerical methods employed to simulate the complex piled raft foundation are mainly the Finite Element Method (FEM), Boundary Element Method (BEM), Finite Layer Method (FLM), Finite Difference Method (FDM) or a combination of two or more of these methods.

i. Boundary Element Methods

In Boundary Element Methods, both the raft and the piles within the system are discretized, and elastic theory is used. Raft is discretized as a two-dimensional thin plate and represented by integral equation. Soil, on the other hand, is treated as elastic homogenous layer, in which piles are embedded. It works by constructing a mesh over the modeled surface, which have been formulated as boundary integral equation.

ii. Combined Boundary Element and Finite Element Analyses

These methods consist of a combination of boundary element analysis for the piles and of finite element analysis for the raft. The soil was modelled as a homogeneous elastic soil mass.

iii. Simplified Finite Element Analyses

A simplified or 2D finite element analysis involved the representation of piled raft as an axi-symmetric or a two-dimensional plain strain problem. In both cases, significant approximations were made. Many computer programs (PLAXIS, AMPS etc.) are available to simulate the behavior. In this approach, both the raft and the soil are discretized into finite elements. Also, the non-linear behavior of the soil and raft can be employed as well as time-dependent effects can be considered.

The problem of this simplified finite element analysis is that, only regular loading pattern can be analyzed and it cannot give the torsional moment in the raft. Piles must be smeared to a wall and given an equivalent stiffness equal to the total stiffness of the piles being represented by the wall. If non uniform loading considered, it may be required to run analyses for each of the directions in order to obtain estimates of the settlement profile and the raft moments.

iv. Three-Dimensional Finite Element Analyses

This method of analysis is the most powerful tool at the moment in terms of modelling a real problem. A more recent attempts for piled rafts were made to produced parametric solutions for the settlement and load distribution within piled rafts (Fisseha, 2019; Mahider, 2018; Kumar, 2016; Sinha, 2013 and Ruel, 2004). This method removes the need for approximate assumptions made in all the above approaches. However, there are still some problems in relation to the modelling of the pile-soil interfaces.

2.5 Previous Studies of PRF Under Vertical Static Load

In this sub section recent studies on piled raft which were done using three-dimensional numerical method will be discussed. The main concerns in piled raft foundation are the load sharing mechanism, the total settlement and differential settlement. The optimum design of piled raft focuses on determining the number of piles, spacing of pile, position of pile, length of pile, raft thickness and pile diameter.

Reul and Randolph (2004) have conducted a numerical investigation on study three case histories, namely Westend 1, the Messe Turm and the Messe Torhaus have been studied by means of three-dimensional elasto-plastic finite-element analyses, and the calculated results have been compared with the in-situ measurements. Torhaus building foundations were designed using a settlement reducing approach with a uniform distribution of piles over the raft area. A total number of 84 bored piles with a length of 20 m and diameter of 0·9 m are located under the rafts. Two pile configurations were examined with the concept of placing piles in the center to reduce settlement. These are configuration A and B having 60 and 40 number of piles having 20 m to 27.5 m length. The overall result in the settlement and load sharing of the real and two modified arrangements are listed in the table 2.2. The pile configurations are shown in the Figure 2.1 below.

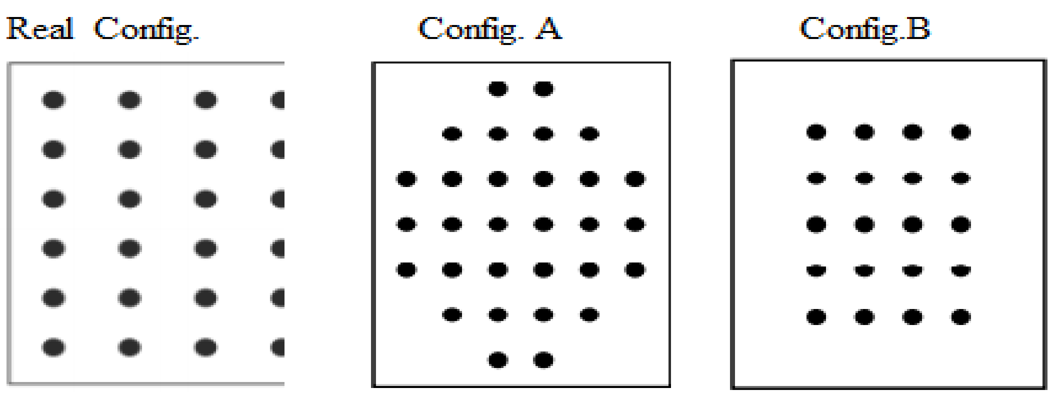

Figure 2.1: Layout of piles on the Messe Torhaus building (Reul and Randolph, 2004)

Table 2.2: The results of parametric study under different configuration

Parameters	real layout	Configuration A	Configuration B
No. of pile ()	84	60	40
Length of pile(m)	20	23.1	27.5
αpr	0.76	0.67	0.52
ξs	0.51	0.51	
ξΔs	0.5	0.16	<0 (hogging)

Sinha and Hanna (2016) have conducted a numerical analysis to examine the effect of the key parameters governing the performance of this foundation during loading and, accordingly, the load shared by the piles and the raft. In addition to the substructure effect different subsoil effect, like angle of shear resistance and cohesion, were examined by this study. In their hypothetical study of piled raft foundation, a variable raft thickness, pile length, pile diameter and pile spacing were considered. The soil was model by the modified Drucker-Prager constitutive model.

Their results show increase of spacing beyond of 6D to carry the whole load by the raft. Increasing the pile length leads to decrease in total and differential settlement. Furthermore, settlement at the center of the raft decrease up to a raft thickness of 1.5m beyond which it will impose addition load for underlying soil. Variation of the internal friction angle and cohesion were under study. Increasing ϕ from 10^o to 15^o decrease settlement appreciably, while by 15^o it is not drastic. The increase in cohesion (c) up to 25 kPa show the same result with ϕ. In this study, homogenous soil layer and vertical loading were considered.

Mahider (2018) conducted a research entitled Assessment of "Piled Raft Foundation" for High Rise Buildings Under Vertical Load in Addis Ababa: The case of Nib, Zemen, and United Bank Headquarter Buildings. He conducted the study using the finite element software package – ABAQUS. The width and depth of the model were 2.5 times pile length and 3 times the raft width respectively. The soil was modeled in an elastoplastic constitutive model called the Mohr-Coulomb while the piled raft was model in a linear elastic model. The maximum settlement obtained in the study was 8.97 mm in Zemen Bank, 3.024 mm Nib Bank, United Bank buildings respectively. He found 90% of the load shared by the pile. The load shared by the raft was increased considerably when the spacing was increased from 3D to 6D.

Moayedi *et al*. (2018) have studied an analytic investigation on the performance of floating piled raft which is found in deep compressible soil layer for controlling angular distortion of the foundation system. A 9*9 pile with 45 combinations had analyzed by varying the spacing, arrangement, length and raft thickness. He found angular distortion is lower when floating pile of different length had used rather than uniform pile length. In his study, a static analysis was only considered with a uniform soil layer.

Fisseha (2019) studied the load sharing behavior of piled raft foundation on the Commercial Bank of Ethiopia Head Quarter building at Addis Ababa. The soil continuum was modeled with a modified Drucker – Prager cap plasticity constitutive model and the raft and pile were modeled with a linear elastic constitutive model. He found that 46 pile has no contribution in settlement reduction but carries the entire load of the structure. The load shared by the pile is 96% of the total superstructure load due to the pile tips resting on hard stratum. Moreover, a parametric study had conducted to see the effect of a weak layer located under hard stratum below pile tips. He found that the effect of this weak layer is negligible for relative stiffness between the weak and hard strata is greater than 0.5. In his study, he considers a homogenous soil layer modeled by the Drucker-Prager constitutive model which may alter the true numerical result.

2.6 Summary of studies on PRF related to vertical static load

In the previous topic several literatures focusing mainly on vertically loaded piled raft foundation have been discussed. It is usually required to specify the major area of the study and their major findings. Table 2.3 summarizes major finding of different authors reviewed in the previous topics.

Table 2.3: Summary of literatures related to statically loaded PRF

Year	Authors	Authors Finding
2004	Reul and Randolph	Smaller settlement obtained on longer piles rather than with a higher number of piles, for uniform loading the installation of piles seems not to reduce the bending moments
2016	Sinha & Hanna	The pile cross-sectional shape doesn't have effect, thinner raft may lead to nonuniform load shared by the piles
2018	Mahider	Up to 90% load was carried by the pile; PRF is effective in reducing settlement
2018	Moayedi *et al.*	Angular distortion is lower when floating pile of different length had used rather than uniform pile length, raft thickness can decrease the angular distortion
2019	Fisseha	The pile has little contribution for settlement reduction but carry the whole load, 96% load carried by the pile tip.

2.7 Earthquake History of Addis Ababa, Ethiopia

Addis Ababa, the capital of Ethiopia is the largest city in population and size. Addis Ababa is a densely populated city of Ethiopia which is expected to be above 7 million people and holds 527 square kilometers of area (CES,2007). Since this city is the economic and political center of Ethiopia, many infrastructures including high-rise building are under construction. Besides, the scarcity of land, technological advancement and others encourage the construction industry in Addis, especially high-rise buildings.

Earthquake event starts from the earth, destroys any structure found on the earth's surface and ends in the earth. Consequently, understanding the internal structure of the earth is a key requirement to clearly understand seismic events. The earth has three consecutive layers starting from the top crust, in the middle mantle and at the bottom core (Figure 2.2). The interior part of the earth is in constant motion due to heat generated by radioactivity in the core (Sucuoğlu and Akkar, 2014). The heat energy transferred to the outer core and then towards the crust in the convection form. This results in the movement of plates to converge or diverge. The relative movement of one plate to other leads to the occurrence of an earthquake (Figure 2.2).

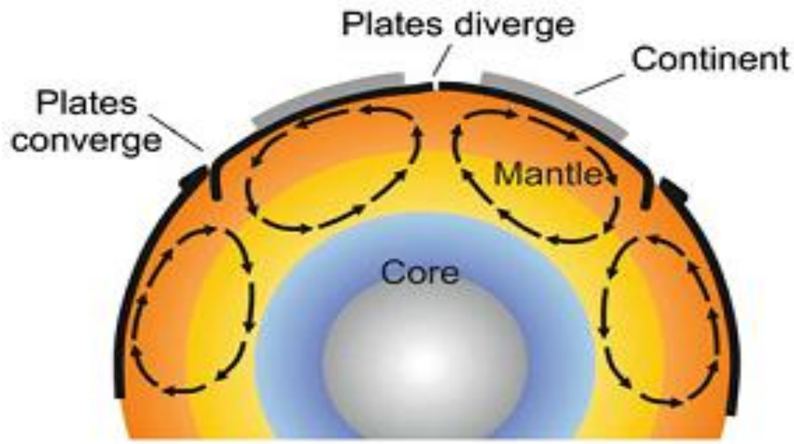

Figure 2.2: Internal earth structure and plate movement (Sucuoğlu and Akkar, 2014)

The parameter used in evaluating the seismicity of the area are (Gouin, 1970):

- Areal distribution of earthquake event
- Magnitude of earthquake
- Frequency of occurrence
- The focal depth of earthquake

The above-listed parameters are essential for evaluating the seismicity of any region for further use of engineers and experts. For Ethiopia, at present time, a good quantity of instrumental data is available on the magnitude, epicentral distribution and frequency of occurrence of damaging earthquakes that have occurred since the beginning of this century (Gouin, 1970). The last hundred and above years data and experience show that Ethiopia is a region where seismic activity often exceeds the threshold of damage. Hence, engineers must assess the magnitude of the problem, develop a way of reducing the problem and construct a structure that remain durable to minimize damage of lives and property.

The East African Rift system (EARS) is a 3,000 km long Cenozoic age continental rift extending from the Afar triple junction, between the horn of Africa and the Middle East, to western Mozambique (Figure 2.2) (Hayes *et al*., 2014). Since Ethiopia is in the horn of Africa this rift valley system (EARS) divides the country in to two. Figure 2.3 below can clearly show Addis Ababa is very close to Main Ethiopian Rift Valley system (EARS) which is about 75-100 kilometers away. According to the Ethiopian building code, Addis Ababa is labeled in zone 3 with a peak ground acceleration (PGA) of 0.1g (CES-160-2015, 2015). In addition to Addis Ababa, other major cities in Ethiopia like Adama, Dire Da'wa and Hawassa are in or very near this fault lines. In this rift system and close to it (Addis Ababa) earthquake events have been occurred which ranges from barely felt to devastating.

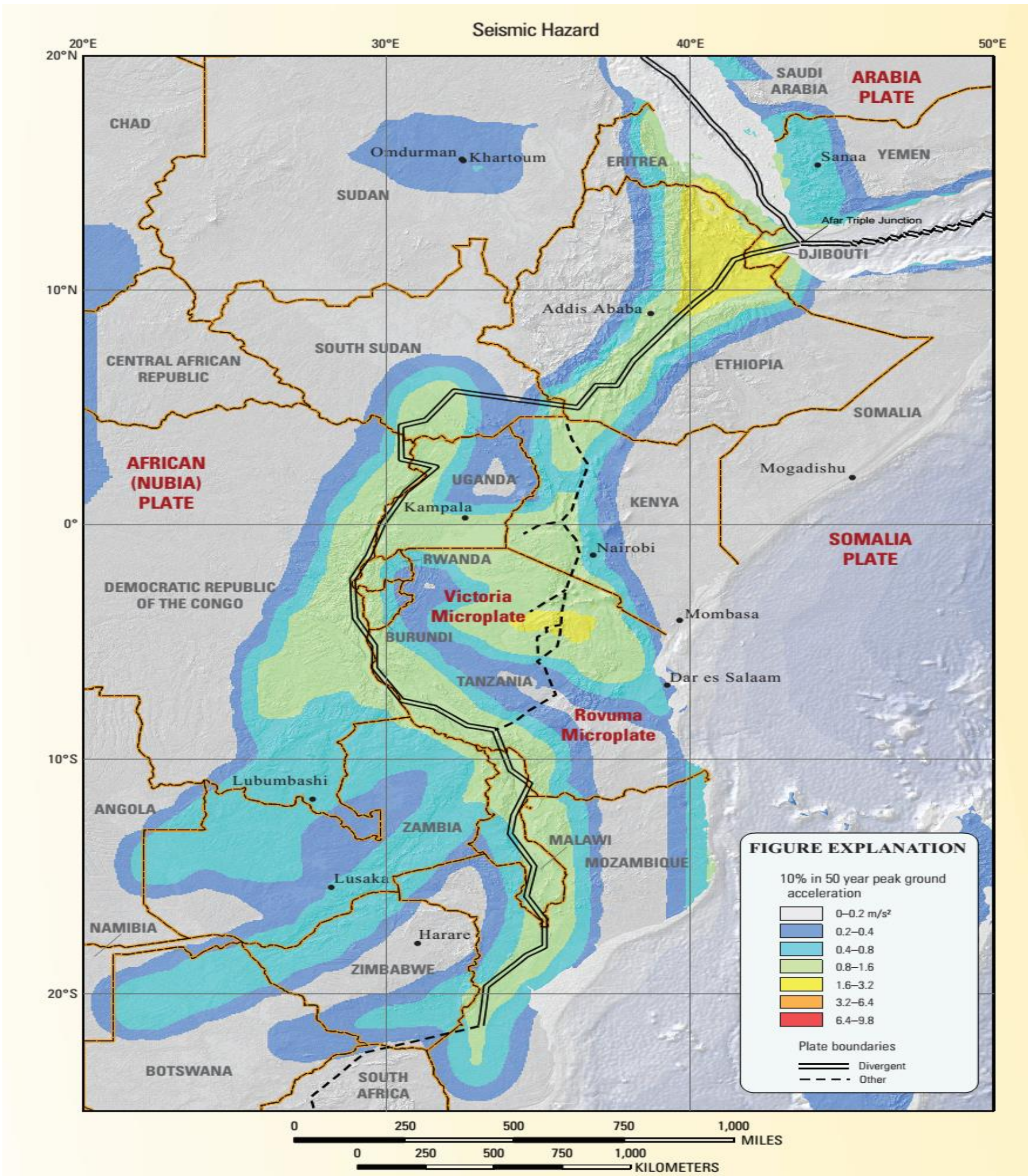

Figure 2.3: The seismic map of east and south Africa (Hayes *et al.*,2014)

2.8 Concept of the Seismic Soil-Structure Interaction

The main concept of the soil structure interaction comes from geotechnical earthquake engineer to construct a civil structure that can resist earthquake strike. This require understanding of geology, seismology, soil dynamics, structural and geotechnical engineering. Analysis of a structure considering fixed base condition is sometimes unreasonable specially when the subsoil condition is poor deposits. It is usually considered in different papers SSI increase the fundamental period of the system leading to higher damping. However, in recent studies it is found that SSI can also increase the lateral deflection and foundation rocking as compared to fixed base condition. (Hokmabadi *et al.,* 2014; Van Nguyen *et al.,* 2016). Earthquake characteristics, local soil properties, travel path, and the soil-structure interaction are the key factors affecting the seismic excitation experienced by the superstructure. A free field condition is a ground motion under the first three specified conditions without the presence of structure. When structure built on poor deposit, the foundation is unable to conform to the deformations of the free-field motion. This deviation and dynamic response of the structure itself induce deformation on the surrounding soil. This process of interaction between the soil, structure and foundation under dynamic loading is called soil structure interaction or simply SSI. This can be defined shortly as: dynamic soil structure interaction is the response of soil for loading of structure (piled raft) in the form of deflection or displacement and then the corresponding response of structure to the soil.

The effect of SSI on the response of civil structure by considering a compliant base can be illustrated by the model suggested by wolf (1985). Under compliant base condition the foundation can rotate and translate. The damping and stiffness characteristics can be represented translational and rotational springs and dashpots of Wolf’s model in the Figure 2.4.

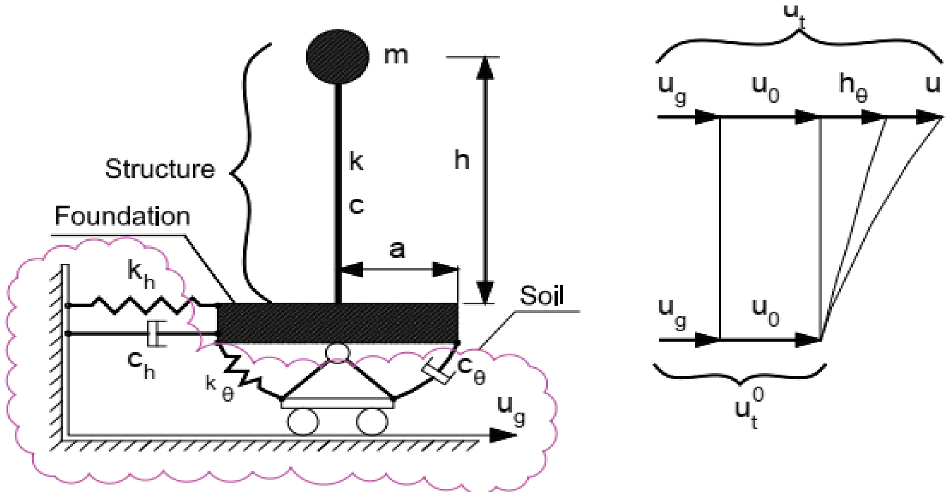

Figure 2.4: Soil-structure interaction model including SDOF structure and idealized discrete system to represent the supporting soil (Wolf ,1985)

Where:

- K_h and C_h are stiffness and damping in the horizontal direction;
- K_θ and C_θ are stiffness and damping in the rotational direction;
- h is the height of the structure; $2a$ is the width of the foundation;
- U_0 is the amplitude of the base relative to the free-field motion (U_g)
- U is the structural distortion; and U_t is the total lateral displacement of the system.

The above three degree of freedom vibration can be replaced in to equivalent model by assuming the foundation as massless as shown in the figure 2.5. Wolf also changed the motion of the figure 2.5 equivalent system in to a matrix form as shown equation 2.8.

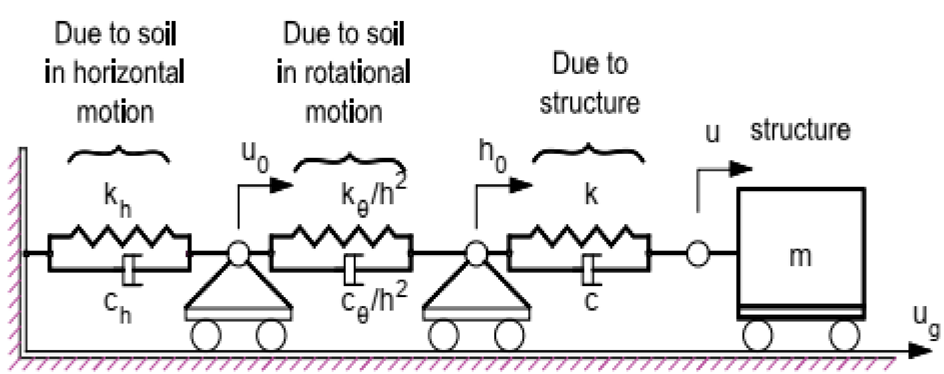

Figure 2.5: Equivalent soil structure interaction model (Wolf, 1985)

$$\begin{bmatrix} K_h + \frac{K_\theta}{h^2} & -\frac{K_\theta}{h^2} & 0 \\ -\frac{K_\theta}{h^2} & k \pm \frac{K_\theta}{h^2} & -k \\ 0 & -k & k \end{bmatrix} \begin{Bmatrix} u_0 \\ u_0 + h\theta \\ u_0 + h\theta + u \end{Bmatrix} + \begin{bmatrix} c_h + \frac{c_\theta}{h^2} & -\frac{c_\theta}{h^2} & 0 \\ -\frac{c_\theta}{h^2} & c + \frac{c_\theta}{h^2} & -k \\ 0 & -c & c \end{bmatrix} \begin{pmatrix} \dot{u}_0 \\ \dot{u}_0 + h\dot{\theta} \\ \dot{u}_0 + h\theta \dot{+} \dot{u} \end{pmatrix} +$$

$$\begin{bmatrix} 0 & 0 & 0 \\ 0 & 0 & 0 \\ 0 & 0 & m \end{bmatrix} \begin{Bmatrix} \ddot{u}_0 \\ \ddot{u}_0 + h\ddot{\theta} \\ \ddot{u}_0 + h\ddot{\theta} + \ddot{u} \end{Bmatrix} = \begin{Bmatrix} 0 \\ 0 \\ -m \end{Bmatrix} \ddot{u}_g \tag{2.8}$$

Where:

$$\xi = \frac{c}{2k_\omega}; \xi_h = \frac{c}{2k_h\omega_h}; \xi_\theta = \frac{c_\theta}{2k_\theta\omega_\theta}; \omega_s = \sqrt{\frac{k}{m}}; \omega_h = \sqrt{\frac{k_h}{m}}; \omega_\theta = \sqrt{\frac{k_\theta}{mh^2}}; \tag{2.9}$$

After solving the equation above

$$u_0 = \frac{\omega_s^2}{\omega_h^2}\frac{1+2i\xi}{1+2i\xi_h}u; h\theta = \frac{\omega_s^2}{\omega_\theta^2}\frac{1+2i\xi}{1+2i\xi_\theta}u \tag{2.10}$$

Hence u can be expressed as:

$$\left(1 + 2\xi - \frac{\omega^2}{\omega_s^2} - \frac{\omega_s^2}{\omega_h^2}\frac{1+2i\xi}{1+2i\xi_h}\frac{\omega_s^2}{\omega_\theta^2}\frac{1+2i\xi}{1+2i\xi_\theta}\right)u = \frac{\omega^2}{\omega_s^2}u_g \tag{2.11}$$

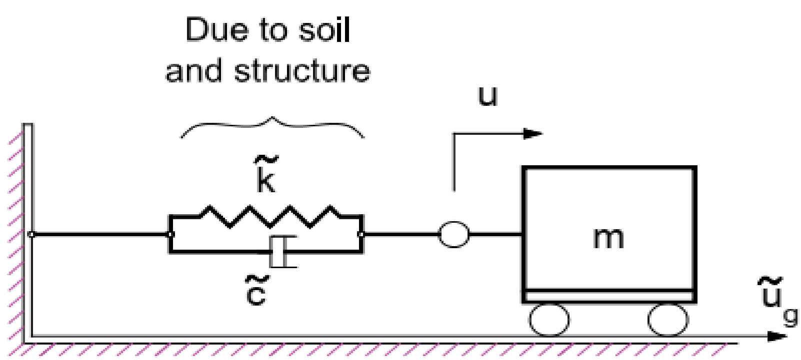

Figure 2.6: Equivalent one degree of freedom SSI (Wolf ,1985)

Figure 2.6 shows the transformation of three degree of freedom SSI in to equivalent one degree of freedom SSI. The symbol m is the mass of the structure, $\tilde{k}$ is equivalent soil structure stiffness, $\tilde{\omega}$ is equivalent natural frequency, $\tilde{\xi}$is equivalent damping ratio,$\tilde{u}_g$ equivalent input motion and $\tilde{c}$ is equivalent damping value. This are obtained as follows:

$$\frac{1}{\tilde{\omega}^2} = \frac{1}{\omega_s^2} + \frac{1}{\omega_h^2} + \frac{1}{\omega_\theta^2} \tag{2.12}$$

$$\tilde{\xi} = \frac{\tilde{\omega}^2}{\omega_s^2}\xi_s + \frac{\tilde{\omega}^2}{\omega_h^2}\xi_h + \frac{\tilde{\omega}^2}{\omega_\theta^2}\xi_\theta \tag{2.13}$$

$$\tilde{u}_g = \frac{\tilde{\omega}^2}{\omega_s^2} u_g \tag{2.14}$$

The above equation clearly depicts that the full compliant base analysis (soil structure interaction) compared with the fixed base results in reduce the natural frequency and increase the damping ratio. This interaction generalized in to inertial interaction and kinematic interaction. Kinematic interaction arises from the variation of stiff foundation motion from the free field motion. While the inertial interaction arises inertial developed to produce base shear, torsion and moment on the foundation.

2.1.1 Kinematic Interaction

This interaction is mainly due the presence of the stiff piled raft foundation elements in the soil resulting in the deviation of the foundation motion from the free field ground motion. Kinematic interaction could be due to the ground motion incoherence, foundation embedment effects, and wave scattering or inclination. In seismic active regions many buildings are susceptible to soil structure interaction effects due to the induced changes in the dynamic characteristics of soil during seismic excitation. Depending mainly on the relative stiffness of the soil and structure, SSI can have an impact on the response of the civil structure. To account for the kinematic interaction of SSI, a full nonlinear dynamic analysis is necessary under the following conditions (Bommer, 2004, Hokmabadi *et al*., 2014).

- Very important structure
- Having special features (base isolation)
- Designed for high degree of ductility
- Minimum expected seismic magnitude is 0.1g
- Poor soil class are common

2.1.2 Inertial Interaction

Inertial interaction is when superstructure start to excite due to the motion inertial forces triggered by the excitation at the foundation level. The inertial forces distributed over the height of the structure cause a resultant base shear and an overturning moment at the foundation, which in turn cause deformation of the soil. This is called the inertial dynamic soil structure interaction.

2.9 Soil Behavior Under Dynamic Load

Soils are often subjected to vibrating forces from different sources like earthquake, machines, bomb blasting, wave actions from the water body and probably other. This creates challenges for civil engineers that requires basic knowledge of property of soil under dynamic loads to handle properly. These problems can be response of machine foundations subjected to cyclic loading, dynamic bearing capacity of foundations, earthquake resistance of dams and embankments and soil structure interaction during the propagation of stress waves generated due to an earthquake (Das and Luo, 2016).

A typical soil subjected to symmetric cyclic loading will create a closed loop of shear stress versus shear strain during loading and unloading. This loop (Figure 2.7a) is called hysteresis loop. For a very small strain magnitude usually 0.005 percent the hysteresis loop is narrow. This hysteresis response of soils can be described using two important characteristics of the hysteresis loop shape: inclination and breath. Kramer (1996) describe inclination represents stiffness of the soil, which can be described at any point during the loading process by the tangent shear modulus (G_{tan}). Obviously, the tangent shear modulus varies throughout a cycle of loading, but its average value over the entire loop can be approximated by the secant shear modulus (G_{sec}) (Equation 2.15).

$$G_{sec} = \frac{\tau_c}{\Upsilon_c} \tag{2.15}$$

where, $\tau_c$and Υ_c are the shear stress and shear strain amplitudes at the defined point, respectively. Therefore, G_{sec} describes the general inclination of the hysteresis loop. The breath of the hysteresis loop, which is related to the area of one hysteresis loop, represents the energy dissipation and can be described by the damping ratio (ξ) as follows (Equation 2.16):

$$\xi = \frac{W_D}{4\pi W_S} = \frac{A_{loop}}{2\pi G_{sec}\gamma_c^2} \tag{2.16}$$

where, W_D is the dissipated energy in one loop, W_S is the maximum strain energy, and A_{loop} is the area of the hysteresis loop (which is equal to W_D). The main parameters for equivalent linear analysis are ξ and G_{sec}. However cyclic nonlinear and advanced constitutive model require the actual path of the hysteresis loop to describe the complete soil behavior under dynamic loading (Kramer, 1996). The stiffness of soil depends on the strain ampliated, void ratio, over consolidation ratio, mean principal stress, plasticity index and more. The shear strain amplitude of soil influences the secant shear modulus highly, at low shear strain amplitude it is high and decrease as the amplitude of shear strain increase. The locus of points corresponding to the tips of hysteresis loops of various cyclic strain amplitudes is called backbone curve as shown in Figure 2.7b.

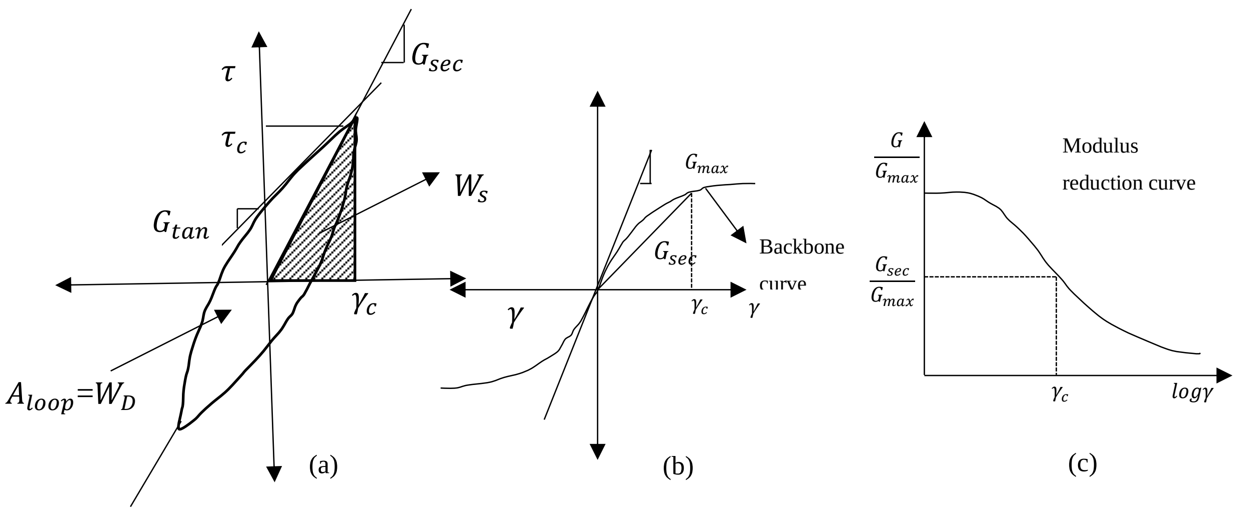

Figure 2.7: (a) Hysteretic loop (b) Backbone curve (c) Modulus reduction curve of soil (Hokmabadi *et al*., 2014)

The slope at the origin of backbone curve represents the largest value of the shear modulus designated by G_{max}. As cyclic shear strain amplitudes increase, the modulus ratio, G_{sec}/G_{max} drops to values less than one. Therefore, in order to characterize the stiffness of the soil element varying with the cyclic shear strain amplitude, both G_{max} and the manner in which the modulus ratio G_{sec}/G_{max} varies with the cyclic strain amplitude. The variation of shear modulus ratio with the cyclic strain amplitude can be described by a graph called the modulus reduction curve amplitude (Figure 2.7c) (Kramer, 1996). Different characteristics of soil that influence the shear modulus also influence the damping ratio. Elastic materials have higher damping ratio than the plastic material. In general, soil damping comprises of two distinct parts: material damping (or viscous damping) and geometrical damping (or radiation damping).

1. Material damping: - is absorption of energy by materials during wave propagation resulting in the reduction of the wave amplitude. This occurs due to the multiple atomic-level actions, such as interface friction and internal hysteresis (Kramer, 1996).

2. Geometrical Damping: - is reduction in the amplitude due to the spreading of energy over a greater volume, even though the elastic energy is conserved (no conversion to other forms of energy takes place), is often referred to as Geometrical Damping (Kramer, 1996).

2.10 Backbone Curve for Geotechnical Material

In the preceding section it was explained what backbone curve is and how it is useful to describe the behavior of geologic material under cyclic load. In this section backbone curve (damping ratio and shear modulus ratio) for clay, sand, gravel and rock will be explained with reference from different previous literatures.

2.1.3 Backbone Curve for Cohesive Soil

The key dynamic property of the soil are the shear modulus reduction ratio and the damping ratio at different shear strain level. It is well known and common that soft soils are highly affected for seismic loads rather than rock or gravel. Considering this fact numerous studies have been conducted dealing with the relation of damping ratio (ξ) versus shear stain (ϒ) and shear modulus ratio (G/G_{max}) versus shear strain (ϒ) (Hardin, 1978; Sun *et al.*, 1998; Zhang *et al.*, 2005). They indicate that the backbone curve for such cohesive soils depends mainly on the plastic index. Sun *et al.*, 1998 have proposed curves of backbone curve of cohesive soils which depend on plasticity index (Figure 2.8).

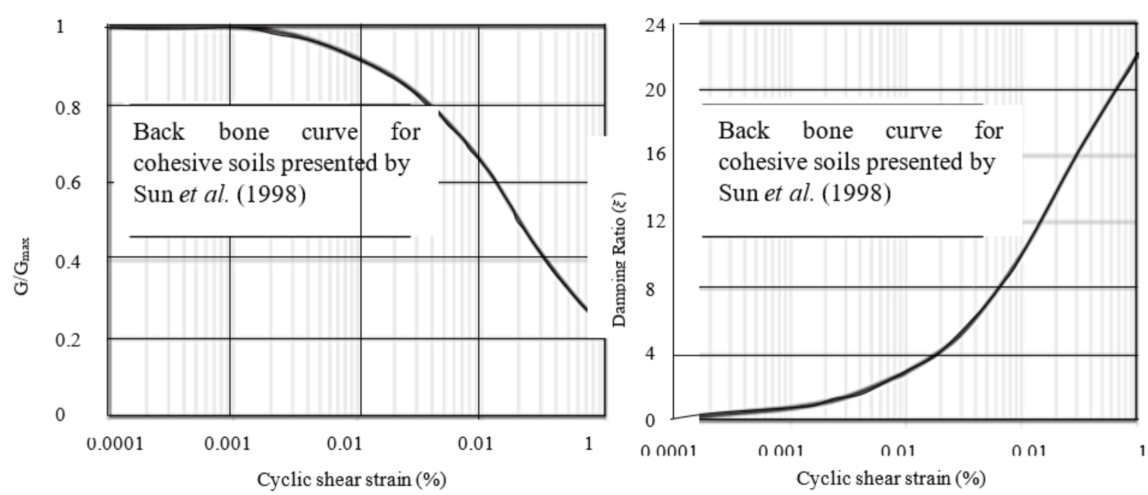

Figure 2.8: Shear modulus and damping ratio curve for clay (Sun *et al.*, 1998)

2.1.4 Backbone Curves for Cohesionless Soils

The main cohesionless soils are sand and gravel. Studies on the dynamic behavior of cohesionless soils indicate that the main factor which influence the damping factor and damping ratio are the confining pressure and strain level (Seed *et al*., 1986). While other factors such as grain size distribution, degree of saturation, void ratio, lateral earth pressure coefficient, angle of internal friction, and number of stress cycles may have minor effects on the damping ratios of sandy and gravely soils. In the figure below a representative backbone curve for sand that is taken from seed *et al*., 1986 is shown in figure 2.9 below.

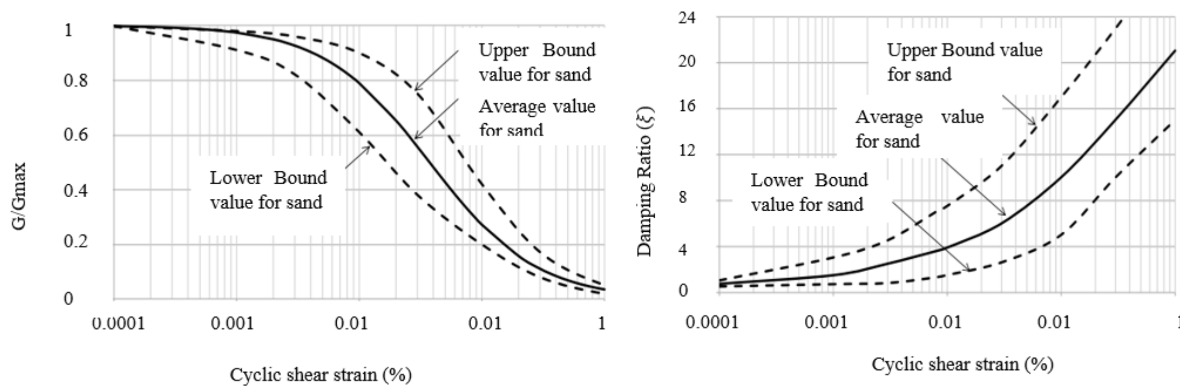

Figure 2.9: Modulus reduction and damping ratio curve for sand (Seed *et al*., 1986)

2.11 Previous Related Studies of Piled Raft Foundation Under Seismic Loading

Some studies that are on piled raft under seismic and dynamic loads will be discussed and reviewed. Some authors compare the centrifuge test with the numerical method and appreciable result were obtained.

Banerjee *et al*. (2007) have investigated the response of clay soil and piled raft foundation using a centrifugal model at Singapore university under three different seismic excitations having a peak ground acceleration of 0.065 g, 0.03 g and 0.015 g. In this experimental study, the clay shows a strain-softening and stiffness degradation after applied cyclic load. The experimental analysis was back analyzed using a numerical software ABAQUS. Hypoelasic and linear elastic model were used for homogenous clay layer and piled raft respectively. The shear stiffness reduction and damping ratio were modeled form the backbone curve of Vucetic and Dobry (1988). The comparison of experimental and numerical studies shows a remarkable agreement (Figure 2.10). However, their study was limited only on clay soil and short length piles.

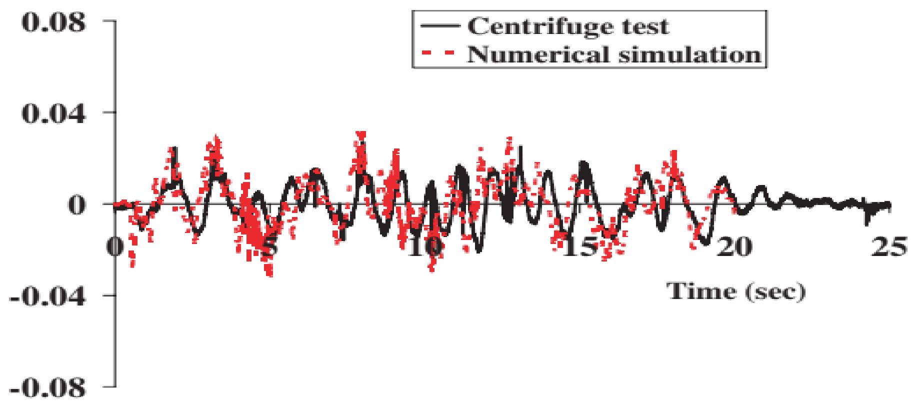

Figure 2.10: TH recorded in centrifuge tests and numerical simulation (Banerjee *et al.*, 2007)

Eslami *et al*. (2011) have studied the seismic behavior of piled rafts and pile groups while the same amount of construction material and excavation is used in their construction. In this study, the El-Centro earthquake was used for the time history analysis of piled raft and pile foundation. In this model, a simple concrete square raft with 6.24 m width and 1.47 m thickness was set up on a 22.5 m × 13.5 m soil (dry Toyoura sand) with a depth of 12 m. In this study, it was observed that the piled raft foundation system is rather better than the pile group system according to the acceleration response of the piled raft which was 36% less than the pile group. The horizontal displacement of the piled raft was 9% less than the pile group and the maximum bending moment was reduced by about 15% for the piled raft system. The effective stress analysis method was employed for this study by considering dry sand.

Saha *et al*. (2015) have conducted a study on the seismic response of a piled raft structure system. In their study, the effect of the soil structure is considered and is the main concern of the study. Their study shows that SSI has a marginal effect on seismic column shear while it may lead to a considerable increase in seismic lateral force in piles because of the additional inertia force contributed by the heavy mass of the superstructure, which is not accounted for in the fixed base condition. In their study, a homogenous soil layer was considered in addition to one seismic excitation.

Kumar *et al*. (2016) have conducted a numerical investigation on the behavior of PRF when subjected to lateral and real earthquake loading conditions in addition to vertical loads with finite-element software called PLAXIS 3D. For pseudo-static loading and real acceleration–time history (dynamic analysis), four real earthquake histories had used. These are El-Centro 1979, Loma Prieto 1989, Bhuj 2001 and Sikkim 2011 real earthquakes. Piled raft foundation having a raft of 4 m width and 1 m thickness was modeled as a plate element. Four fixed headed piles each having 9 m in length, 500 mm in diameter and having a center-to-center spacing of 2 m was modeled with the use of the embedded pile element option inbuilt in PLAXIS 3D, as shown in Figure 2.11. To remove the unnecessary reflection of seismic wave a boundary condition of viscous damping was used. In addition, the existing PRF of MesseTurm Tower was modeled and analyzed under static and pseudo-static loading conditions. Lumped mass of superstructure on the foundation concept was employed to consider the superstructure dead load. The results obtained show a good correlation with the static field-measured results. Results in terms of bending moment in piles, total settlements, and normalized lateral displacement (u/D) are reported. Their study is limited to16m depth homogenous sandy soil and modeled with a Mohr-Coulomb constitutive model.

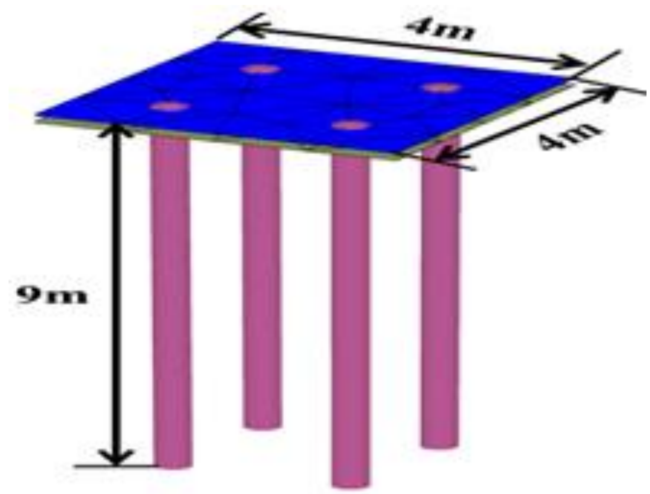

Figure 2.11: Schematic representation of piled raft model (Kumar *et al.*,2016)

Zhang *et al*. (2017) have studied the effect of long-term earthquake load on the response of piled raft foundation using centrifuge test and finite element analysis. They focused mainly on soft kaolin clays soil for a duration of up to 200 sec. The experimental investigation focused on the influence of group size on both raft acceleration and pile bending moment. The centrifuge test result was compared with the finite element analysis result on which the soils modeled by hyperbolic hysteresis constitutive model. The result shows that the response spectrum between computed and measured accelerations at both clay surface and raft shows a good agreement as shown in the figure2.12 below. The computed and measured maximum pile bending moment profiles for 4 different pile-raft models generally shows some variations in the range of 4% to

36%. In their study, the 3D finite element modeling procedure with a hyperbolic-hysteretic soil constitutive model can be extended to complement seismic centrifuge tests.

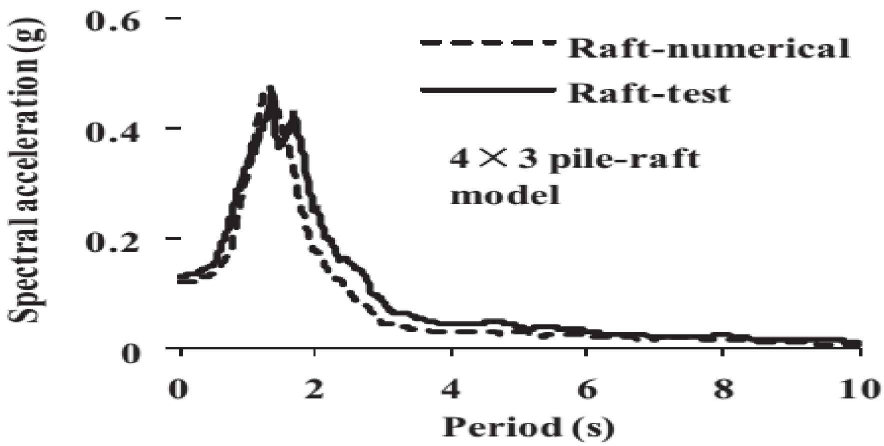

Figure 2.12: Comparisons of acceleration response spectra at raft and clay surface between centrifuge test and numerical simulation (Zhang *et al.*, 2017)

2.12 Summary of Studies on PRF Related to Seismic Load

In the previous sections, several works of literature focusing mainly on laterally and seismic excited piled raft foundations have been discussed. It is usually required to specify the major area of the study and its findings. Table 2.4 summarizes the main focuses of the study and their findings.

Table 2.4: Summary of literatures related to seismic loaded PRF

Year	Author	Authors Finding
2007	Banerjee *et al*.	Shaking results in strain softening and stiffness degradation, aggravated softening of the soil around the pile, lengthening of the resonance period of the clay layer.
2011	Eslami *et al*.	piled raft foundation system is rather better than the pile group system.
2015	Saha *et al*.	The study shows that SSI has a marginal effect on seismic column shear while it may lead to a considerable increase in seismic lateral force in piles because of the additional inertia force contributed by the heavy mass of the superstructure.
2016	Kumar *et al*.	Numerical analysis is in close agreement with the centrifuge test results, Amplification was observed for all cases of earthquake input motion, input motion plays a significant role in resonance condition of foundation.
2017	Zhang *et al*.	The centrifuge and FEM analysis show good agreement, acceleration and pile bending moment response were influenced by stiffness-to-mass ratio of the pile-raft system.

2.13 Conclusion of Literature Review

A comprehensive literature review has been presented in this chapter in regards to performance and investigation of piled raft foundation under static and seismic loads, available in English literature. The authors main focusses of study and their major finding have been described. Although a great deal of effort has been made to study the performance and response of piled raft foundation under static and dynamic loads, the following areas still needs the attention of researcher.

1. Most works on statically loaded piled raft foundation focused on clayey soil or one soil type and layered soils were modeled as equivalent homogenous soil. A limited research is available on the parametric study of piled raft foundation to understand their influence. Others focused either to reduce the settlement to allowable limit or assessed the load sharing of pile and raft on one particular case study.

2. In spite of limited studies, it is observed from the literature review of piled raft foundation under seismic load, countless investigators focused on short length friction piles on a homogenous soil type. There is also observed limitation in considering the effect of different magnitude of earthquake and proper modeling of the soil structure interaction (SSI).
3. The future of geotechnical engineering is in the use of the numerical methods with the goal of modeling the soil, the foundation, and the structure all in one model. The use of software's such as SHAKE2000 and FLAC3D V6 is limited.

Based on these, in this study it is intended to use a properly modeled geologic material that is layered and composed of different soil and rock types to represent the true physical replica adequately. The influence of pile raft geometric properties (pile length, diameter, spacing, raft thickness and size) on its performance will be studied and an optimized pile raft configuration will be provided with acceptable design criteria. Besides these, performance of piled raft foundation considering a kinematic soil structure interaction will be investigated and evaluated. These will be performed by a command driven finite difference software called FLAC3D V6.

CHAPTER – 3: MATERIAL AND METHODOLOGY

3.1 Introduction

In general, the two main classes of piled raft foundation for numerical study are under static (only vertical) and dynamic (seismic) loads. This study is conducted by FLAC3D V6, which is a powerful and suitable finite difference based numerical software. Optimized design of PRF by reducing maximum and differential settlement, increasing load sharing of the raft and finally saving economy is the main objective of PRF study under vertical static load. While under dynamic load the general response, performance and the effect of SSI on this foundation are the main concern of the study.

In the Commercial Bank of Ethiopia, extensive geotechnical field and laboratory test had done. Even though some parameters are obtained from correlation and empirical formula, extensive results are directly used for base model. Loads from superstructures is obtained using average of buildings that are close in weight and height to the Commercial Bank of Ethiopia. Earthquake data of Addis Ababa is not directly available but two digital earthquakes have selected based on some criteria and recommendations from EBCS (1995), CES-160-2015 (2015) and literatures. Dynamic analysis of PRF is performed from designed PRF having three by three (3×3) pile configuration, spaced 3m apart. Floating pile and end bearing pile are also analyzed under two different earthquakes having unique PGA and duration. At the end of this study, validation analysis will be conducted from other similar works of literature.

3.2 Description of Study Area

Addis Ababa is located at 9°1′48″N 38°44′24″E and lies at average elevation of 2,355 m above mean sea level. Addis Ababa is the largest city in land size and population density. According to the 2007 census, Addis Ababa has a population of over 3,384,569 (CSA,2007). It is the political, economic and historical capital of both Ethiopian and African. It is also the main seat for numerous national and international organization. The city hosts the headquarters of The African Union (AU), United Nations Economic Commission for Africa (ECA) and other international organizations that initiates construction of huge building and skyscrapers.

The commercial bank of Ethiopia headquarter building is located around Biherawi along Ras Desta Damtew street (Figure 3.1). The building has above 48 floors including 4 basements which is still under construction (2020) since 2015 and costs around 5.3 billion Ethiopian birrs. The main contractor is China State Construction Engineering Corporation consulting by the Ethiopian Construction Design Share Company. The geotechnical and geophysical investigation were done by the Construction Design Share Company and Addis Ababa University Seismology Department. The geotechnical investigation revealed that at shallow depth the predominate soil type is silty clay soil having a high swelling potential. While going deep down the profile consist of sandy clayey silt, weathered rock, medium weathered rock and hard rock. (Emmanuel, 2017; Mahider, 2018; Fisseha, 2019). The ground water table was found at relatively shallow depth (<10 m). This results in a high initial cost for pumping out of water for the construction of foundation and basements.

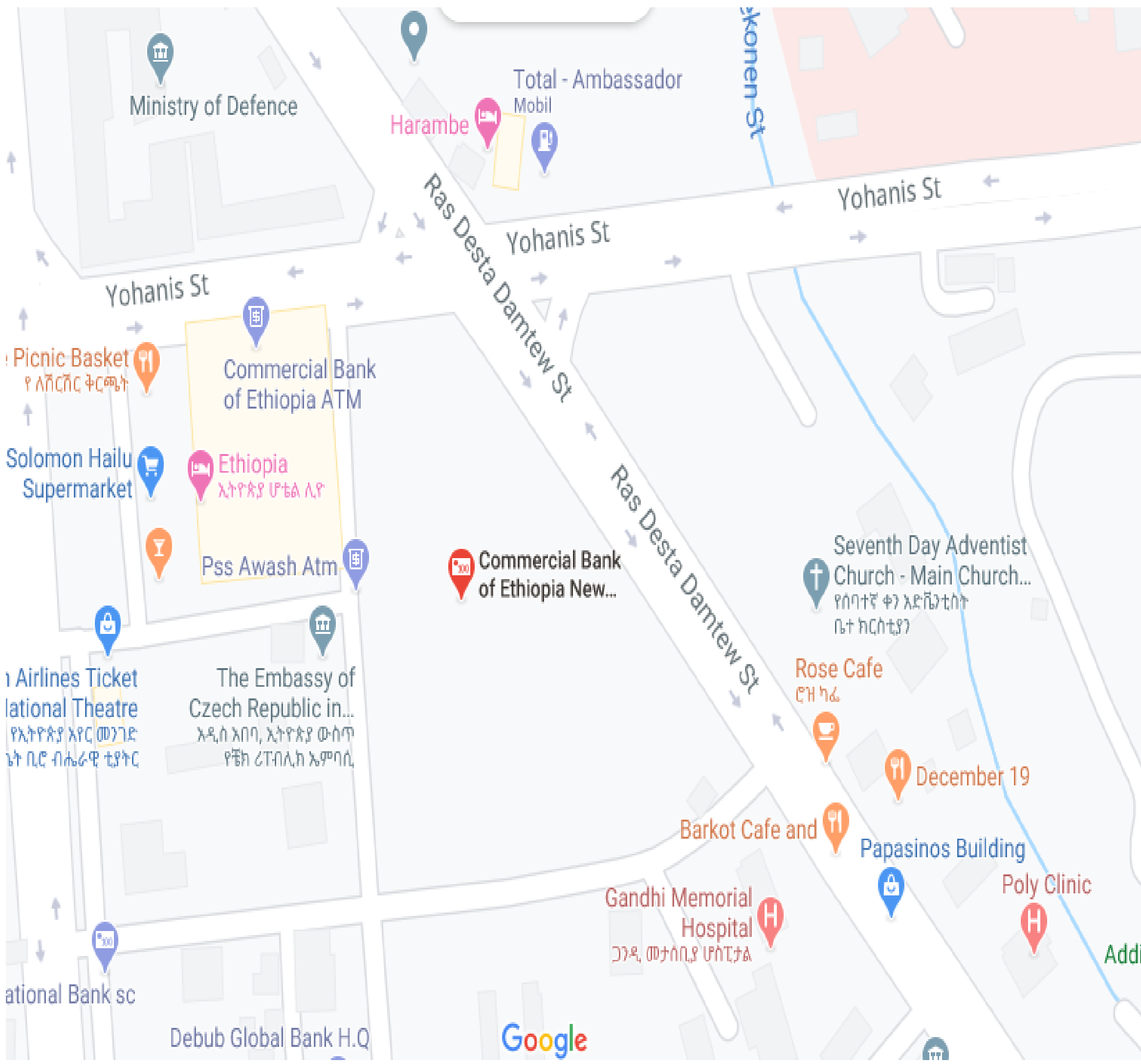

Figure 3.1: Location of commercial bank of Ethiopia headquarter building

3.3 Geologic Conditions and Parameters for Base Model

A wide range of field and laboratory test were conducted in the year 2015 in order to get reliable data and sufficient information about the geotechnical nature of the selected site. A total of 10 bore holes were used to take standard penetration test, unconfined compressive strength (UCS) test of both rock and soil, modulus of elasticity of rock, undrained unconsolidated triaxial test, consolidation test and water test. In this investigation a total of 26 SPT test, 9 UCS for soil, 43 UCS test for rock and 6 moduli of elasticity of rock were conducted in addition to index property test.

The subsurface exploration discovered that the underlying geologic condition is highly stratified consisting of silty clay to hard basaltic rock (Table 3.1). Loose variegated, poorly graded fill material was encountered above 6.5 m while the second layer has 15.5 m with a relatively dense silty clay soil. The third layer is a medium weathered basaltic rock of 6m thickness underlaid by 9 m thick dense silty clay soil with a mixture of scoriaceous basaltic rock. The last layer is located at 47 m below the natural ground level having strong basaltic rock increasing in stiffness with depth. The complete depth range and description of the revealed soil profile are described in Table 3.1 next page. The groundwater table was encountered at an average depth of 6.5 m below the ground level in the majority of the boreholes (BH). This result to high investment for pumping out of the water for the construction of 4 basements.

The stiffness parameters for soil depend on SPT, overburden pressure and other. Hence, the stiffness parameters for soil increase with depth while for rock it is constant throughout depth. The top 22 m is silty clay and it is under layered by a relatively weathered rock of 10 m thick. Equation 3.1 and 3.2 are used to define the stiffness for the top 22 m silty clay soil and the under layered weathered rock consecutively in mega pascal. Therefore, the shear and young modulus will be calculated based on their poisons value and equations written below.

$$E_{top\ 22\ m} = 6.15 + 3.63z - 0.15z^2 + 0.0026z^3 \tag{3.1}$$

$$E_{22-32\ m} = 77.5 + 2.54z - 0.0263z^2 \tag{3.1}$$

Table 3.1: Soil profile stratification under CBE bank headquarter building

Layer	Depth (m)	Description of the layer
1	0-6.5	Loose variegated, poorly graded fill material composed of various proportion of demolished material (concrete, brick), sand silt and clay.
2	6.5-22	Dark brown silty clay
3	22-32	Weak, grey, completely weathered Basalt. Occasionally, fresh or discolored rock is present
4	32-38	Medium strong, grey, intensively fractured and fragmented, slightly to moderately weathered Basalt. Fractured surfaces are rough and yellowish stained. Joints are nearly horizontal and partially filled with altered material.
5	38-47	Weak to strong silty clay consisting of swelling clay with some gravel
6	47-end	Relatively strong rock

Most parameters for a particular constitutive model cannot directly obtained because only limited data are available or the available data are not directly usable for application at hand. The model parameters can be selected based on incorporating the limitation of source test representing the true field condition and influence on the problem at hand. Laboratory tests have the advantage of performing a controlled environment of test with a drawback of representing the true geotechnical condition. Field tests have advantage of representing the true field condition but parameters cannot be directly taken instead they need further processing in some equation (Brinkgreve, 2005).

Several soil parameters that will be used directly in order to model the underlying soil and rock are obtained directly from the investigation report. However, some necessary data are not included in the investigation report. This was tackled from the standard and norms especially the AASTHO 1996. SPT is the most widely used method for measuring relative resistance and the degree of compaction of the soil strata to penetration. This test result has a direct empirical relation with the internal angle of friction, cohesion and Poisson’s ratio for both rock and soil. The modulus of elasticity (for the 1st upper layers) and angle of internal friction (for the last three bottom layers) were determined using correlation relation reported by the 1996 AASHTO standard using Equation 3.3, 3.4 and 3.5. Raw geotechnical data of the commercial bank are attached in **APPENDIX 3A**.

$$E = 400(N_1)_{60} \tag{3.3}$$

$$E = 1200(N_1)_{60} \tag{3.4}$$

$$(N_1)_{60} = CN \times N_{60} \tag{3.5}$$

Where E is the young modulus of the soil; $(N_1)_{60}$ is normalized and standardized corrected blow count and calculated using Equation 3.5 above. CN is correction factor for overburden and it is calculated using Equation 3.6 below. Equation 3.3 is used to get Young's moduli for silty clay soil of the first two upper layers while Equation 3.4 is for highly weathered (Gravel) rock found in third layer. The Poisson's ratio is taken from Bowles (1996).

$$CN = \left[0.77\log10\left(\frac{20}{\sigma_v'}\right)\right] < 2.0 \tag{3.6}$$

Where N_{60} is the N-value corrected for energy efficiency; σ_v' is the vertical effective stress at SPT location in ton per square foot. Putting all the above common empirical correlations for field tests with direct laboratory test results the following parameters are obtained (Table 3.2).

Table 3.2: Soil parameters for base model

Layer	υ (-)	E (MPa)	G (MPa)	K (MPa)	c (kPa)	ϕ (°)	ρ (kgm^{-3})	SPT
1	0.32	Eq. 1	-	-	25.3	19.5	1524	28
2	0.35	Eq. 1	-	-	27	21.3	1743	38.5
3	0.3	Eq. 2	-	-	28	37.4	2359	43
4	0.25	1027	410.80	684.67	5000	40	2626	49
5	0.32	265.5	100.57	245.83	25	35	1871	36
6	0.25	1680	672.00	1120.00	5000	45	2886.7	>50
Conc. C-35	0.15	31,368	13638.26	14937.14	_	_	2500	

3.4 Finite Difference Software, FLAC3D V6

FLAC3D is a three-dimensional explicit Lagrangian finite-difference program for engineering mechanics computation. In order to achieve mathematical model description, general principles such as strain definition and motion laws together with the use of constitutive material equations are implemented in FLAC3D (Itasca, 2017). The resulting mathematical expressions are a set of partial differential equations, relating mechanical (stress) and kinematic (strain rate, velocity) variables, which are to be solved for particular geometries and properties, given specific boundary and initial conditions. Many studies have been conducted using this tool involving a soil structure interaction under seismic and static load, slope stability analysis, shallow and deep foundation analysis, seepage analysis and many days to day engineers and researcher's activity (Lin *et al*.,2016; Akl *et al*., 2014; Rayhani and El Naggar, 2008). Generally, FLAC3D encompass many areas involving, civil, mining, Oil & Gas, Power Generation, Manufacturing and so on.

The equation of motion by applying continuum form of momentum yields Cauchy's equations of motion (Equation 3.7). This law governs the motion of elementary volume when subject by a force. ρ is the mass-per-unit volume of the medium, b is the body force per unit mass, d[v]/dt is the material derivative of the velocity, and $\sigma_{ij,j}$ is the stress tensor. Hence this equation governs the motion of any medium under both static and dynamic forces (Itasca, 2017).

$$\sigma_{ij,j} + \rho b_i = \rho \frac{dv_i}{dt} \tag{3.7}$$

For static analysis of continuum, the equation of motion will be changed in to Equation 3.8.

$$\sigma_{ij,j} + \rho b_i = 0 \tag{3.8}$$

3.5 Selection of Soil Constitutive Mode

A constitutive model is mathematical expression to describe the stress strain relationship of a material for any type of loading condition. A geologic material specially, Soil is a complicated material that behaves non-linearly and often shows anisotropic and time dependent behavior when subjected to different loading types (Ti *et al*., 2009). Generally, when a soil loaded with different stress level it shown completely different property during loading, unloading and reloading time. This initiate modeling of each geologic material to simulate the soil behavior with enough accuracy under different loading condition. For the selection of appropriate constitutive model to simulate the true soil behavior the following are basic but not enough criteria (Lade, 2005):

i. Ability to get the desired parameter
ii. Able to handle 3D condition
iii. Quality of the model to fit with the observed experimental test

iv. Simplicity of the model

The computational geotechnicques has shown a tremendous growth in the implementation of constitutive model, these model ranges from simple (Hook's Law) to a fancy one. Numerous geotechnical commercial software's allow the implementation of such models. However, the fancy models are too complicated to use due to requiring several numbers of parameters which are usually costly to determine in the laboratory and filed tests.

Based on the criterion described above an elastic perfectly plastic Mohr-Coulomb model has selected to model the soil (Figure 3.2). This model is applicable for any type of soil and it can handle 3D conditions. The model requires 5 parameters among these 2 parameters from Hooks law Young's modulus and Poisson's ratio ν that describe the strength. Additionally, two parameters which define the failure criteria are the friction angle ϕ and cohesion c. Dilatancy angle (ψ) is also to used describe the flow rule which comes from the use of non-associated flow rule which is used to model a realistic irreversible change in volume due to shearing (Lade, 2005; Brinkgreve, 2005; Ti *et al.*, 2009; Briaud, 2013). Mohr-Coulomb model was used by different studies including piled raft foundation, slope stability and more giving a satisfactory result.

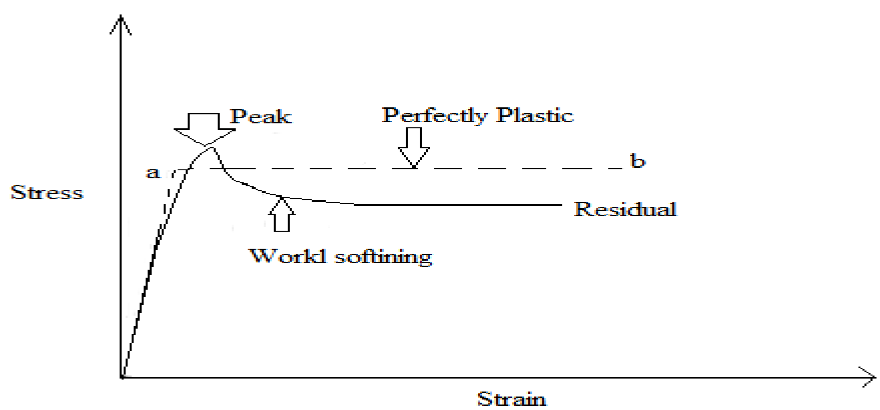

Figure 3.2: Elastic perfectly plastic assumption of Mohr Coulomb mode (Ti *et al.*, 2009)

3.6 Selection of Geometric parameters of PRF

Piled raft foundation is a foundation system in which both structural components (piles and top raft) interact with each other and with the surrounding soil to sustain vertical, lateral or moment loads coming from any sources. The interaction of the three bearing elements (pile, raft and soil) is a three-dimensional problem involving several geometrical, mechanical and interrelating parameters. The geometrical parameters are related to pile geometry (e.g. pile length, diameter, areas, number & spacing) and raft geometry (raft length, breadth and thickness). Whereas, the mechanical properties include the soil properties (e.g. modulus of elasticity, Poisson's ratio etc.) and the interaction parameters can include the various interaction factors (e.g. pile-raft, pile-soil, raft-soil and vice versa) and other derived parameters. This parametric study focuses on the above-listed parameters under gravity loading.

The minimum initial pile spacing is 3D, which fulfills the recommendation of EBCS-7 (1995) for bored piles and common practices (Sinha and Hanna, 2016; Mahider, 2018)**.** Table 2.1 shows the minimum pile length is between 5 m and 10 m in Commercial Bank headquarter building while the maximum length is 28 m in the United Bank building. Hence, pile length taken covers the most widely used ranges in those projects. The minimum pile length taken is 1m which is close to diameters used by United and Nib Banks (0.8 m). In piled raft foundation the pile geometry is important than the raft, so a uniform pile thickness from the average of four projects subjected uniformly distributed load of 926.7 kPa. (Sinha and Hanna, 2016; Reul and Randolph, 2004).

In the parametric study square, unpiled rafts and piled rafts with an edge length of B = 39 m has been considered. Three different pile spacing, three different pile length and three different pile diameters were considered with a combination of each component to twenty-seven different piled raft foundations. The selection of piled raft geometry is taken from the average of buildings listed in Table 2.1 with fulfilling some common regulation and common practices. Hence, the geometric nature of the piled raft foundation that will be under numerical investigation is summarized in Table 3.3 below.

Table 3.3: Summary of parametric values for numerical study of PRF

Parameters	Unit	1st trial	2nd trial	3rd trial
Raft Plane (B×L)	m×m	39 ×39	39 ×39	39 ×39
Raft thickness	m	3	3	3
pile length	m	10	15	20
pile diameter	m	1	1.5	2
pile spacing	m	3D	5D	7D

3.7 Simulation of Single Pile Capacity

The pile installation method employed was bored and cast in place type. The pile capacity for axial load can be approximately calculated using analysis method driven from empirical formulas which depend on the soil type, the method of installation, the pile type and other. Considering this, it is possible to determine the pile capacity approximately and subsequent simulation on FLAC3D V6 is possible. The following formula are obtained from different literatures that are used to calculate the pile capacity under different soil conditions. A pile transfer load from superstructure in two mechanisms skin friction and tip resistance.

The skin friction involves transferring force through the rough surface of pile in cohesionless soil and the cohesion between the pile and surrounding soil in cohesive soil. Skin friction can be calculated from both effective and total stress. But the effective stress analysis of pile capacity is usually recommended since it is useful to include the future capacity. Different methods are available to calculate the pile capacity. Among these α, β and λ methods are the common. Equation 3.9 is used for clay and sandy soils under effective and total stress analysis (Bowles, 1996).

$$Q_S = \sum_1^n A_s f_s \tag{3.9}$$

where A_s = effective pile surface area on which f_s acts; $f_s$is the shear stress capacity along the pile shaft which depend mainly on the unconfined shear strength of the soil (f_s) for fine grained soils. The shear stress f_s of bored and cast in place pile on weathered and coarse-grained soil is calculated using the correlation with standard penetration test in Equation 3.10 (Yamashita *et al.*,1987).

$$\mathrm{f_s} = \mathrm{A1} + \mathrm{B1N} \leq 200\mathrm{kPa} \tag{3.10}$$

Where A1 = 20; B1 $= 2\mathrm{N} = 72$. Since the soil is highly weathered rock taking $\mathrm{f_s} = 200\mathrm{kPa}$ using this equation for a pile of length 10 m and diameter of 1m the surface area $A_S = \pi DL = 31.4\ m^2$. The total skin resistance of the pile $\mathrm{Q_s} = \mathrm{A_s f_s} = 6280$ kN. The tip resistance of this pile is calculated from the unconfined compressive strength of the bedrock. Goodman *et al*., 1980 in 1980's proposed in Equation 3.11 bearing capacity a pile standing on a rock.

$$\mathrm{q_p} = \mathrm{q_{u(deisgn)}}(\mathrm{N_\phi} + 1) \tag{3.11}$$

Where $N_\phi = tan^2(45 + \phi'/2) = 4.11$, $\mathrm{q_{u(deisgn)}} = 37.8/5 = 7.56\mathrm{MPa}$ is the design unconfined compressive strength of the rock and it is laboratory result divided by a factor of five, $\phi' = 37.4°$ is drained angle of internal friction of rock. Using the Goodman *et al*. (1980) formula, the end resistance of pile ($\mathrm{Q_b}$) is 30.3MN. Using a factor of five to account for discontinuity in the rock mass the allowable end resistance is 6.06MN. The total load capacity using a factor of three for the skin (Fisseha, 1996; GEO, 2006) resistance is 8.15MN.

The bearing behavior of a single pile is modeled using a brick and structural pile element for soil and pile simulation respectively. The interface between pile, the surrounding soil and the base rock have both cohesive and frictional nature. These properties are called the shear and normal coupling spring. The shear coupling spring consists of the shear spring stiffness (K_s), shear direction friction angle ($\emptyset'_s = tan^{-1}[(2/3) \times tan\emptyset']$) and shear direction cohesion ($c'_s = 2/3c'$). The normal spring stiffness (K_n), normal direction friction angle ($\emptyset'_n = tan^{-1}[(2/3) \times tan\emptyset']$), normal direction cohesion ($c'_n = 0.9c'$) are used to model the interface in the direction to normal to the pile periphery. The above interface parameters are determined through a parametric study (trial and error) until the required bearing capacity and allowable settlement is achieved. Different study indicates that the interface parameters for initial simulation can be approximated instead of initial assumptions (Lin et al, 2016; Itasca, 2017; Hokmabadi, 2014). While the shear and normal spring stiffness (K_n, K_s) are approximated in Equation 3.12 below.

$$K_s = K_n = (10 - 100) \times \left[\frac{K + \frac{4}{6}G}{\Delta Z_{min}}\right] \tag{3.12}$$

Where, K and G are bulk and shear modulus of neighboring zone, respectively, and ΔZ_{min} is the smallest width of an adjoining zone in the normal direction. Substituting bulk modulus (K) 11.2 GPa, shear modulus (G) 13.64 GPa, and a minimum grid size of (ΔZ_{min}) 0.5 m the shear and normal spring stiffness is 428.6 GPa/m using a factor of 10. The other parameters simulating the pile soil interface are listed in the Table 3.4 below. The variation of the above interface parameters will be varied until 1% and 10% of the pile diameter is mobilized for shaft and end resistance respectively (Orr & Farrell, 2012). Considering the above criteria, the following Figure 3.3 shows the simulation result. The coding sequence for simulation of this single pile is attached in the **APPENDIX 3B**.

Table 3.4: Input initial and final parameters to model the soil pile interaction

Description	Unit	Initial parameter	Final parameter
Normal direction cohesion (c'_n)	kPa	0.9×28 =25.2	30
Shear direction cohesion (c'_s)	kPa	2/3×28 = 16.7	20
Shear direction friction angle ($\emptyset'_s$)	°	27	30
Normal direction friction angle ($\emptyset'_n$)	°	27	30
Shear spring stiffness (K_s,)	Pa/m	4.28×10^{11}	8×10^{11}
Normal spring stiffness (K_n,)	Pa/m	4.28×10^{11}	8×10^{11}
Minimum grid size (ΔZ_{min})	m	0.5	0.5

Table 3.4 outlines the final coupling normal and shear stiffness parameters after several tri and error. These parameters are cohesion, friction and stiffness in the normal and shear direction of the pile. End bearing and friction capacity are appreciably simulated to be further used in the succeeding topics. These interface parameters will be used to simulate any pile in the PRF for further geometric parametric study. The figure 3.3 below depict the simulation result of single pile for 10 mm of pile diameter displaced.

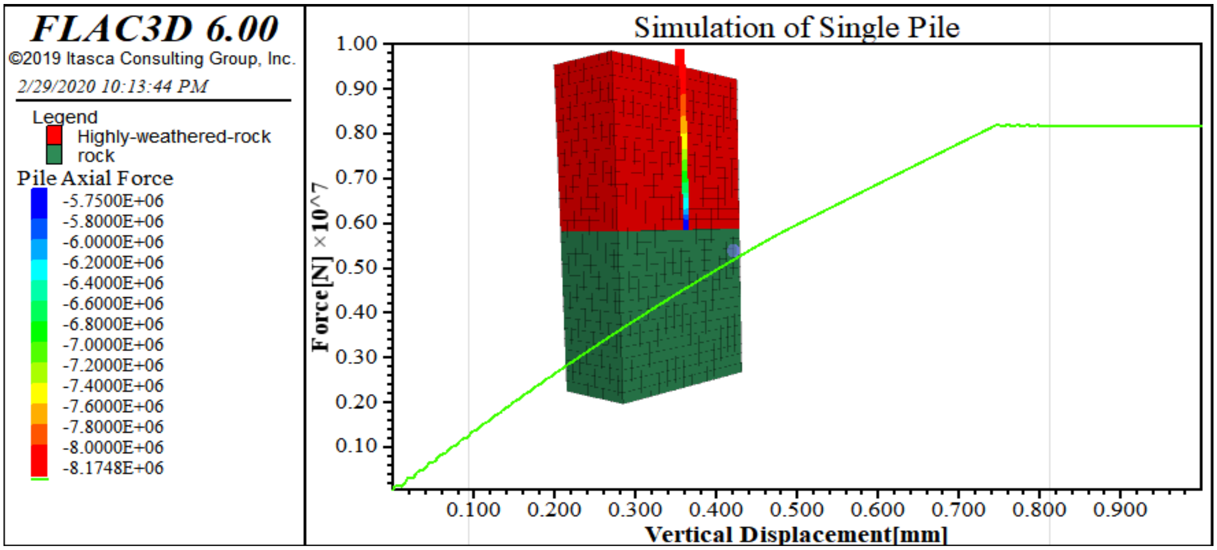

Figure 3.3: Plot of force displacement for a single pile having end and frictional resistance

3.8 Static Analysis Procedure

In this finite difference analysis, the soil and rock are modeled as eight nodded brick elements including wedge shaped meshes. The long-term behavior of the geologic condition was taken since the water was pumped out before installation of pile, higher static vertical load results in the expulsion of water from the pores of the soil medium. To compare the performance and influence of piles, an analysis of the raft foundation has performed. The result of the numerical solution depends on the reproducing true in-situ stress condition and general procedure for the construction of PRF. Figure 3.4 shows the procedure used for the simulation of all twenty-seven piled raft foundations under vertical static load.

The ratio of the horizontal (in the two orthogonal directions) to the vertical effective stress ratio cab be approximately expressed in terms of effective angle of friction by Jaky’s formula. Equation 3.13 was derived in a more elaborate form by Jaky (1944) from an analysis of the stress field in a wedge prism of a loose granular material. It is a good approximation for normally consolidate clay, granular materials that are not previously densified by vibration (Michalowski, 2005; Mesri & Hayat, 1993). At rest earth pressure coefficient of Jaky will be used to calculate horizontal pressure for each layer.

$$K_o = 1 - \sin\phi' \tag{3.13}$$

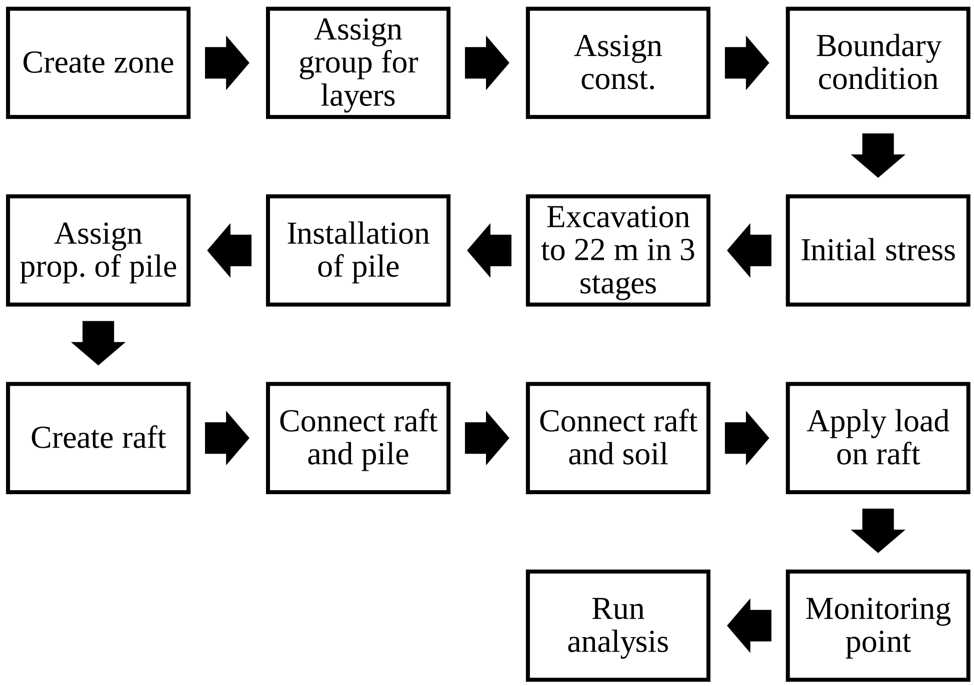

Figure 3.4: Static analysis procedure analysis for parametric study

3.9 Selection of Strong Ground Motion

Nonlinear dynamic analysis is usually done for seismic prone area and a civil structure that is very complex and having high importance in terms of economy or culture. This detailed nonlinear analysis requires the use of real accelerogram that may be obtained easily from different sources. Acceleration time history (ATH) can be made available or made synthetic from three alternatives;

1. Artificial spectrum-compatible accelerograms,
2. Synthetic accelerograms by accounting path and site effect,
3. Real earthquake records from different sources (Bommer, 2004).

In this particular study it is intended to use a real earth accelerogram record during earthquake occurrence for full dynamic analysis of PRF. This can be obtained USGS (United States Geological Survey) which has collection of over 1500, National Geophysical Data Center (NGDC) and the PEER databank which includes 1557 record are some. Real Earthquake record can be made useful from estimation of some key features of ground motion. The geographical location of the site, expected magnitude, source distance and expected duration are some. Selection of real accelerogram record may contain some or all-of the following criteria:

- Expected magnitude (Mw)
- Source distance (R)100Km
- Soil class (S) (depends usually on Vs,30)
- Duration(T)
- Peak ground acceleration
- Focal depth

In Ethiopia, specially Addis Ababa different study were conducted focusing on the seismicity and amplification character of the site. This study indicate that the expected magnitude of earthquake is between 6 to 8 (Yoseph and Ramana 2008). The source distance of 100km from Addis Ababa and soil class of C and D based on the shear wave velocity of the top 30m is common (Emmanuel 2017; Gouine 1978). EBCS 1995 recommend a peak ground acceleration between 0.g1 and 0.2g having a duration greater than 10 sec is common (EBCS 1995; Yoseph and Ramana 2008). The focal depth of the source earthquake is between 8 m to 14 m is found in recent studies (Keir *et al.*, 2006). It is also usual to use accelerogram which matches the site shear wave velocity. Among the above listed earthquake parameters, in dynamic analysis of geotechnical structures different scholars use the magnitude (Mw) and peak ground acceleration (PGA) main criteria for the selection of the appropriate acceleration time history (Assefa *et al.*, 2017; Chatterjee *et al.*, 2015). Assefa *et al.* (2017) in the dynamic slope stability of a railway embankment along the Kombolcha hara gebeya rail road, the 1940 El Centro earthquake having Mw of 6.7 were used by scaling to 0.3g peak ground acceleration.

The 1940 El Centro earthquake, which happened at 21:35 Pacific Standard Time on May 18 in California near the border of Mexico and USA. This earthquake has a moment magnitude of 6.7 and a maximum perceived intensity of X (Extreme) on the Mercalli intensity scale. It is the first earthquake event to be recorded by strong ground motion seismograph and cased death of nine peoples and widespread damage to irrigation systems. As shown in Figure 3.5 this earthquake has a peak ground acceleration of 2.8 m/sec^2 and duration of 53 sec (Ahmad and Najar, 2016). The site condition is specified by the average shear wave velocity of the top 30m. The site condition of California is in the range of C and D with average shear wave velocity of 191m/sec (Tso and Hsu, 1978; Wills and Silva, 1998). Hence, this earthquake is selected for this study.

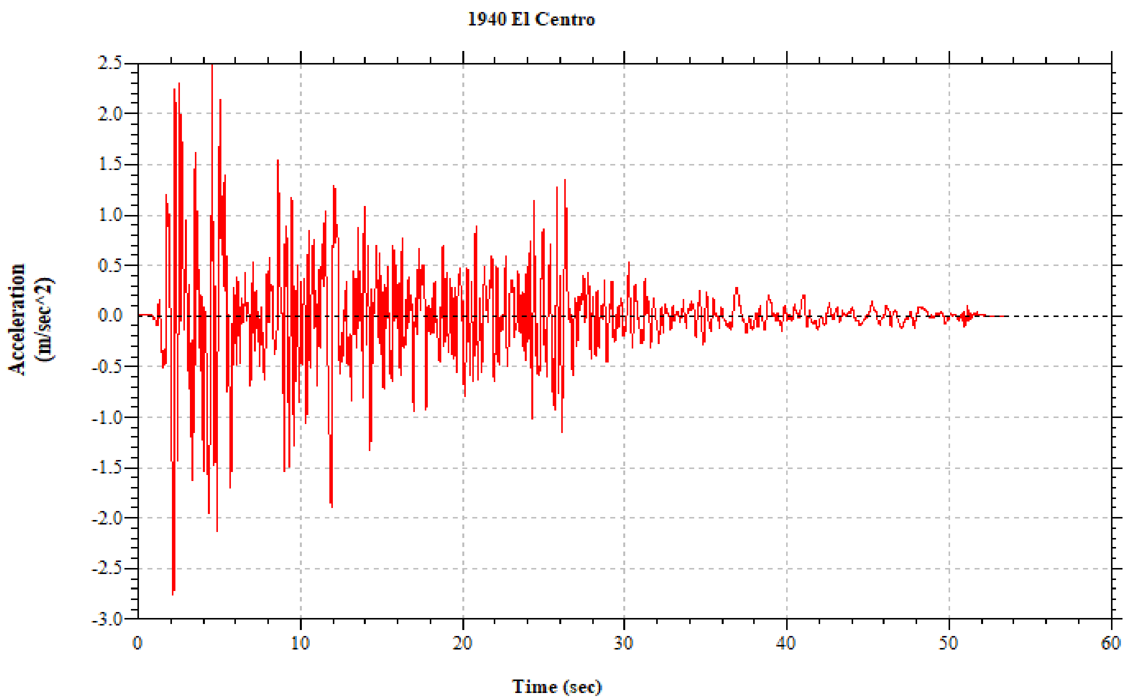

Figure 3.5: Acceleration time history of the 1940 El Centro Earthquake (PEER, 2014)

3.10 Estimation of Dynamic Soil Property

Dynamic soil properties are useful in order to completely describe the response of soil under dynamic loading. The main dynamic property of a geomaterial are the shear modulus and damping ration for a specified strain level. As it was previously explained in chapter two of the literature review the shear moduli and damping of soil depends on the strain level. The backbone curve for silty clay soil and rock needs estimation of the shear moduli at the origin. This means the shear modulus at zero shear strain level which is maximum. After estimating this soil and rock parameter the shear modulus reduction factor (G/G_{max}) and damping ratio (ξ) versus shear strain (ϒ) will be governed by the graph 3.7 (Ordonez, 2000) below. Dynamic shear moduli of soils are computed at strain level of less than or equal to 10^{-6}. Ohta and Goto (1976) conducted numerous field shear wave velocity test and they presented empirical formula to estimate the shear wave velocity of any soil type (Equation 3.14). This equation will be used to estimate the shear wave velocity of upper two layer which in turn is useful to calculate dynamic shear moduli based on Equation 3.14 (Seed *et al*., 1986). The third layer (22 to 32m) is a relatively weathered basalt and the maximum shear moduli is calculated using the shear wave velocity of 1 km/sec using the Equation 3.15 (the shear wave velocity for rock is usually greater than 1000 m/sec but to reduce effect of discontinuity and approximation) (Ordonez, 2000). The back bone curve for silty clay soil and rock are shown in the Figure 3.7. This curve is used for estimation of the Rayleigh damping parameters by SHAKE2000 (Assefa *et al.*, 2017; Mejia & Dawson 2006). The strain-compatible shear modulus and damping ratio parameters for each specific layer under investigation are determined using SHAKE 2000 (Assefa *et al.*, 2017).

$$v_s = 69{N_{60}}^{0.17} D^{0.2} \times F_1 \times F_2 \tag{3.14}$$

Where v_s is the shear wave velocity in m/s; D is depth of the soil below the ground surface; F_1depends on the soil type and is 1 for alluvial deposits; F_2 also depend on the soil type and it is 1.1 for silty clay soil (Seed *et al.*, 1986). Furthermore, the maximum dynamic moduli (G_{max})are calculated from the Equation 3.15 given below (Kramer, 1996). Substituting the above parameters, the shear wave velocity (v_s) for the first and second silty clay soil are $204\ \mathrm{m/s}$ and $275\ \mathrm{m/s}$ respectively.

$$G_{max} = \rho V_s^2 \tag{3.15}$$

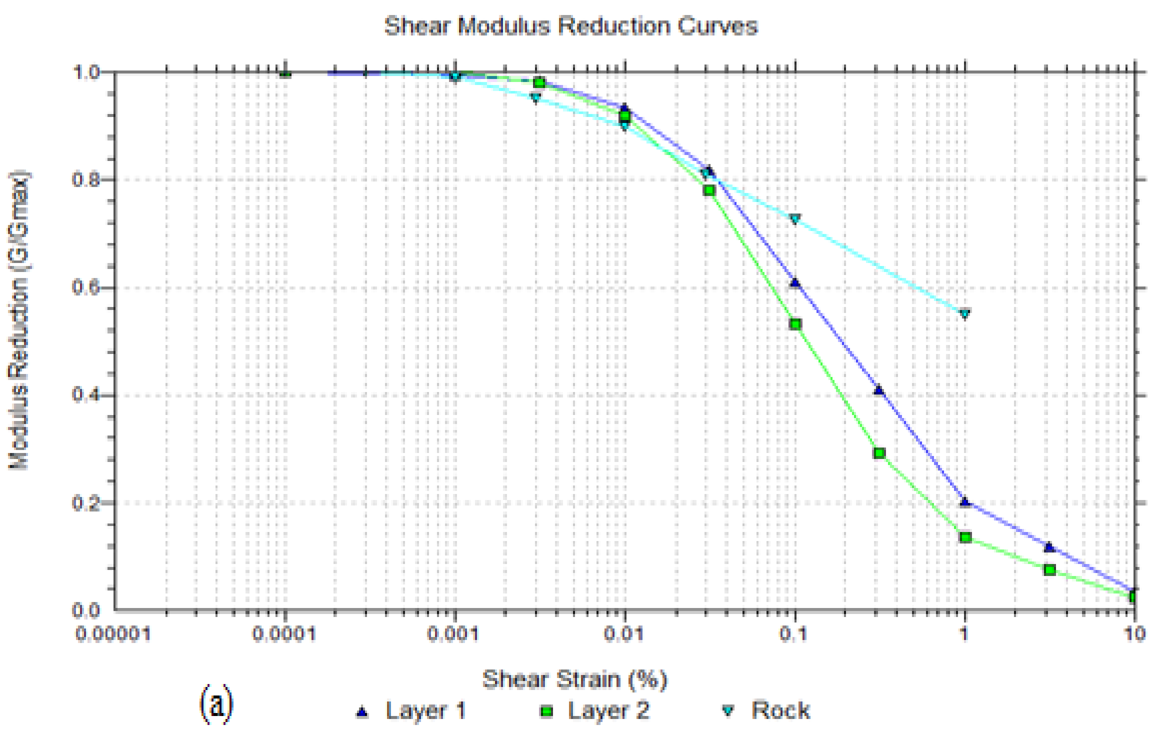

(a)

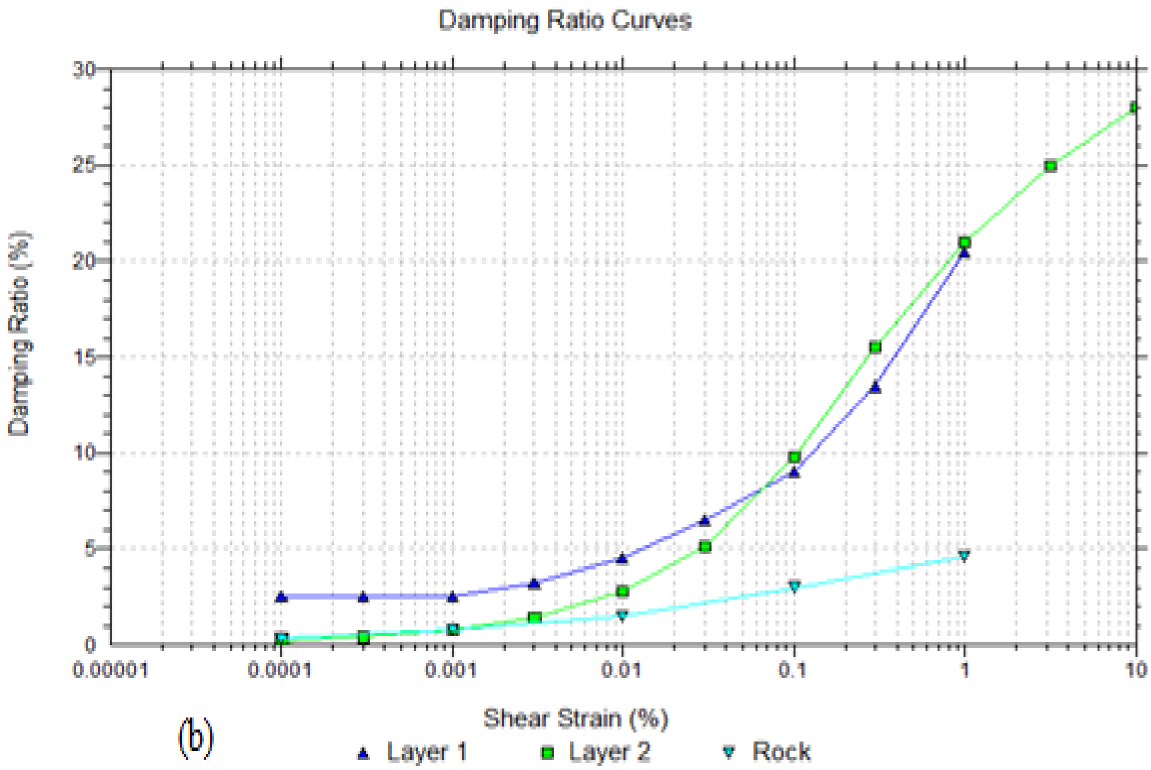

Figure 3.7: Modulus reduction (a) and damping ratio curve (b) of 3 layers (Ordonez, 2000)

Most of the dynamic study and evaluation of geotechnical structure recommend to incorporate the top 30m of the geology. This is due to the fact that any amplification or attenuation of dynamic events occur in this range of depth (EBCS-8, 1995; Xu & Fatahi, 2019; Hokmabadi *et al.*,2014). The inelastic cyclic behavior of the soil and rock is simulated using Rayleigh parameters from SHAKE2000 results. For this 1D analysis of geotechnical earthquake engineering software a free filed column is created having three different soil layers with specific shear moduli, shear wave and density. The thickness of each layer in SHAKE2000 can be in the range of 1.5 m at the surface to 15.25 m below 30 m. Keeping this rule the first layer is divided in two, second layer also divided in to four and one bottom layer (Half Space). The ratio of the equivalent uniform strain to maximum strain was kept 0.5 as recommended by Itasca (2017). The outputs are used to simulate the behavior of cyclically loaded soil and rock in the FLAC3D V6 model. The results SHAKE2000 analysis is shown in the Table 3.5 below.

Table 3.5: Strain compatible damping and shear moduli reduction for the top 30m (Result of SHAKE2000)

Thickness	Uniform strain	Damping (%)	G/Gmax
3.25	0.016	5.4	0.896
3.25	0.055	7.8	0.883
3.875	0.046	7.4	0.58
3.875	0.0792	8.7	0.658
3.875	0.113	9.7	0.78
3.875	0.139	10.5	0.896
8 (Half space)	0.782	9.74	0.924

The weighted average damping and modulus reduction factor are 8.71% and 0.81 respectively. the common damping factor for geologically material is usually 5% which is less that the results obtained from SHAKE2000 analysis (Briaud, 2013; Kramer, 1996). In order not to overestimate the damping and reduce some errors for modeling and approximation 5% damping is employed. While the moduli reduction factor obtained from the result will be directly used. The shear moduli of each layer will be reduced by a factor of 8.1%.

3.11 Deconvolution of Input Earthquakes

Strong ground motions that are recorded during seismic events are situated at the ground surface. These records describe about the ground surface motion during the incident while the rock motion is unknown. There are different available tools (SHAKE2000 and FLAC3D V.6) which can help to estimate the motion at the rock level. A method of reverse process of estimating the rock motion from the observed ground motion is called Deconvolution. This is a very important technique for dynamic numerical simulations that feed the input motion at the base of model like FLAC3D. This technique is employed for this study and its process is described in the subsequent articles.

The target motion is usually given at the ground surface (for this case $3\ m/sec^2$ and $1.5\ m/sec^2$ peak ground acceleration). If this record is used directly as input motion at the base of the model it will result higher acceleration time history and erroneous result due to amplification or attenuation. The input motion at the quite base can be approximately taken half of the target motion (Mejia & Dawson, 2006; Assefa *et al.*, 2017). But for this study the input motion for the compliant base is directly estimated from the deconvolution analysis by SHAKE2000. Three layers are further subdivided in to several layers resulting in to seven layers. The target earthquake motion (two scaled El Centro earthquake) are applied at the first layer (surface) as outcropping motion. The acceleration time history at rock level are estimated by specifying the output to within the profile mode at the rock in the seventh layer. The deconvolution analysis by a 1-D wave propagation equivalent linear program code, SHAKE2000 is shown in the Figure 3.8.

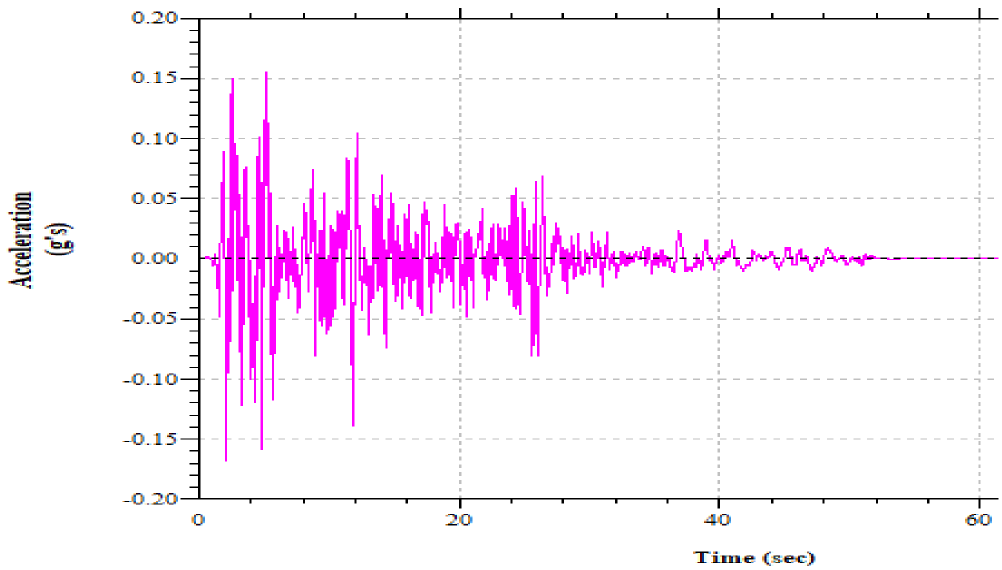

Figure 3.8: Deconvolution analysis result of El Centro Earthquake's

The natural frequency of piled raft foundation having n piles is calculated using Equation 3.16 (Kang *et al*., 2012; Kumar *et al*., 2016).

$$\omega_{PRF} = \sqrt{\frac{nk}{m_{raft}}} \tag{3.16}$$

Where k is flexural stiffness of pile and it is calculated using Equation 3.17; n is the number of piles and m_{raft} is the mass of the raft (Kang *et al*., 2012).

$$k = \frac{EI}{l^3} \tag{3.17}$$

Where E is the Young's modulus (31.37 GPa); I is the second moment of area (0.0064 m^2) and *l* the length of the pile (10 m for friction pile and 30 m for end bearing pile). Therefore, the natural frequency of piled raft foundation having 9 piles is calculated using Equation 3.18. The natural frequency of the pile raft foundation for friction and end bearing pile are 4.2 Hz and

0.812 Hz consecutively. These frequency's will be useful in order to evaluate the occurrence of resonance.

$$\omega_{PRF} = 3\sqrt{\frac{EI}{m_{raft}l^3}} \tag{3.18}$$

3.12 Processing of Strong Ground Motion

The results from deconvolution analysis result from shake have a PGA of $1.8\,m/sec^2$ and $1\,m/sec^2$ for $3\,m/sec^2$ and $1.5\,m/sec^2$ peak ground acceleration of El Centro earthquakes respectively. These ATH will be applied at the base of the model after performing a ground motion processing. Ground motion processing is processing a raw accelerogram data to remove high-frequency noise and instruments effects and it involves filtering and baseline correction. Applying this ATH having higher frequency content without filtering may require a very fine mesh and this leads higher computational effort. Since most of the energy are stored in the lower frequency contents, removing higher frequency content without affecting the predominant frequency of the motion will result in coarser meshes. A Fast Fourier Transform employed by the dynamic input wizard of FLAC3D will be used to convert and ATH to power spectrum. Hence, it is possible to identify the dominant frequency and specify the limit beyond which frequency is to be removed. Acceleration response spectrum plot of the 1940 El Centro shows that the dominant frequency is 2 Hz with highest frequency contents less than 10 Hz and majority of them below 8 Hz. A Butterworth-type low-pass filter with a cutoff frequency of 8 Hz is applied to remove the frequency components above 8 Hz. The resulting filtered and unfiltered response spectrum are shown in the Figure 3.9 in red and green colors respectively.

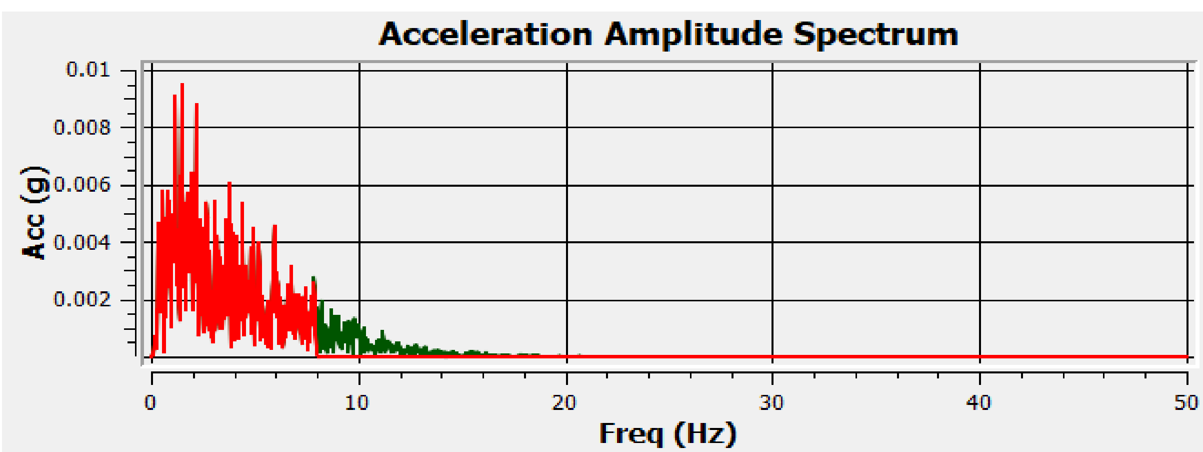

Figure 3.9: Plot of filtered and unfiltered power spectrum for 1940 El Centro earthquake

Strong ground motions record available from different sources are of great interest for engineers dealing with seismic problems. Unfortunately, experience indicates that the digital recordings are often plagued by what we call baseline offsets: small steps or distortions in the reference level of motion (Boore *et al.*, 2002). This offset in the acceleration time series; upon integration, linear and quadratic trends observed in the velocity and displacement time series, respectively. The main reason for this baseline offset is incapability of the accelerograph to differentiate translational and rotational motion. Accelerographs are capable of recording translational motions, hence rotational motions are recorded as a fake translational motion leading to small baseline drift (Boore *et al.*, 2002; Melgar *et al.*, 2013). A direct use of an acceleration or velocity record outcomes the numerical model to exhibit continuing velocity or residual displacements after the motion has finished. This can be solved using the built-in dynamic input wizard of FLAC3D thus, the final displacement of the result become zero. The 1940 El Centro; upon double integration has a final drift in displacement of 1.02 cm. This is removed by applying a polynomial function of degree one without affecting the overall shape as shown in the Figure 3.11. Green color indicates baseline corrected while the red one indicate uncorrected displacement plot of the 1940 El Centro earthquake (Figure 3.11).

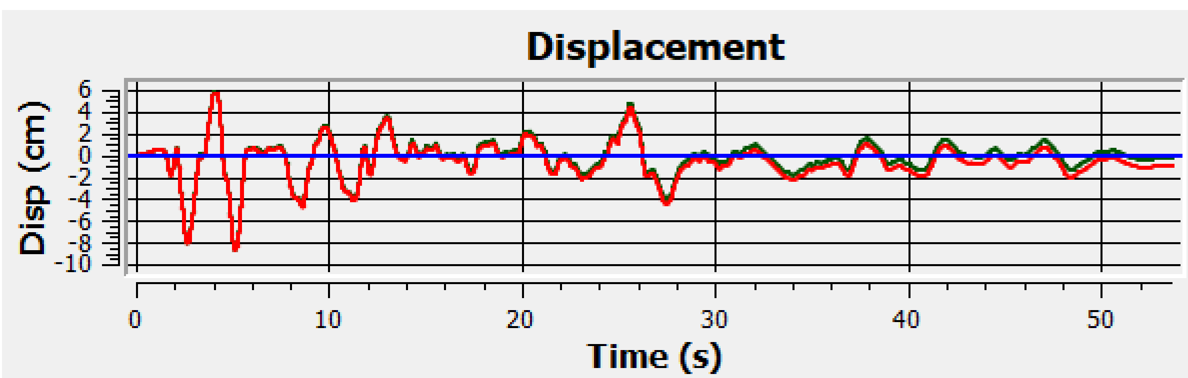

Figure 3.11: Baseline corrected and uncorrected plot of the 1940 El Centro earthquake

Appropriate wave propagation through an element is possible when the maximum zone size $\Delta X, \Delta Y, \Delta Z$ are smaller than one-tenth to one-eighth of the wave length, λ (Kuhlemeyer and Lysmer 1973). The highest frequency of the 1940 El Centro earthquake is 8 Hz; the lowest shear wave velocity is $204\ \mathrm{m/s}$ corresponding to the first layer. Taking these parameters, the shortest wavelength is 25.5 m (Equation 3.19). Therefore, the maximum zone size which allow smooth wave propagation without crumbling the elements is 3.2 m. This method of mesh size determination was employed by different studies including Berhe *et al*. (2010) and Assefa *et al.* (2017). Hence, the maximum zone size that will be employed for this numerical dynamic analysis will be 3.2 m.

$$\lambda = \frac{c_s}{f} \tag{3.19}$$

3.13 Determination of Interface Parameters

An interface is a connection between subgrids that can separate (e.g., slide or open) during the calculation process. Interfaces in FLAC3D are collections of triangular interface elements, each of which is defined by three interface nodes. Interface elements are attached to a zone boundary through interface nodes. As shown in the Figure 3.12 the interface constitutive model is defined by a linear elastic-perfectly plastic Coulomb shear strength criterion that limits the shear force acting at an interface node, normal and shear stiffnesses (K_n and K_s), tensile and shear bond strengths (T_s and s_s), and a dilation angle (ψ) that causes an increase in effective normal force on the target face after the shear-strength limit is reached(Itasca, 2017).

In this study a total of three interface zones are required between different material having distinct physical property. These are between pile shaft and the surrounding soil; pile end and the bottom soil; raft bottom with the underlaying soil. However, for pile foundation the interface element is not applied between the raft and the underlying soil since it is assumed the load transfer between raft and soil is considered insignificant while in piled raft it is mandatory. The relative interface movement is controlled by interface stiffness values in the normal K_n and tangential K_s directions.

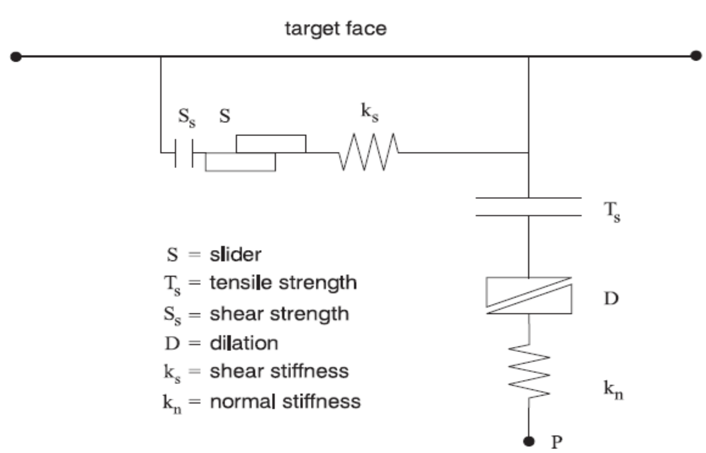

Figure 3.12: Components of the interface element (Itasca, 2017)

The normal and shear direction stiffnesses are determined using Equation 3.12 based on the recommendation of Itasca Consulting Group (2017) and Rayhani & El Naggar (2008). Using Equation 3.12 the relative shear and normal stiffness value both pile-skin and pile-end is 1651.6 GPa. The interface between raft and soil (raft-soil) has 330.3 GPa shear and normal stiffness (Figure 3.13). Furthermore, the tensile strength is set to be zero in order to allow some gaping and slide between different material models (Itasca, 2017).

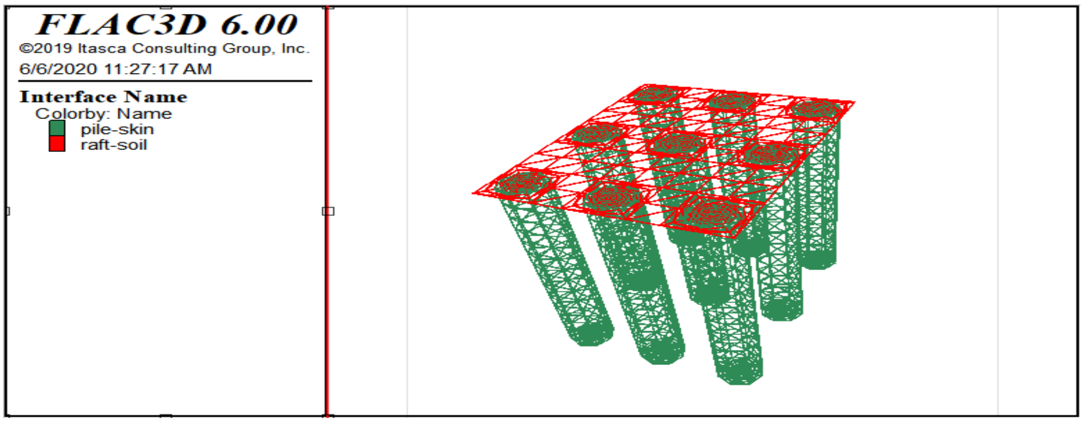

Figure 3.13: Interface modeled between pile-soil and raft-soil

3.14 Boundary Condition and Size for Seismic Analysis

In static analysis of geotechnical structural analysis, the boundary condition can be placed a certain distance from a region of interest using sensitivity analysis. In dynamic analysis using finite boundary size causes reflection of propagating wave and it also prohibit radiation of energy. In order to remove such problems two solutions are available. These are quite (Viscous) and Free-filed boundary condition. The former uses independent dashpot in the normal and shear direction to absorb energy. This boundary condition is only used when the dynamic source is within the grid of the model. Free-field boundary is useful to account the effect of free filed which exist when piled raft foundation is absent (Figure 3.14). This boundary condition is used when the dynamic source is from external source or at the boundary of the model. This system of boundary condition involves the execution of free-field calculations in parallel with the main-grid analysis. Therefore, free-field boundary condition is applied at the lateral boundary while fixed base boundary is used at the base of the model to simulate the underlying bedrock.

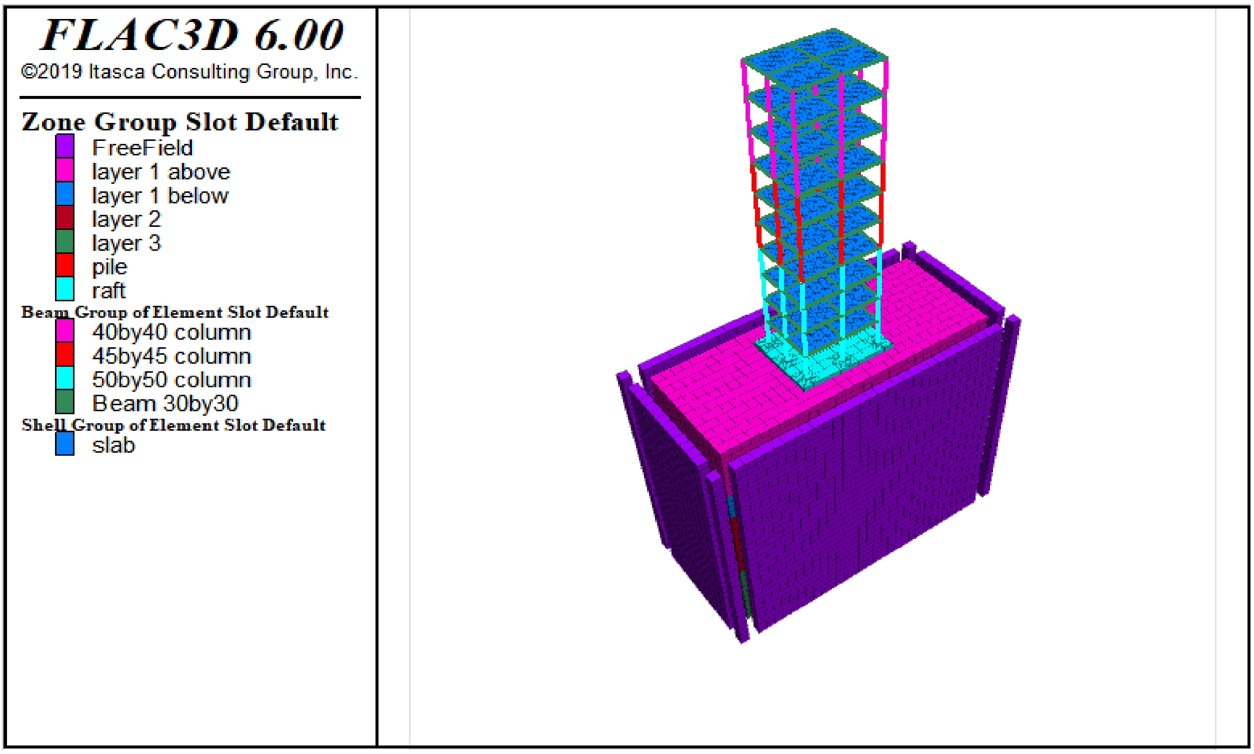

Figure 3.14: Free-filed boundary applied for seismic analysis of PRF

The boundary size to be employed for dynamic analysis is usually dependent on computational effort and reflection of propagating waves. A maximum depth of 30m bedrock is usually recommended by different study and codes (EBCS, 1995; Hokmabadi *et al.*, 2015;). This is because of most of the amplification and attenuation of seismic wave happens in the top 30m. The lateral size in the shaking direction is greater than three times the foundation size. Therefore, 30m total lateral size is employed in the shaking direction (Y-axis).

3.15 Seismic Analysis Procedure

Some major procedural issues are addressed in the previous sub-topics and some are to be explained in this subsection. Mesh size, boundary size, filtration and deconvolution of earthquakes are first done in the previous sub-sections. The procedures that are displayed in Figure 3.15 are only to show the coding sequence used. The major part of the procedures that are essential input for this seismic analysis are described in the previous section.

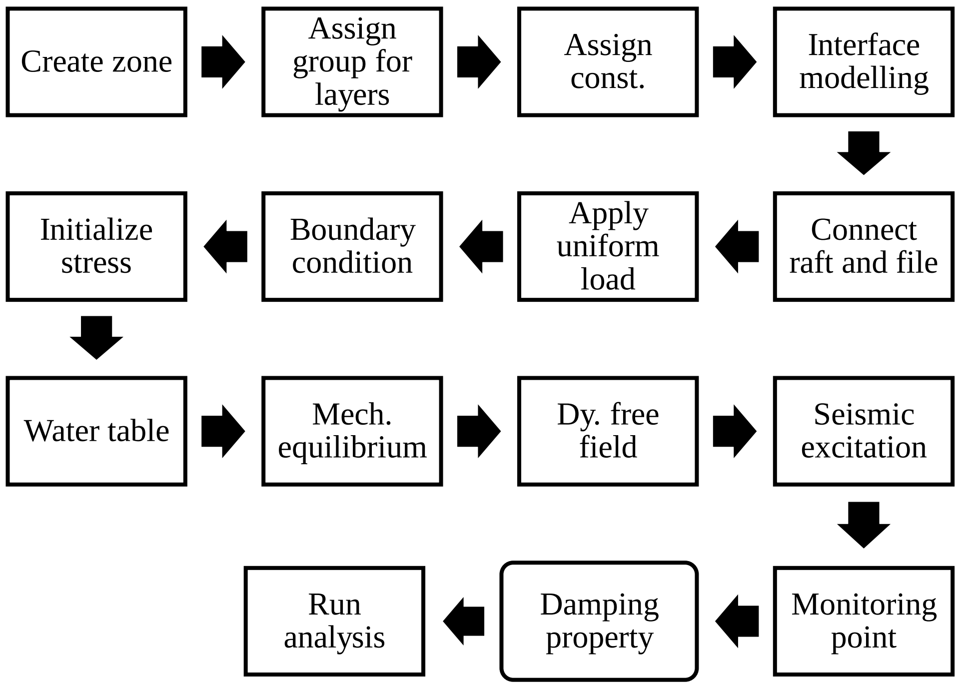

Figure 3.15: Procedure for seismic analysis of PRF

CHAPTER – 4: RESULTS AND DISCUSSIONS

4.1 Introduction

The result of the studies is divided into vertically static and Seismic analysis and these are discussed in detail. The static analysis result focuses mainly on the differential settlement, total settlement and load sharing between pile and raft. Thus, help to select the optimum configuration of piles fulfilling the design requirements. The Seismic analysis result focuses on attenuation or amplification, pile head displacement, settlement of PRF and finally the effect of different PGA on the acceleration record at the top of the raft.

4.2 Parametric Study of PRF Under Vertical Static Load

The parametric study includes a twenty-eight piled raft configuration. These include three different pile lengths, three different pile diameter, three different pile spacing and finally one unpiled raft. The main aim of this pile raft configuration is an investigation of the response of different pile geometric positioning under the raft. The magnitude of the superstructure load is represented by a distributed load on the surface of the raft. This lumped mass of the superstructure on the foundation method was previously used by Reul & Randolph in 2004, Sinha and Hanna in 2016, Fisseha in 2019 and others.

In this numerical parametric study, the soil is modeled using the hexahedral element (brick) and pile and raft are models using a structural element of pile and shell respectively. The number of piles will vary hence depends on the available space on the raft. Due to the bisymmetric nature of the piled raft foundation (square) quarter of the foundation will be taken to reduce very high computational effort.

4.1.4 Sensitivity Analysis and Grid Independency Test

Sensitivity analysis is a useful parametric study to obtain the optimum boundary size, mesh size and mesh quality. The finite number of mesh and distance of boundary from the piled raft will influence the results. To investigate the influence of the above-listed condition on a settlement, bearing capacity and load sharing of PRF a sensitivity analysis will be conducted while keeping the material property constant.

Considering the above conditions four different boundary sizes and mesh quality are investigated and their influence is studied in detail. The settlement at the center and edge, an axial load of the pile at the center and edge and lateral load at the center and edge were investigated. Depending on the result a boundary size of $50 \times 50 \times 60$ m ($length \times width \times depth$) and 142,800 number of zones were selected for further parametric study under vertical loading (Table 4.1 and Table 4.2). This selection has a very good aspect ratio (> 0.7), volume ratio (> 0.9), orthogonality (> 0.7). Therefore, further parametric study will be valid and results will not be highly influenced by the selected mesh fineness, mesh quality and boundary size (Figure 4.1). The coding sequence of sensitivity analysis of piled raft under vertical load is attached in **APPENDIX 4A.**

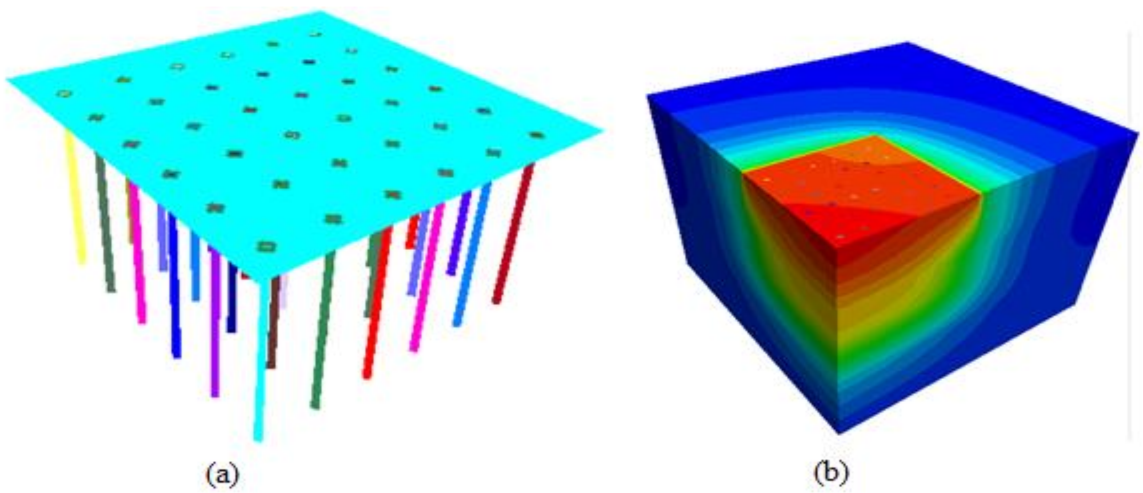

Figure 4.1: Model of piled raft (a) and overall boundary of the analysis (b)

Table 4.1: Influence of boundary size on the PRF foundation

Boundary size ($X \times Y \times Z$) m	No. of zones	Settlement (mm)		Axial Load (MN)		Y-Lateral Load (MN)		Z-Lateral Load (MN)	
		center	edge	center	edge	center	edge	center	Edge
$40 \times 40 \times 60$	13,606	39	29	8	19	-0.2	-0.8	0.2	0.84
$45 \times 45 \times 60$	21,756	40	29	8	18.7	-0.2	-0.8	0.2	0.82
$50 \times 50 \times 60$	24,864	41	30	8	18.6	-0.2	-0.8	0.2	0.78
$60 \times 60 \times 60$	29,008	43	30.5	8.2	18.4	-0.2	-0.8	0.2	0.78

Table 4.2: Influence of grid number on the PRF analysis

Trial	No. of zones	Settlement (mm)		Axial Load (MN)		Time taken (hr.)
		center	edge	center	edge	
1	17,234	33	22	11	21.3	0.5
2	24,864	41	30	8	18.6	1
3	142,800	46	40	7.2	15	4.5
4	306,516	48	45	6.5	13.4	13.5

4.1.5 Unpiled Raft Foundation

The behavior of unpiled raft is taken as a reference for evaluating the performance of piled raft foundation in terms of the settlement and bearing capacity. Figure 4.2 shows the settlement profile at the center, at some point and edge of the raft. The settlements at the center of the raft and edge are 196 mm and 104 mm. This results in a higher differential settlement of 92 mm. According to Boussinesq (1985) the distribution of stress in an elastic medium by a point load decrease towards the edge. This increase in stress at the center leads to higher settlement at the center than at the edge to make a bowel shaped settlement. The coding sequence of the parametric study of piled raft under vertical load is attached in **APPENDIX 4B**.

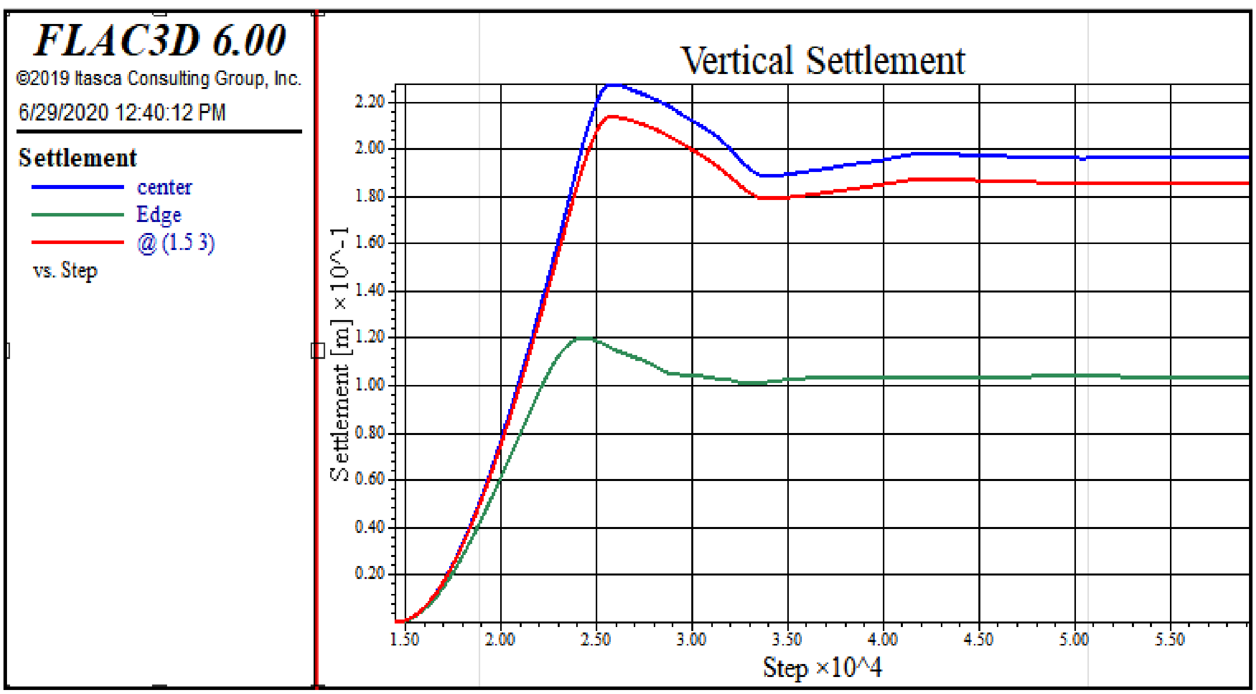

Figure 4.2: Settlement profile of Unpiled raft

The maximum positive bending moment is observed at the corners of the raft having a magnitude of 2. 25 MN.m (Figure 4.3). The negative maximum bending moment is -1. 1 MN.m located at the midsection of the raft in both x and y directions. This plot is helpful to assess the benefit and disadvantages of installing a pile in the bending moment of the raft.

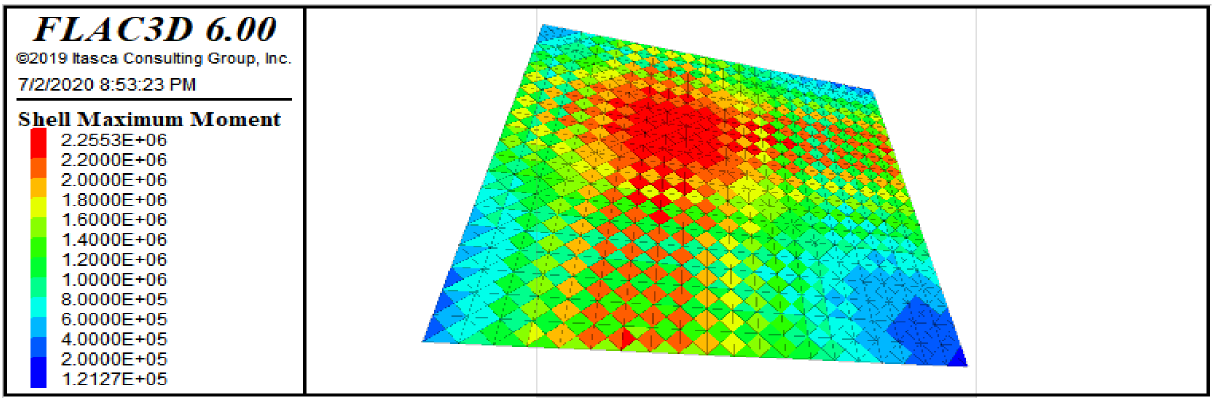

Figure 4.3: Maximum positive Bending Moment in unpiled raft foundation

4.1.6 Influence of Pile Spacing

The PRF components are pile, raft and their size. Hence, this numerical investigation considers mainly the pile size, pile diameter, pile spacing, number of pile and the outer edge size of the raft. A uniform raft thickness is considered throughout the study.

Pile spacing is the center to center distance between two consecutive piles. This spacing determine the number of pile and the overall structural stiffness. Three different pile spacing (3D, 5D and 7D) as a function of pile diameter are considered. Since most PRF systems in Addis Ababa have a spacing of 3D and above. Therefore, the spacings selected have covered most of the trends in the design of piled raft foundation.

The analysis output of FLAC3D V6 for a three different pile spacing (3D,5D and 7D), a pile length of 10 m and 1 m diameter have been plotted in Figure 4.4 below. The figure depicts that increasing the spacing results in increase of differential and total settlement. Specially at a spacing of 7D the differential and total settlement increase abruptly to 53 mm and 93 mm respectively. This phenomenon indicates that the pile spacing lower than 7D should be considered to alleviate settlement related problems. From the ratio of settlements piled raft and unpiled raft the following total settlement reduction factor (ξs) and differential settlement reduction factor (ξΔs) are obtained. These factors are helpful to indicate the reduction in settlements by addition of piles under the raft.

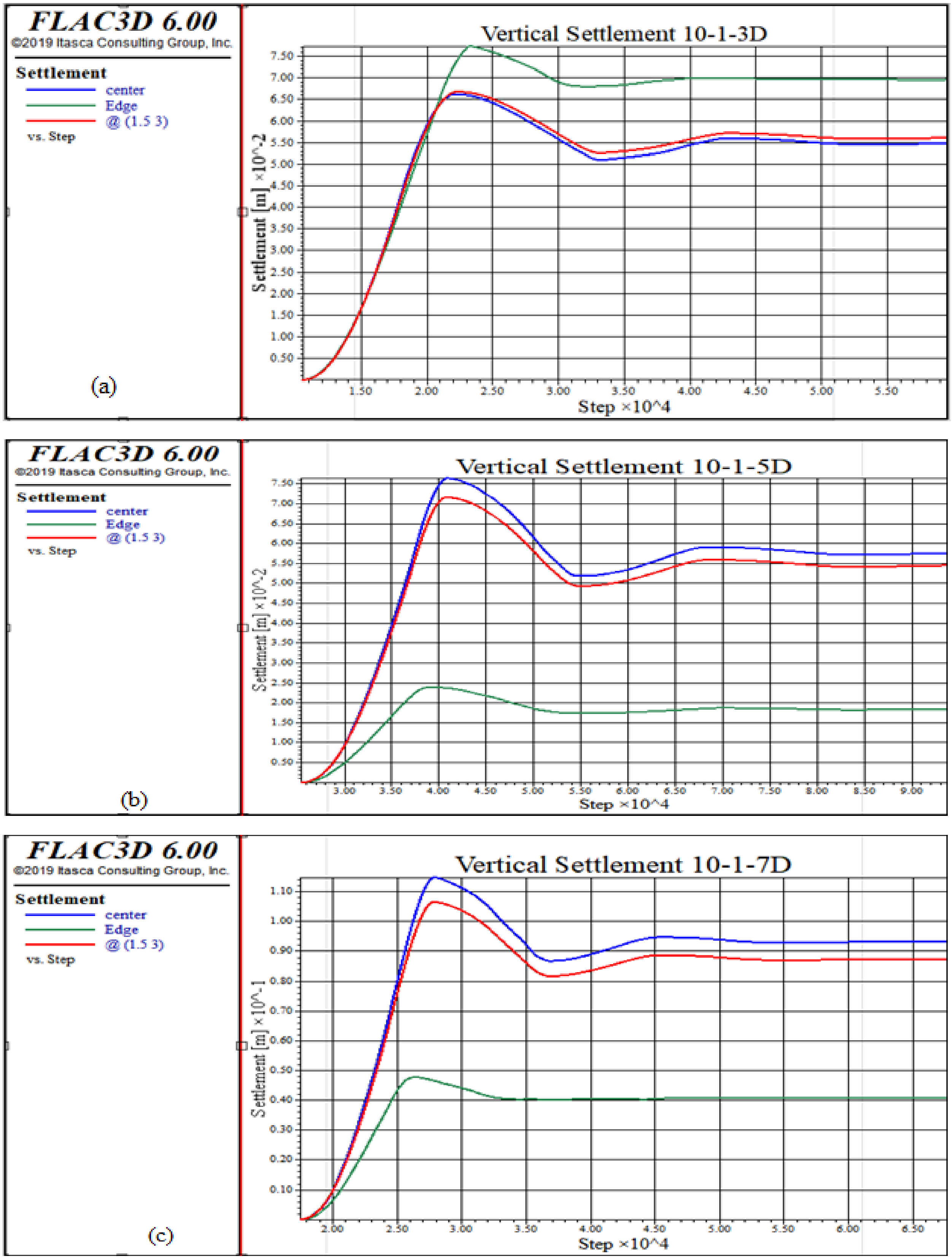

Figure 4.4: Settlement for PRF having 1m pile diameter with a) 3D b) 5D c) 7D spacing

The effect of different pile spacing on settlement reduction factors are listed in the Table 4.5 below. From the table a spacing of 3D have total settlement reduction factor of 0.35 while the 7D spacing have 0.47. This indicates 3D pile spacing almost reduce the total settlement more than that of 7D. However, a spacing of 5D is very effective in reducing the total settlement due the outer edge of the raft is very small. Differential settlement reduction factor increases as the pile spacing increase form 3D to 7D.

Table 4.3: The results of parametric study under different configuration

Spacing	UPR	3D	5D	7D
No. of pile (-)	_	144	64	36
Length of pile(m)	_	10	10	10
Total settlement (mm)	196	69	57	93
Differential settlement	92	15	39	53
ξs	_	0.35	0.29	0.47
$\xi \Delta s$	_	0.16	0.42	0.57
αpr	_	0.76	0.67	0.53

The maximum and minimum pile load capacity is 8.2 MN and 6 MN at some distance from the raft periphery and the center of the raft respectively. This result is obtained for a PRF with 3D pile spacing, 1m pile diameter and 10 m pile length. The piled raft coefficient is the ratio of the load carried by the pile and the whole expected load. Table 4.3 shows the reduction in pile raft coefficient as the spacing increase. As shown in the Figure 4.5 the total load carried by the piles for a spacing of 7D is 740 MN while for a spacing of 3D the load is 1086 MN. This reduction of load sharing is due to decrease of number of piles resulting in load to be shared by the raft. Load sharing of the raft has increase by 11.5% consecutively as the spacing increase. This result is close to numerical result obtained from the Reul and Randolph (2003).

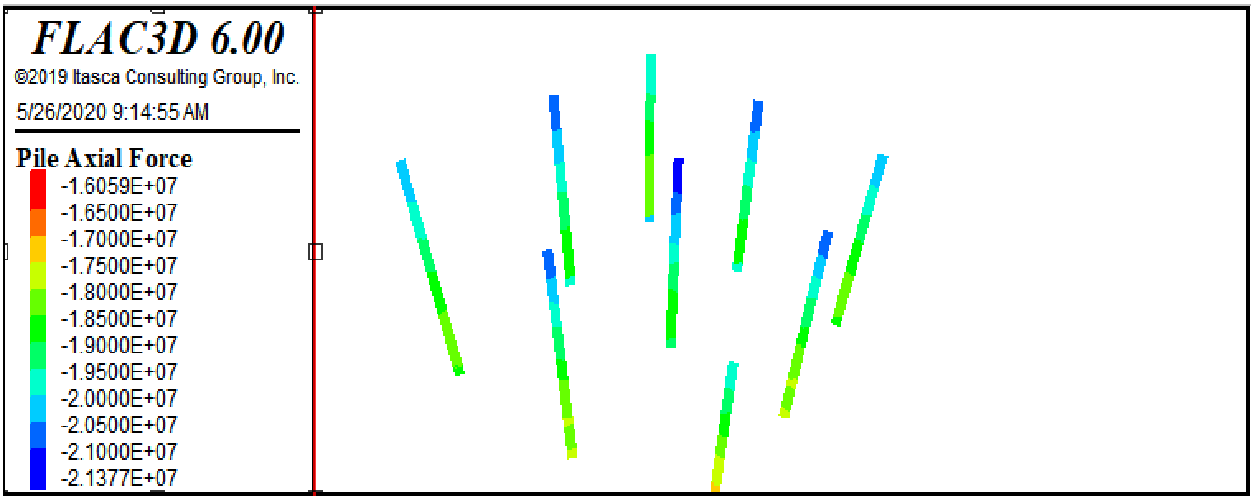

Figure 4.5: Axial load for a pile of 10 m length, 1 m diameter and 7D spacing

For all piles, the maximum bending moment and normalized lateral displacement were observed near the pile head, which decreased with an increase in the depth of the pile. The raft maximum and minimum bending moment is observed in connection between pile-raft and corner of raft respectively. A pile of 10 m length and 1 m diameter with different spacing consisting of 3 different spacings shows that increase of spacing results to increase in bending moment of both pile and raft as shown in Table 4.4. Compared with unpiled raft foundation, piled raft has increased the rafts negative bending moment due to rigid connection of pile and raft leading the tendency of raft to bend rather than settle and distributed load changed to axial load in the pile.

Table 4.4: Summary bending moment in pile and raft for different spacing

	Pile		Raft	
Config.	Maximum moment (MN.m)	Minimum moment (MN.m)	Maximum moment (MN.m)	Minimum moment (MN.m)
10-1-3D	0.36	0	1.2	-3.2
10-1-5D	7.8	0	1.5	-5.47
10-1-7D	11.7	0	2.1	-5.5
15-1.5-3D	2.7	0	1.2	-4.9
15-1.5-5D	9.6	0	3	-4.9
15-1.5-7D	5.3	0	1.7	-2.6

4.1.7 Influence of pile length

Pile length is a very crucial geometric component of PRF specially for skin friction pile. In this study the pile tip ends on hard rock stratum. Hence majority of the loads transfer to soil largely through end bearing and in small fraction through skin friction. To capture the effect of pile length on the overall performance of PRF three different pile length (10 m, 15 m and 20 m) are considered. The selected range of piles are commonly used in Addis Ababa specifically at Commercial Bank, Nib Bank and other (Kiros,2019; Mahider, 2018).

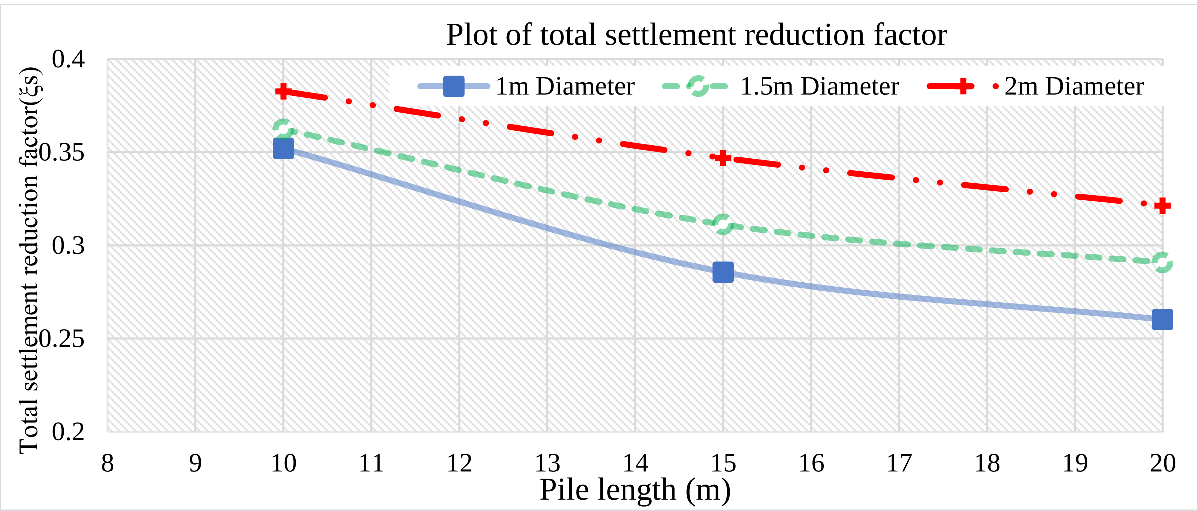

Figure 4.6: Total settlement reduction for different pile length and 3D spacing

In the Figure 4.6 above, it is clearly shown that increasing pile length reduce total settlement with different rate. This reduction rate is very high for a pile diameter of 1 m due to smaller spacing between piles. The effectiveness increasing pile length depends on the spacing between piles. Hence, for optimal design of PRF it is necessary to balance between spacing and length. Increasing pile length by 5 m from 10 m with a spacing of 3D reduces differential settlement is by 1 mm. A similar trend is observed for different pile configurations. Therefore, increasing pile length for reduction of differential settlement is not significant.

The load sharing behavior also modified due to increase in pile length. A pile of diameter 1.5 m, 5D (5 times the pile diameter) spacing and 10 m length shares 37% of the total load and the addition of pile length by 5 m increase the load sharing by 8%. Further increase of pile length by 10 m leads increase of the load sharing by 6%. Hence, pile raft coefficient increases when there is increase in pile length with a relatively small percentage.

The pile bending moment has shown increase in bending moment as the pile length increase. This is due to increase slenderness ratio which intern reduce the resistance to bending moment. Table 4.5 shows this increase in pile bending moment for the same pile diameter and spacing but different spacing. However, the raft positive and negative bending moment has shown undefined pattern with the pile length. This variation of bending moment in the raft is insignificant compared with the piles bending moment change. The raft has higher bending moment at the connection of pile and raft due to stiffness variation between pile and soil.

Table 4.5: Pile and raft bending moment with different pile length

Config.	Bending Moment		
	Pile (MN.m)	Raft (+) (MN.m)	Raft (-) (MN.m)
10-2-3D	1.1	0.72	4
15-2-3D	3.7	1.01	5.5
20-2-3D	3.8	0.55	3.5

4.1.8 Influence of Pile Diameter

In this parameter, three different pile diameters (1 m, 1.5 m and 2 m) are considered. From this study it is possible to note increasing pile size has reduced settlements. A pile of 10 m length and 1 m diameter and 9 number of piles has a total settlement of 93 mm. While the same number and length of pile but a diameter of 2 m has a settlement of 63 mm. However, a pile of size 1.5 m and spacing of 5D has higher settlement of 113 mm due to higher center to center spacing and long raft edge size (Figure 4.7). Thus, pile spacing and raft outer edge length plays significant role in settlement reduction of PRF than pile diameter. Differential settlement reduces from 55 mm to 26 mm for the increase of diameter from 1 m to 2 m.

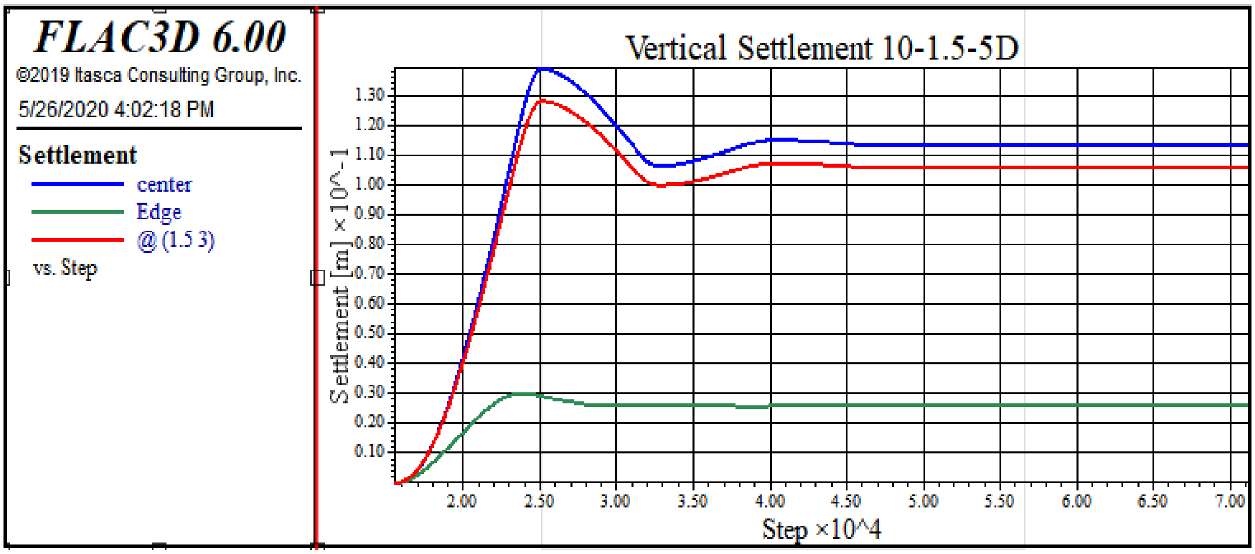

Figure 4.7: Settlement for a pile of 10m length, 1.5m diameter and 5D spacing\

The generalized relation between load sharing and pile diameter is direct. Figure 4.8 shows the variation of pile raft coefficient for a pile of 15 m length spaced at 5D. A diameter of 1 m has 64 total pile and piled raft coefficient of 0.87. Increase of pile diameter to 1.5m reduce pile numbers to 36 and the coefficient to 0.45. This shows further increase of diameter leads in reduced pile raft coefficient to increase the load carried by the raft. The percentage of load shared by the pile can be estimated from the curve fitting functions given in Figure 4.8.

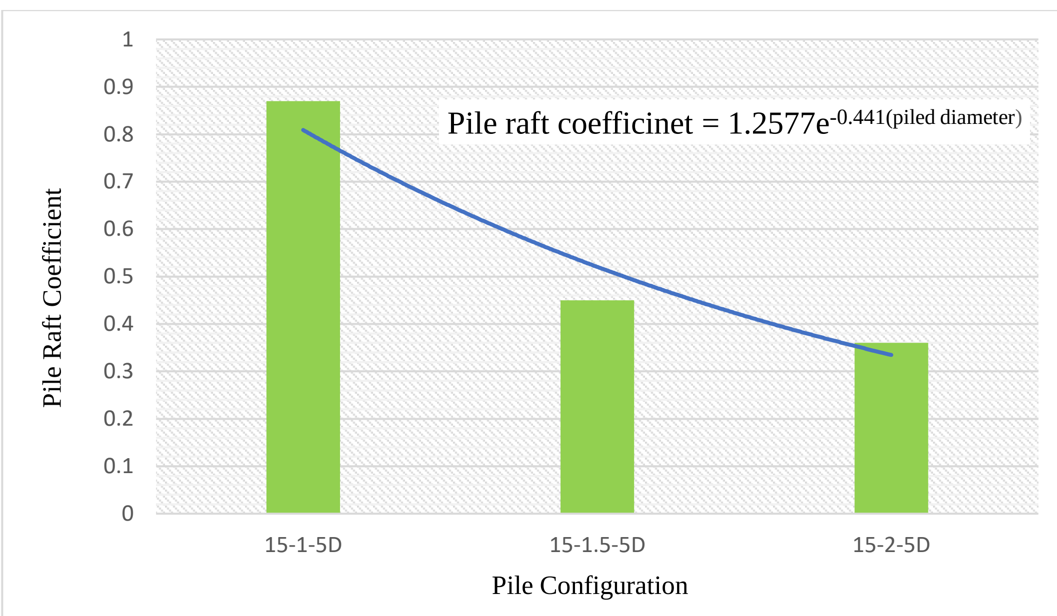

Figure 4.8: Piled raft coefficient for different pile diameter

4.1.9 Influence of Raft Edge Dimension

The raft considered is a square of dimension 39*39 m and 3 m thick. The spacing between and number of piles determine the outer edge dimension of the raft. This intern has influence on differential and total settlement. As frequently observed from this numerical parametric study higher settlement is recorded either at the center or at the corner of the raft. A PRF having 20 m pile, 4.5 m spacing and 0.75 m outer raft length has corner settlement of 51 mm. However, addition of outer raft dimension by 3 m increase the raft corner settlement by 13 mm (Figure 4.9). The general settlement trend is clearly dependent by the center to center spacing of pile and raft edge dimension.

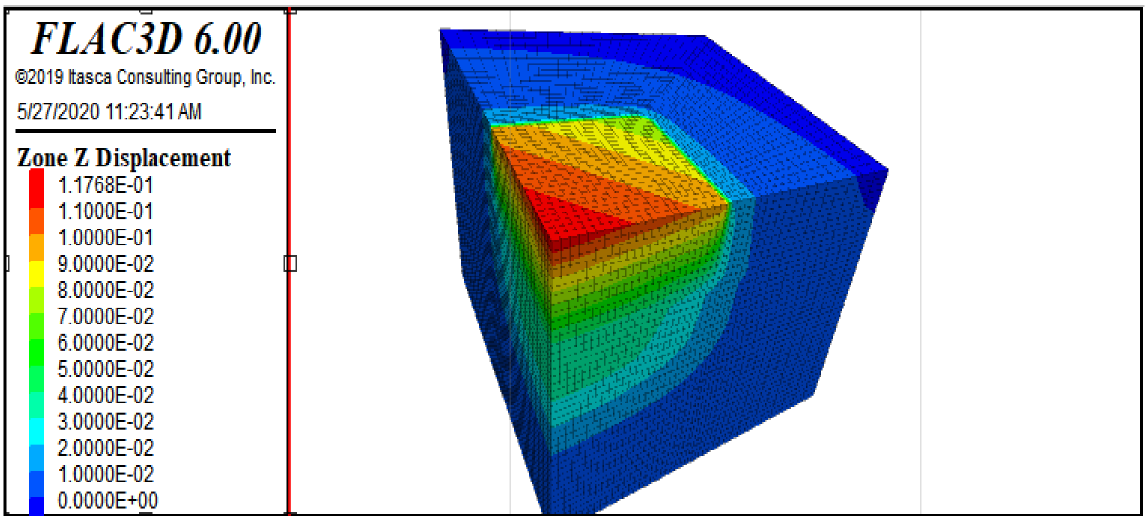

Figure 4.9: Settlement of PRF with 3.75m raft edge dimension

4.1.10 Optimized Design of PRF

The foundation design depends on the geologic condition, load type and magnitude, foundation type and intended purpose. Relying on this, the aim may be to reduce total settlement, differential settlement, or increase the load sharing of the raft, these configurations are obviously not optimized design solutions. Since the main aim of optimized design is achieving maximum economy while providing a safe foundation system. Accordingly, in this paper it is assumed that optimized design is providing a small total pile length with acceptable limit of design requirement.

The main task of geotechnical engineer is providing a foundation system that have adequate beading capacity, tolerable total and differential settlement. The load sharing between pile and raft is not the main concern instead settlements should be controlled. In the previous topics, it has found that the main parameters that control total, differential settlement and load sharing of PRF are the pile spacing and raft edge dimension from pile periphery. Hence, to achieve an optimized design a new pile configuration, piles are placed under the center and edge of the raft is proposed (Figure 4.10) and its performance will be evaluated. In this configuration piles at the center cover one quarter of the raft area ($A_G/A_R = 0.25$) in addition to edges. Performance of this pile configuration will be compared with a uniformly pile distributed ($A_G/A_R \sim 1$) having a pile length of 10 m, diameter of 1 m and spacing of 3 m.

The allowable differential and total settlement are dependent on the load magnitude, load type and importance of the structure. Different codes have their own allowable limit of differential and total settlement. Moyes *et al.* (2005) have limited the allowable total and differential settlement of PRF to 50 cm and 15 cm respectively. Reul and Randolph (2004) set allowable settlements to 10cm and 3cm respectively and this is taken for this optimization criteria. In the pile configuration of optimized design, the total number and length of pile provided are 88 and 880 m. This pile configuration has saved 56 number of piles (560 m) but it did not fulfill the required design criteria. Hence, another pile configuration with piles at the center ($A_G/A_R = 0.25$) and two rounds of edge piles has full filled the design requirement criteria. This configuration has reduced pile number of 84 (840 m pile length) and is saves 40% pile numbers from a uniform pile provision.

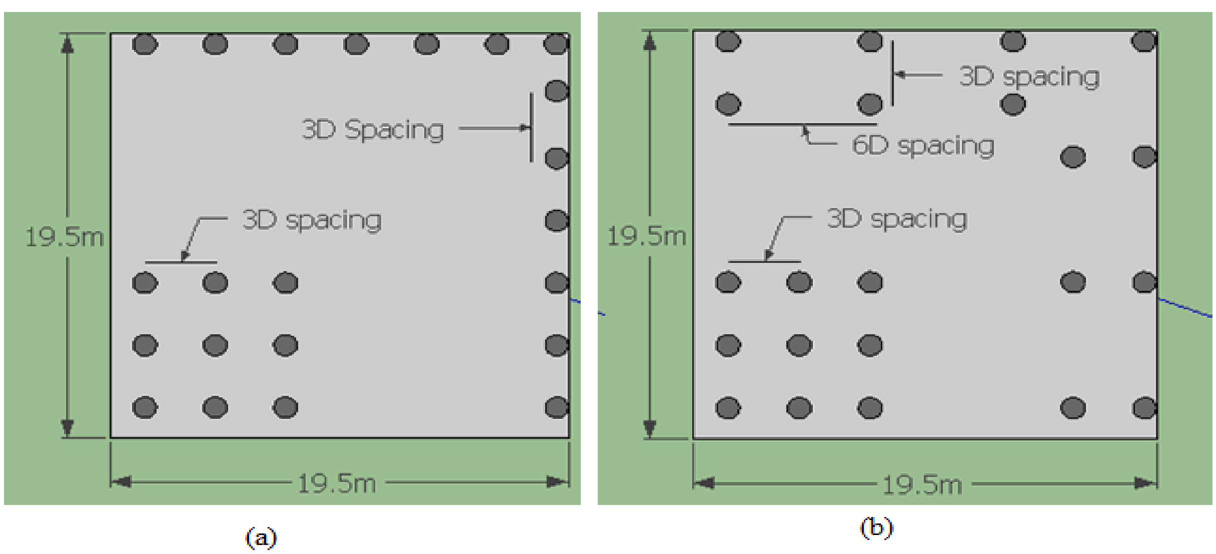

Figure 4.10: Modified Pile configurations (a) pile at the center and edge (b) pile at the center and two rounds of edge

Table 4.6: Results of optimized piles raft configuration

Parameters	Uniform pile	Configuration A	Configuration B
No. of pile (-)	144	88	84
Total pile length (m)	1440	880	840
αpr	0.76	0.53	0.49
ξs	0.35	0.4	0.4
ξΔs	0.16	0.32	0.04

High differential settlement causes distorted structure, increase angular distortion, result unfunctional door and window which reduce overall function of the structure. This puts many codes to limit differential settlement well under the total settlement. Figure 4.11shows the total and differential settlement for modified pile raft configuration B. The overall differential settlement was only 4mm (has reduced 95% differential settlement) due to addition of second round of piles around the raft edge. Table 4.6 shows the modified pile raft configuration B transfer 50% of the super structural load to the raft and the rest to pile which is usually appreciated. The coding sequence of selected optimized piled raft under vertical load is attached in **APPENDIX 4C**.

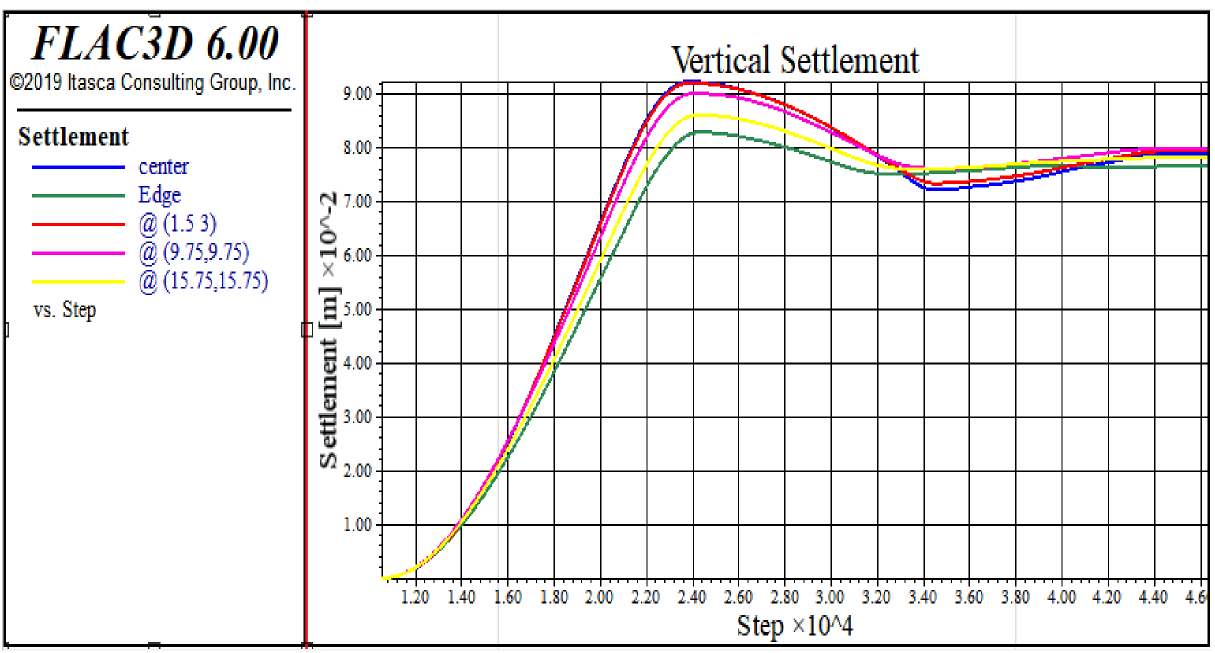

Figure 4.11: Settlement of optimized piled raft configuration B

4.2 Dynamic Analysis of Piled Raft Foundation

In this this section, the results of a piled raft foundation under the influence the 1940 El Centro earthquakes for friction pile and end bearing pile will be discussed. These results are lateral deflection at the pile and raft, amplification or attenuation of input earthquake and finally acceleration at the top of the raft will be discussed considering soil structure interaction. The coding sequence of seismic analysis of piled raft is attached in **APPENDIX 4D**.

4.2.1 Friction Piles Under Seismic Loading Considering SSI

Figure 4.12 illustrate the pile head displacement for the edge pile under the excitation of the 1940 El Centro earthquake. This pile has displaced 8 cm in the y direction but under different PGA excitation and the same earthquake it has only displaced by 4 cm. From this result it is noticeable that PGA has a predominant effect than duration of earthquake.

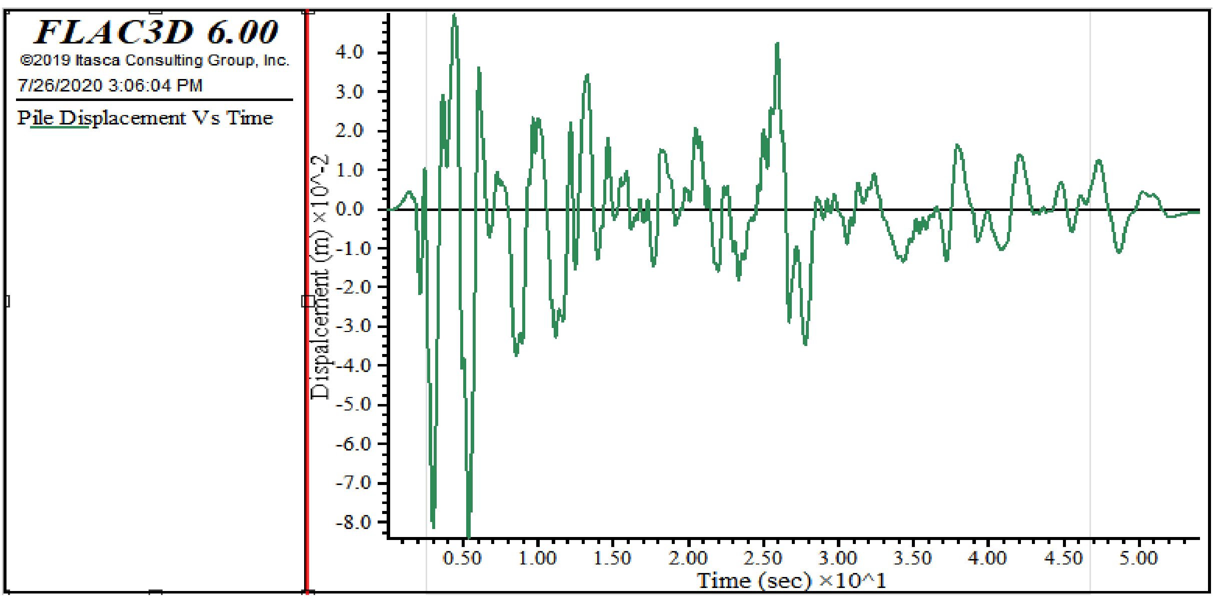

Figure 4.12: Lateral displacement of pile head at (9,19,30) in excitation direction

The destructiveness of earthquake can aggravate by the stratigraphy and formation of the top 30 m soils at a given area. This aggravation or reducing the seismic shaking is called site effect. This effect usually depends on the composition of the soil and stratification. Soils with a higher stiffness are effective in attenuation of seismic waves but loose soils having a very low stiffens value attenuate seismic waves which lead to increasing of both PGA and duration. In the Figure 4.13 it is shown the acceleration plot at the top of the piled raft. Figure 4.13 has PGA of 3 m/sec^2 but the input earthquake has a PGA of 1.5 m/sec^2 . The same was observed for earthquake having PGA of 3 m/sec^2 but it amplified to 6 m/sec^2 . This is due to the presence of silty clay soil up to 22 m from the ground surface. This amplification of earthquake has a negative influence by increasing the intensity of earthquake which intern increase lateral deflection in the pile and story.

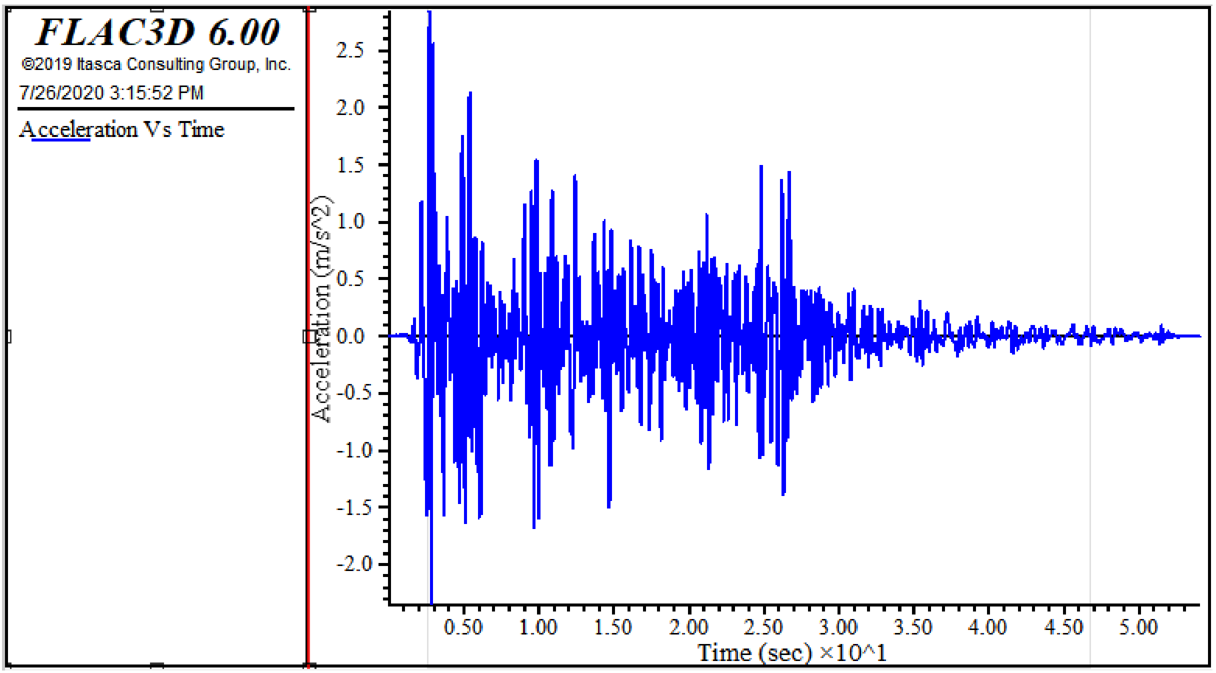

Figure 4.13: Acceleration time history at the top of PRF induced PGA of 1.5 m/sec^2

The PRF has not experienced residual horizontal displacement (after the end of shaking duration) of under two different amplitude earthquakes. Figure 4.14 shows the result of pile head displacement under the 1940 El Centro earthquake having PGA of 1.5 m/sec^2. Based on the conventional design of pile group foundation and Japan Road Association (2002) the horizontal displacement allowed is 1% of pile diameter which is 6 mm. But the recorded pile head displacement is 0 mm. The predominant period of 1940 El Centro earthquake is 3 sec, while the friction PRF fundamental period is 0.24 sec. Hence, the condition of resonance has not occurred for this earthquake.

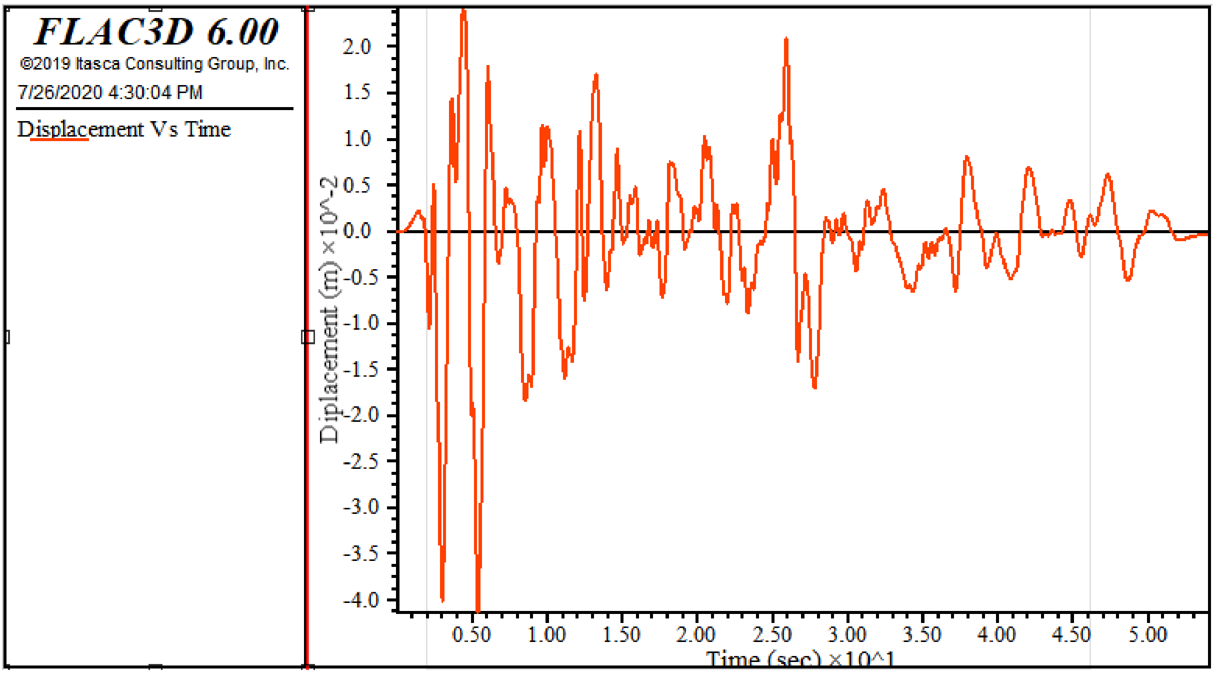

Figure 4.14: Pile head displacement of friction pile under the 1940 El Centro earthquake with 1.5 m/sec^2 PGA

4.2.2 End Bearing Piles Under Seismic Loading Considering SSI

The influence of earthquake on piled raft foundation for floating and end bearing pile is not that much different. This is observed in the analysis of PRF having 9 piles with 0.6 m diameter piles using El Centro earthquakes with two different PGA. Figure 4.15 shows the plot of pile head displacement versus the duration of El Centro earthquake. In this figure the maximum horizontal displacement of the pile is 3.5 cm at 5 sec of the earthquake. This result shows the pile head displacement under end bearing pile by 1.5 m/sec^2 PGA has a reduced displacement compared with friction piles. The maximum acceleration at the top of piled raft is 1.6 m/sec^2 which is smaller compared with friction piled raft foundation.

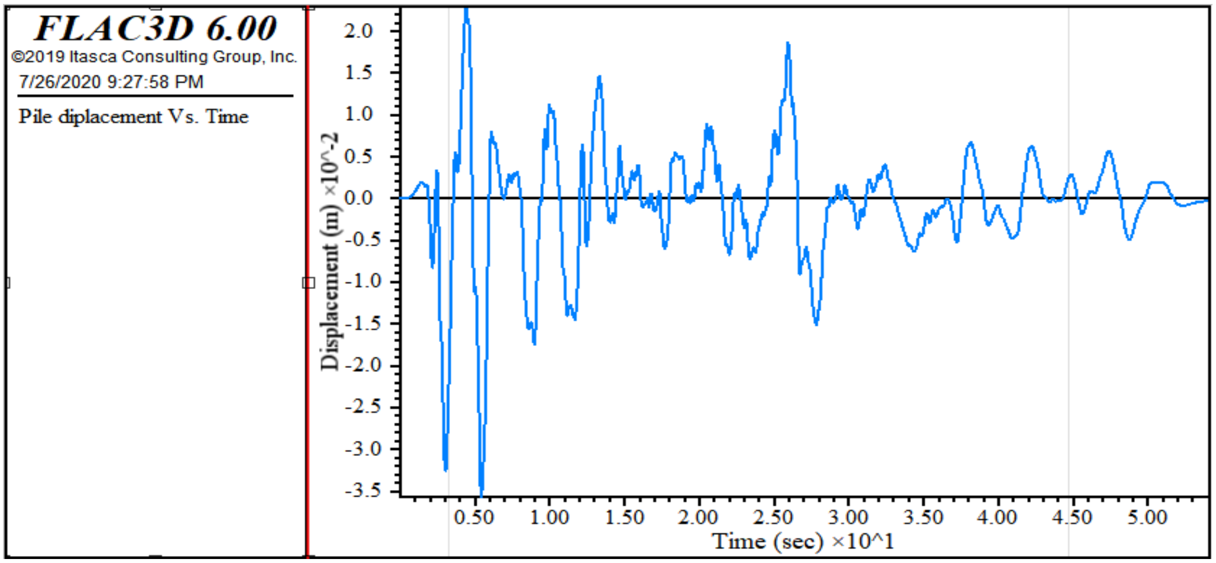

Figure 4.15: Pile head displacement on end bearing PRF by the 1940 E l Centro earthquake under PGA of 1.5 m/sec^2

The overall analysis result for end bearing and floating PRF by the two earthquakes is shown in the Table 4.7 below. Hence both floating and end bearing piled raft foundation respond closely similar but end bearing PRF has reduced the pile displacement and acceleration at the raft top.

Table 4.7: Performance of friction and end bearing PRF under 1940 El Centro earthquake

PRF type	Friction		End bearing	
PGA (m/sec^2)	1.5	3	1.5	3
Pile displacement (m)	0.4	0.8	0.35	0.7
Acceleration at the top (m/sec^2)	1.9	3.7	1.3	2.5
Velocity at the top (m/sec)	0.18	0.36	0.13	0.27
Acceleration at the top of PRF (m/sec^2)	3	6	1.6	3.1

The total and differential settlement for piled raft foundation shows appreciable difference in end bearing and friction PRF. Figure 4.16 shows an end bearing pile has a total and differential settlement of 3 mm and 1 mm excited by the 1940 El Centro earthquake with a PGA of 3 m/sec^2. However, the same pile raft arrangement excited by El Centro earthquake but a floating pile has a total settlement of 4.2 mm. Using end bearing PRF has reduced the total settlement by 25% of the floating PRF. The predominant period of 1940 El Centro earthquake is 3 sec, while the end bearing PRF has a fundamental period of 1.2 sec. Hence, the condition of resonance has not occurred for this piled raft foundation type.

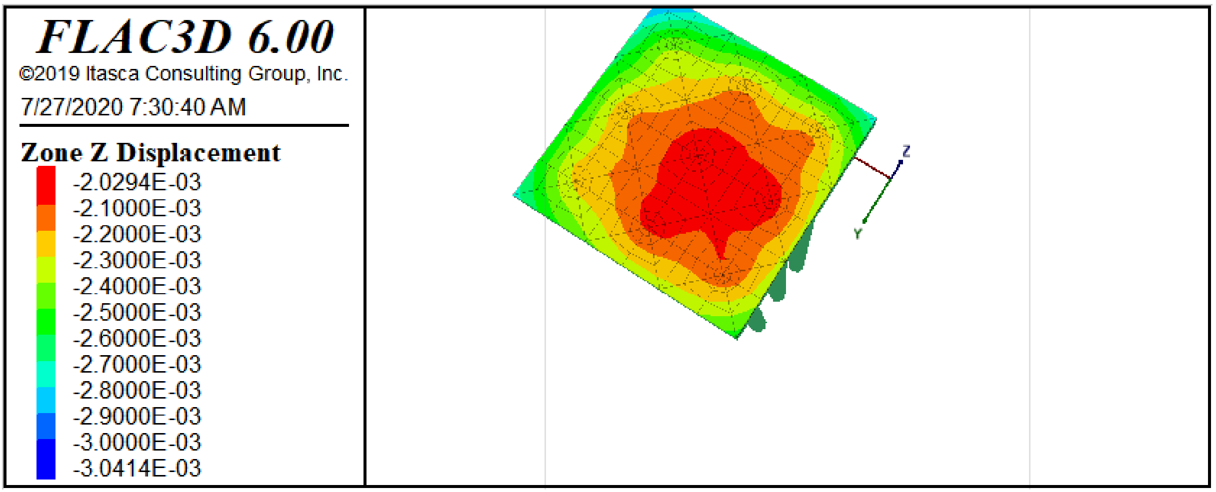

Figure 4.16: Settlement of end bearing PRF excited by the 1940 El Centro earthquake

Magnitude of earthquake, especially peak ground acceleration, has also shown a considerable effect on the settlement of PRF. An increase of peak ground acceleration from 1.5 m/sec^2 to 3 m/sec^2 has increased the settlement end bearing PRF by 4 folds. In addition to end bearing PRF, friction PRF total settlement has increased from 1 mm to 4.2 mm by the increase of peak ground acceleration from 1.5 m/sec^2 to 3 m/sec^2. This is due to change and adjustment of the stress distribution by seismic waves.

End bearing PRF experienced no residual horizontal displacement (after the end of shaking duration) earthquakes. Based on the conventional design of pile group foundation the horizontal displacement allowed is 1% of pile diameter. The allowable displacement according to Japan Road Association (2002) is 6 mm, hence, end bearing piled raft responds well for earthquake loads.

4.3 Validation of Numerical Studies

Validation of the numerical study is very important in order to accept and justify the results of both static and dynamic numerical studies. Numerical studies should be compared with physical models or analytical solution under the same soil and soil conditions. The analytic method reported on Poulos (2001) by Technical Committee TC18 of Piled Foundations has been used in this thesis for validation purpose. The soil and geometric property of the piled raft foundation is summarized in the Table 4.8.

Table 4.8: Model parameters for validation of numerical study (Poulos., 2001)

Geometry	size(m)	Unit weight (kg/m^3)	Young modulus (MPa)	Load (MN)	Poisson's ratio
Pile	D=0.5, L=10	2500	30000	2MN middle rows; 1MN on other	0.2
Raft	10 × 6 × 0.5	2500	30000	-	0.2
Soil	20 × 20 × 20	1700	20	-	0.3

Th American Society of Civil Engineers (ASCE) Technical Committee–18 (TC -18) report in 2001, has been used in this thesis for validation purpose. The results of the simulated model through different rigorous and simplified method has a settlement of around 50 mm. While in FLAC3D V6 the piled raft has a settlement of around 59 mm which is 85% accurate (Figure 4.17). This validation is customary for both static and dynamic analysis since the same software is used throughout the analysis. The codding sequence for validation of PRF under static loading is attached in **APPEDIX 4E**. The validation performed shows that a numerical software FLAC3D is adequate to simulate the true experimental results from physical model with acceptable limit of accuracy.

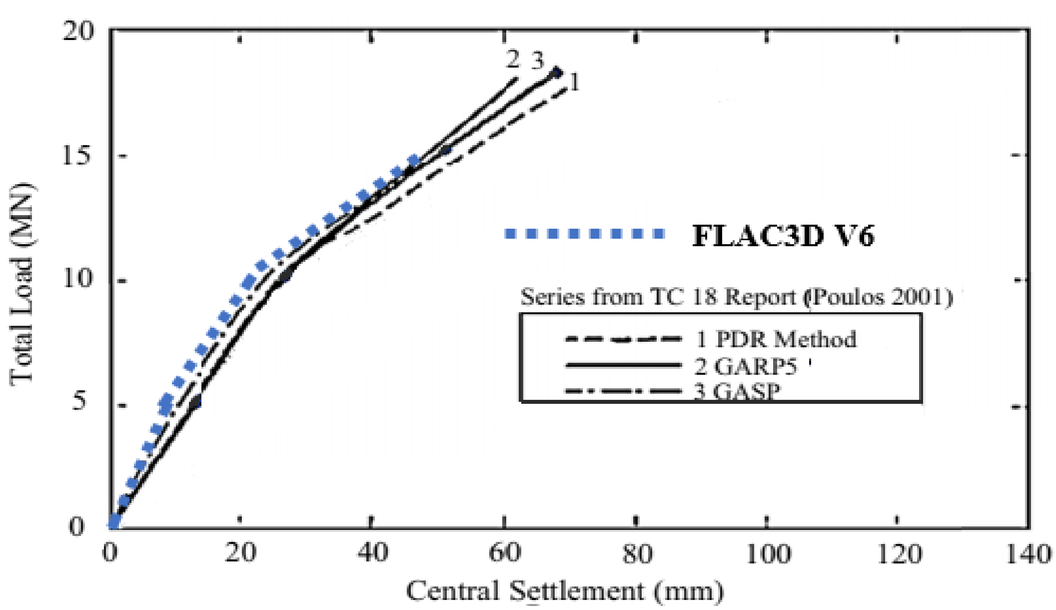

Figure 4.17: Settlement of piled raft for validation of software

CHAPTER – 5: CONCLUSIONS AND RECOMMENDATIONS

5.1 Conclusions

In the preceding sections an attempt has been made to summarize results from outputs of analysis and discus major finding concerning on both statically and seismically loaded piled raft foundation. Important conclusion in this thesis is summarized in to the following points.

- Pile spacing and length of raft from the outer most pile to the edge of raft are basic parameters which influence settlements. The raft settles at the center more than any other portion of the PRF in the shape of a bowl. Increasing pile length from 10 m to 20 m for 2 m diameter has reduced the settlement by 9%, which show pile length is not efficient in reducing settlement. The differential settlement is governed by the raft edge length from outer most pile periphery. Hence, pile diameter should be balanced with raft edge dimension to control differentials settlement.
- Spacing has a considerable effect in increasing the load shared by raft. Increasing pile length has reduced the load shared by the raft but which is not appreciable to achieve economical design. Increase of pile diameter has increased the load shared by the raft effectively. A close load sharing between pile and raft was achieved at a spacing of 7D with different pile length and diameter but settlement should be controlled.
- The installation of piles result increase of negative bending moment of the raft compared with unpiled raft. Generally bending moment (maximum positive and minimum negative) in the raft increase as the spacing and pile diameter increase. The piles bending moment has shown increase with length and diameter of the piles.
- An optimized design of piled raft foundation depends mainly on the pile center to center spacing and raft outer edge dimension from the periphery of the pile. Optimized design of piled raft is attained by placing piles at the center and edge of the raft. While pile length and diameter variation have no significant influence on optimized design. An optimized piled raft configuration (piles covering area at the center $A_G/A_R = 0.25$ and two rounds of pile around the edge of the raft) provided can reduce the number of piles by 40% and differential settlement by 95%.
- The dynamic numerical study of PRF considering SSI has shown that magnitude of earthquake (specially PGA) has predominant effect on lateral deflection of the pile head

and settlement. The subsoil found on the commercial bank of Ethiopia have poor soil composition resulting in amplification of seismic waves.

- Compared with friction PRF, an end bearing PRF has lower amplification, pile head displacement and vertical settlement under the 1940 El Centro earthquake with different peak ground acceleration. The condition resonance was not observed for both end bearing and friction piled raft foundation under different peak ground acceleration by the 1940 El Centro earthquake. The residual pile head displacement for both end bearing and friction pile by El Centro earthquake is well below the allowable limit.

5.2 Recommendations

In this study, the main objectives are investigation of PRF under vertical static load, evaluate the performance and investigate the influence of kinematic SSI under the seismic excitation of PRF and optimization of PRF for vertical static load. There are many areas beyond the scope of this study that should be addressed by future works. The following are recommended for future study.

1. The numerical studies involving both static and seismic load should also be investigated through experimental method.
2. In order to have a better understanding on the performance of piled raft foundation in Addis Ababa, buildings on PRF should be studied through a highly experimentation and comparison should be made with the numerical studies.

SPECIAL ACKNOWLEDGEMENT

This research project is funded by Adama Science and Technology University under the grant number:

ASTU/SM-R/045/19

Adama, Ethiopia

REFERENCE

1. AASHTO, L. (1996). Bridge Design Specifications (1994). *The American Association of State Highway and Transportation Officials, (ed.), Washington, DC,*
2. Ahmad, B., & Najar, I. A. (2016). Comparative Seismic Analysis of EL Centro and Japan Earthquakes using Response Spectra Method. *International Journal of Current Engineering and Technology*, *6*(5).
3. Akl, A. Y., Mansour, M. H., & Moustafa, H. K. (2014). Effect of changing configurations and lengths of piles on piled raft foundation behavior. *Civil Engineering and Urban Planning*, *1*(1).
4. Assefa, E., Lin, L. J., Sachpazis, C. I., Feng, D. H., Shu, S. X., & Xu, X. (2017). Slope Stability Evaluation for the New Railway Embankment using Stochastic Finite Element and Finite Difference Methods. *Electronic Journal of Geotechnical Engineering*, *22*, 51-79.
5. B. Yoseph & G. Ramana (2008) Earthquake ground-motion parameters at stiff sites in Addis Ababa, Ethiopia, International Journal of Geotechnical Engineering, 2:1, 45-58
6. Banerjee, S., Goh, S. H., & Lee, F. H. (2007). Response of soft clay strata and clay-pile-raft systems to seismic shaking. *Journal of Earthquake and Tsunami*, *1*(03), 233-255.
7. Berhe, T. G., Wang, X. T., & Wu, W. (2010). Numerical investigation into the arrangement of clay core on the seismic performance of earth dams. In *Soil Dynamics and Earthquake Engineering* (pp. 131-138).
8. Bommer, J. J., & Acevedo, A. B. (2004). The use of real earthquake accelerograms as input to dynamic analysis. *Journal of Earthquake Engineering*, *8*(spec01), 43-91.
9. Boore, D. M., Stephens, C. D., & Joyner, W. B. (2002). Comments on baseline correction of digital strong-motion data: Examples from the 1999 Hector Mine, California, earthquake. *Bulletin of the Seismological Society of America*, *92*(4), 1543-1560.
10. Boussinesq, J. (1969). Application of potentials to the study of equilibrium and movement of solid elastic bodies [Application des Potentiels à l'Etude de l'Equilibre et du Mouvement des solides élastiques]. *Paris: Albert Blanchard*.
11. Bowles, J. E. (1996). Foundation Analysis & Design 5th Edition McGraw-Hill Companies.
12. Briaud, J. L. (2013). *Geotechnical engineering: unsaturated and saturated soils*. John Wiley & Sons.

13. Brinkgreve, R. B. (2005). Selection of soil models and parameters for geotechnical engineering application. In *Soil constitutive models: Evaluation, selection, and calibration* (pp. 69-98).
14. Bull, J. W. (Ed.). (2014). *Linear and non-linear numerical analysis of foundations*. CRC Press.
15. CES-160-2015. Design of Structures for Earthquake Resistance (2015). *Ministry of construction, Addis Ababa*.
16. Chatterjee, K., Choudhury, D., & Poulos, H. G. (2015). Seismic analysis of laterally loaded pile under influence of vertical loading using finite element method. *Computers and Geotechnics, 67*, 172-186.
17. CSA. (2007). Central Statistical Agency of Ethiopia, Addis Ababa
18. Cunha, R. P., Poulos, H. G., & Small, J. C. (2001). Investigation of design alternatives for a piled raft case history. *Journal of geotechnical and geoenvironmental engineering*, *127*(8), 635-641.
19. Das, B. M., & Luo, Z. (2016). *Principles of soil dynamics*. Cengage Learning.
20. Dash, S. R., Govindaraju, L., & Bhattacharya, S. (2009). A case study of damages of the Kandla Port and Customs Office tower supported on a mat–pile foundation in liquefied soils under the 2001 Bhuj earthquake. *Soil Dynamics and Earthquake Engineering*, *29*(2), 333-346.
21. Emmanuel, J. (2017). *Parametric Study on Analysis and Design of Permanently Anchored Secant Pile Wall for Earthquake Loading* (Doctoral dissertation, Addis Ababa University).
22. Eslami, M. M., Aminikhah, A., & Ahmadi, M. M. (2011). A comparative study on pile group and piled raft foundations (PRF) behavior under seismic loading. *Computational Methods in Civil Engineering*, *2*(2), 185-199.
23. Fisseha, K. (2019). Investigating the Load Sharing Behaviour Of Piled Raft with Pile Tips on Hard Strata Using Finite Element Method: Case of Commercial Bank of Ethiopia Headquarters Building (Master thesis, Addis Ababa University).
24. GEO, G. (2006). Foundation Design and Costruction-Publication No. 1/2006.
25. Giannopoulos, K. Numerical Analysis of the Reuse of Piled Raft Foundations.
26. Goodman, R. E. & Kulhawy, F. H. (1980). Design of foundations on discontinuous rock. In *International Conference on Structural Foundations on Rock, 1980, Sydney, Australia*.

27. Gouin, P. (1970). Evaluating seismic activity in Ethiopia. *Zede Journal*, *4*, 5-9.
28. Hardin, B. O. (1978, June). The nature of stress-strain behavior for soils. In *from Volume I of Earthquake Engineering and Soil Dynamics--Proceedings of the ASCE Geotechnical Engineering Division Specialty Conference, June 19-21, 1978, Pasadena, California. Sponsored by Geotechnical Engineering Division of ASCE in cooperation with:* (No. Proceeding).
29. Hayes, G. P., Jones, E. S., Stadler, T. J., Barnhart, W. D., McNamara, D. E., Benz, H. M., ... & Villaseñor, A. (2014). *Seismicity of the Earth 1900-2013 East African Rift* (No. 2010-1083-P). US Geological Survey.
30. Hokmabadi, A. S. (2014). *Effect of Dynamic Soil-pile Structure Interaction on Seismic Response of Mid-rise Moment Resisting Frames* (Doctoral dissertation, University of Technology, Sydney).
31. Hokmabadi, A. S., Fatahi, B., & Samali, B. (2014). Seismic response of mid-rise buildings on shallow and end-bearing pile foundations in soft soil. *Soils and Foundations*, 345-363.
32. Itasca Consulting Group, Inc. (2017). "FLAC3D- Fast Lagrangian Analysis of Continua in 3 Dimensions, version 6.0." Minneapolis, Minnesota.
33. Japan Road Association. (2002). Specifications for highway bridges part IV: substructures. *Tokyo, Japan*.
34. Kang, M. A., Banerjee, S., Lee, F. H., & Xie, H. P. (2012). Dynamic soil-pile-raft interaction in normally consolidated soft clay during earthquakes. *Journal of earthquake and tsunami*, *6*(03), 1250031.
35. Katzenbach, R., Schmitt, A., & Turek, J. (2005). Assessing Settlement of High-Rise Structures by 3D Simulations. *Computer-Aided Civil and Infrastructure Engineering*, *20*(3), 221-229.
36. Keir, D., Ebinger, C. J., Stuart, G. W., Daly, E., & Ayele, A. (2006). Strain accommodation by magmatism and faulting as rifting proceeds to breakup: Seismicity of the northern Ethiopian rift. *Journal of Geophysical Research: Solid Earth*, *111*(B5).
37. Kramer, S. L. (1996). *Geotechnical earthquake engineering*. Pearson Education India.
38. Kuhlemeyer, R. L., & Lysmer, J. (1973). Finite element method accuracy for wave propagation problems. *Journal of Soil Mechanics & Foundations Div*, *99*(Tech Rpt).

39. Kumar, A., Choudhury, D., & Katzenbach, R. (2016). Effect of earthquake on Combined piled raft foundation. *International Journal of Geomechanics*, *16*(5), 04016013.
40. Lade, P. V. (2005). Overview of constitutive models for soils. In *Soil constitutive models: Evaluation, selection, and calibration* (pp. 1-34).
41. Lin, D. G., Liu, W. T., & Chou, J. C. (2016). Load transfer and deformation analyses of piled-raft foundation in Taipei Metropolitan. *Journal of Marine Science and Technology*, *24*(4), 798-806.
42. Mahider, M. (2018). Assessment of "Piled Raft Foundation" for HighRise Buildings Under Vertical Load in Addis Ababa: The case of Nib, Zemen, and United Bank Headquarter Buildings (Mater thesis, Addis Ababa University).
43. Mandolini, A., Di Laora, R., & Mascarucci, Y. (2013). Rational design of piled raft. *Procedia Engineering*, *57*, 45-52.
44. Mejia, L. H., & Dawson, E. M. (2006, May). Earthquake deconvolution for FLAC. In *4th International FLAC symposium on numerical modeling in geomechanics* (pp. 04-10).
45. Melgar, D., Bock, Y., Sanchez, D., & Crowell, B. W. (2013). On robust and reliable automated baseline corrections for strong motion seismology. *Journal of Geophysical Research: Solid Earth*, *118*(3), 1177-1187.
46. Mesri, G., & Hayat, T. M. (1993). The coefficient of earth pressure at rest. *Canadian Geotechnical Journal*, *30*(4), 647-666.
47. Michalowski, R. L. (2005). Coefficient of earth pressure at rest. *Journal of geotechnical and geoenvironmental engineering*, *131*(11), 1429-1433.
48. Moayedi, H., Nazir, R., Ghareh, S., Sobhanmanesh, A., & Tan, Y. C. (2018). Performance analysis of a piled raft foundation system of varying pile lengths in controlling angular distortion. *Soil Mechanics and Foundation Engineering*, *55*(4), 265-269.
49. Moyes P, Poulos HG, Small JC, Badelow F (2005) Piled raft design process for a high-rise building on the gold coast, Australia. www.coffey.com. pp 1–9
50. OHTA, Y. (1976). Estimation of S-wave velocity in terms of characteristic indices of soil. *Butsuri-Tanko*, *29*(4), 34-41.
51. Ordonez, G. A. (2000). SHAKE2000: A computer program for the 1D analysis of geotechnical earthquake engineering problems. *Geomotions, LLC, USA.*

52. Orr, T. L., & Farrell, E. R. (2012). *Geotechnical design to Eurocode 7*. Springer Science & Business Media.
53. PEER, P. (2014). Ground motion database. *2014-03-26]. http://peer. berkeley. edu/peer_ground_motion_database*.
54. Poulos, H. G. (2001). Methods of analysis of piled raft foundations. A Report Prepared on Behalf of Technical Committee TC18 of Piled Foundations.
55. Poulos, H. G. (2002). Simplified design procedure for piled raft foundations. In *Deep Foundations 2002: An International Perspective on Theory, Design, Construction, and Performance* (pp. 441-458).
56. Poulos, H. G., & Bunce, G. (2008). Foundation design for the Burj Dubai–the world's tallest building.
57. Poulos, H. G., & Davis, E. H. (1980). *Pile foundation analysis and design* (No. Monograph).
58. Randolph, M. F. (1994). Design methods for pile groups and piled rafts. In *International conference on soil mechanics and foundation engineering* (pp. 61-82).
59. Rayhani, M. H., & El Naggar, M. H. (2008). Numerical modeling of seismic response of rigid foundation on soft soil. *International Journal of Geomechanics*, *8*(6), 336-346.
60. Reul, O., & Randolph, M. F. (2004). Design strategies for piled rafts subjected to nonuniform vertical loading. *Journal of Geotechnical and Geoenvironmental Engineering*, *130*(1), 1-13.
61. Saha, R., Dutta, S. C., & Haldar, S. (2015). Seismic response of soil-pile raft-structure system. *Journal of civil engineering and management*, *21*(2), 144-164.
62. Seed, H. B., Wong, R. T., Idriss, I. M., & Tokimatsu, K. (1986). Moduli and damping factors for dynamic analyses of cohesionless soils. *Journal of geotechnical engineering*, *112*(11), 1016-1032.
63. Sinha, A., & Hanna, A. M. (2016). 3D numerical model for piled raft foundation. *International Journal of Geomechanics*, *17*(2), 04016055.
64. Sisay, Y. (2005). Correlation between standard penetration and unconfined compressive strength of Addis Ababa clay soils. A thesis presented to Graduate Studies, Addis Ababa University.
65. Standard, E. B. C. EBCS-8 Design of Structures for Earthquake Resistance (1995). *Ministry of Works and urban Development, Addis Ababa*.

66. Sucuoğlu, H., & Akkar, S. (2014). Basic Earthquake Engineering. *Switzerland: Spring International Publishing*.
67. Sun, J. I., Golesorkhi, R., & Seed, H. B. (1988). *Dynamic moduli and damping ratios for cohesive soils*. Berkeley: Earthquake Engineering Research Center, University of California.
68. Ti, K. S., Huat, B. B., Noorzaei, J., Jaafar, M. S., & Sew, G. S. (2009). A review of basic soil constitutive models for geotechnical application. *Electronic Journal of Geotechnical Engineering*, *14*, 1-18.
69. Tso, W. K., & Hsu, T. I. (1978). Torsional spectrum for earthquake motions. *Earthquake Engineering & Structural Dynamics*, *6*(4), 375-382.
70. Van Nguyen, Q., Fatahi, B., & Hokmabadi, A. S. (2016). The effects of foundation size on the seismic performance of buildings considering the soil-foundation-structure interaction. *Structural Engineering and Mechanics*.
71. Viggiani, C. (2001). 'Analysis and Design of Piled Foundations. In *Proceedings* (pp. 47-75).
72. Vucetic, M., & Dobry, R. (1988). Degradation of marine clays under cyclic loading. *Journal of Geotechnical Engineering*, *114*(2), 133-149.
73. Wills, C. J., & Silva, W. (1998). Shear-wave velocity characteristics of geologic units in California. *Earthquake Spectra*, *14*(3), 533-556.
74. Wolf, J. P. (1985). Soil-structure interaction. *Prentice Hall Inc., Englewood Cliffs, New Jersey ISBN 0 l3*, *221565*(9), 01.
75. Xu, R., & Fatahi, B. (2019). Impact of In Situ Soil Shear-Wave Velocity Profile on the Seismic Design of Tall Buildings on End-Bearing Piles. *Journal of Performance of Constructed Facilities*, *33*(5), 04019053.
76. YAMASHITA, K., TOMONO, M., & KAKURAI, M. (1987). A method for estimating immediate settlement of piles and pile groups. *Soils and foundations*, *27*(1), 61-76.
77. Yoseph, B., & Ramana, G. (2008). Earthquake ground-motion parameters at stiff sites in Addis Ababa, Ethiopia. *International Journal of geotechnical engineering*, *2*(1), 45-58.
78. Zhang, G., Fu, P., & Liang, F. (2013). Mathematical and numerical modeling in geotechnical engineering. *Journal of Applied Mathematics*, *2013*.

79. Zhang, J., Andrus, R. D., & Juang, C. H. (2005). Normalized shear modulus and material damping ratio relationships. *Journal of Geotechnical and Geoenvironmental Engineering*, *131*(4), 453-464.
80. Zhang, L., Goh, S. H., & Liu, H. (2017). Seismic response of pile-raft-clay system subjected to a long-duration earthquake: centrifuge test and finite element analysis. *Soil Dynamics and Earthquake Engineering*, *92*, 488-502.

APPENDIX

APPENDIX 3A

Sample of geotechnical and geological data collected from Commercial bank headquarter building is shown in the following figures below.

PROJECT NEW HEAD QUARTERS BUILDING (CBE) BORING TYPE ROTARY CORING
LOCATION ADDIS ABABA GROUND WATER LEVEL 5.50m
CLIENT CHINA STATE CONSTRUCTION ENGINEERING Co. LTD BH ELEVATION 2354m
DATE STARTED 23/07/2015 INCLINATION VERTICAL
DATE COMPLETED 04/08/2015 COORDINATES 0472991E 0996648N
BH 1

DEPTH (m)	CASING SIZE (mm)	DRILLING SIZE (mm)	SAMPLE RECORD	S.P.T. /N-VALUE/	DEPTH (m)	PROFILE	TCR (%)	RQD (%)	STRATA DESCRIPTION	REMARK
0–1	130	130			0.00–1.00		100, 100		Loose to medium dense, variegated poorly graded fill material. It is mainly composed of varying proportions of demolished materials (concrete and brick gravel) sand, silt and clay	
1–6.5			4.50		1.00, 3.00, 4.50, 5.70, 6.40, 6.50		100, 100, 100, 100, 100		Soft, light brown to light grey expansive silty CLAY	
6.5–10.7					7.00, 7.40, 8.90, 9.10, 10.00, 10.70		100, 100, 100, 100, 100, 100		Medium dense, grey silty SAND with gravel (completely weathered Basalt)	
10.7–15	100	100			11.00, 12.40, 14.90		100, 89, 85	0, 15, 20	Medium strong, grey, intensively fractured and fragmented slightly to moderately weathered BASALT. Fracture surfaces are rough and yellowish stained. Joints are nearly horizontal and Filled with altered materials	

(Nc) CONE PENETRATION TEST
N BLOWS/30cm
RS ROCK SAMPLE
W WATER SAMPLE
TCR TOTAL CORE RECOVERY
RQD ROCK QUALITY DESIGNATION
DISTURBED SOIL SAMPLE
UNDISTURBED SOIL SAMPLE
SPT STANDARD PENETRATION
END OF DRILLING

CREW Daniel Furgasa DRAWN BY Bezunesh W/Tsadik
SUPERVISOR Berhanu Beyene SIG
LOGGED BY Berhanu Beyene SIG
APPROVED BY Matewos Bekele SIG

Project :- Head Quarter Building Of CBE
Client :- China State Construction Engineering Ethiopia PLC
Location :- A.A (Ambasader)
Object :- Nineteen Undisturbed Soil Samples

N°	BH N°	Depth (m)	Atterberg Limit			Free	Organic	Swelling	Natural	Natural	Unconfined	Triaxial Shear Test		Direct Shear Test	
			LL (%)	PL (%)	PI (%)	Swell (%)	Content (%)	Pressure (KN/m2)	Moisture Content (%)	Unit Weight (Kg/m3)	Compressive Strength (KN/m²)	C (KN/m²)	Ø Degree	C (KN/m²)	Ø Degree
1	1	4.50	-	-	-	-	-	-	30.50	1670	64	-	-	14	21
2	1	18.60	75.48	49.35	26.13	-	-	-	54.22	1519	-	12	19	-	-
3	1	43.00	109.17	48.59	60.58	220	-	-	20.11	1643	-	-	-	19	17
4	3	5.50	62.09	25.82	36.27	70	-	-	18.07	1550	-	-	-	17	20
5	5	6.40	83.06	43.89	39.17	170	-	480	26.17	1876	144	-	-	36	25
6	5	22.00	144.50	49.99	94.51	240	-	-	30.69	1774	61	-	-	28	7
7	6	5.00	70.94	33.45	37.49	120	-	260	36.18	1889	130	-	-	30	10
8	6	20.50	119.50	52.25	67.25	-	-	-	64.25	1444	-	90	8	29	25
9	6	38.20	-	-	-	-	-	-	31.45	1658	241	94	5	-	-
10	6	41.00	-	-	-	-	-	-	36.98	1590	254	-	-	26	17
11	6	42.00	-	-	-	-	-	-	30.92	1962	265	84	15	-	-
12	7	3.00	76.03	38.91	37.12	110	-	-	20.50	1823	-	-	-	33	25
13	7	38.50	-	-	-	-	-	-	31.13	1543	386	-	-	20	18
14	7	39.50	77.51	28.25	49.26	140	8.28	-	39.02	1645	-	-	-	30	23
15	7	41.50	88.86	35.30	53.56	-	-	-	39.61	1747	-	85	16	-	-
16	8	40.00	84.09	34.66	49.43	-	-	-	33.36	1740	-	31	12	-	-
17	8	47.50	64.64	21.51	43.13	110	4.20	-	34.20	1790	-	-	-	32	13
18	9	19.00	93.55	55.49	38.06	-	-	-	80.27	1459	-	-	-	1	20
19	9	3.20	-	-	-	-	-	-	35.69	1649	132	-	-	22	16

Note :-

1. Nineteen graphs for grain size distribution test result are drawn and attached herewith.
2. Fourteen graphs for direct shear test result are drawn and attached herewith.
3. Six graph for UU triaxial test result is drawn and attached here with.
4. Eight Time - settlement, void ratio- pressure curve and the necessary data sheets for one - dimensional consolidation test result are attached herewith.

Project :- Head Quarter Building Of CBE
Client :- China State Construction Engineering Ethiopia PLC
Location :- A.A (Ambasader)
Object :- Six Rock Samples

N°	BH N°	Depth (m)	Rock Strength Test		
			Unit Weight (Kg/m3)	Compressive Strength (KN/m2)	Modulus of Elasticity (KN/m²)
1	12	29.00	2684	26702	1027000
2	12	47.50	2701	30237	222331
3	12	53.60	2812	48670	3080380
4	12	56.00	2792	58877	1863196
5	12	69.00	2814	31620	1550000
6	12	73.00	2783	48526	1708662

Project :- Head Quarter Building Of CBE
Client :- China State Construction Engineering Ethiopia PLC
Location :- A.A (Ambasader)
Object :- Two Soil & Thirty Seven Rock Samples

N°	BH N°	Depth (m)	Permeability			Rock Strength Test	
			Maximum Dry Density (Kg/m3)	Optimum Moisture Content (%)	Coefficent (K) (M/s)	Unit Weight (Kg/m^3)	Compressive Strength (KN/m^2)
1	1	32.00	-	-	-	2765	25660
2	2	32.80	-	-	-	2734	21923
3	2	40.00	-	-	-	2424	8251
4	2	41.40	-	-	-	2433	26816
5	3	26.20	-	-	-	2934	60069
6	3	30.50	-	-	-	2776	38584
7	3	32.50	-	-	-	2676	37269
8	3	38.30	-	-	-	2825	92107
9	3	40.00	-	-	-	2808	105002
10	4	25.00	-	-	-	2836	69083
11	4	32.60	-	-	-	2824	24151
12	5	26.40	-	-	-	2886	27345
13	5	29.80	-	-	-	2749	32743
14	5	32.50	-	-	-	2883	43774
15	5	33.50	-	-	-	2791	75740
16	5	47.00	-	-	-	2939	62868
17	6	32.70	-	-	-	2824	48723
18	6	48.60	-	-	-	2517	26541
19	6	54.30	-	-	-	2387	55706
20	6	56.40	-	-	-	3030	59068
21	6	58.20	-	-	-	3093	16613
22	7	36.00	-	-	-	2567	64834
23	7	49.00	-	-	-	2428	48783
24	7	52.00	-	-	-	2930	16248
25	7	58.00	-	-	-	2696	22308
26	7	71.50	-	-	-	3046	64178
27	7	76.50	-	-	-	2823	62967
28	8	33.00	-	-	-	2796	32351
29	8	52.00	-	-	-	3285	38729
30	8	55.00	-	-	-	3637	46712
31	8	58.00	-	-	-	2603	60542
32	8	69.50	-	-	-	2891	48279
33	8	76.50	-	-	-	2882	41840
34	8	79.50	-	-	-	2675	53584
35	9	54.00	-	-	-	2741	67519
36	9	59.00	-	-	-	2847	15444
37	9	82.00	-	-	-	2840	73904
38	1	18.60	1184	35.82	1.99×10^{-6}	-	-
39	3	5.30	1339	29.58	8.09×10^{-6}	-	-

APPENDIX 3B

Coding sequence for simulating single pile capacity.

```
FILE: single-pile-simulation.f3dat, DATE: Fri Jul 3 21:00:58 2020
-------------------------------------------------------------------
; simulation of single pile
model new
model title "Single_pile_simulation"
; Create the grid
zone create brick point 0 (0 0 0) Point 1 (10 0 0) point 2 (0 10 0) point 3 (0 0 20) ...
size 15 15 30
;================================
; Label model boundaries
;===============================
zone face skin
;================================
;Assign Boundary conditipon
;================================
zone face apply velocity-normal 0 range group 'East' or 'West'
zone face apply velocity-normal 0 range group 'North' or 'South'
zone face apply velocity-normal 0 range group 'Bottom'
;=================================
;Assign Group for each material
;=================================
zone group "rock" range position-z 0 10
zone group "Highly-weathered-rock" range position-z 10 20
; Assign constitutive model and propertie
;========================================
;layer one
;===========================
zone cmodel assign mohr-coulomb range group "Highly-weathered-rock"
zone property bulk=80e6 shear=40.62e6 density=2359 friction 37.4 cohesion 28e3 ...
range group "Highly-weathered-rock"
;===========================
;layer two
;===========================
zone cmodel assign mohr-coulomb range group "rock"
zone property bulk=684.67e6 shear=410.8e6 density=2626 friction 40 cohesion 5000e3 ...
range group "rock"

; Initial conditions
model gravity 10
zone initialize-stresses
model solve ratio-local 1e-4 ; Should be instant
; =====================================================
; Create a pile in the center of the soil block
struct pile create by-line (5, 5, 21) (5, 5, 10) segments=33
struct pile property young=31.37e9 poisson=0.15 cross-sectional-area=0.7854 moi-polar=0.0 moi-y=0.0
moi-z=0.0 ...
            perimeter=3.14 coupling-stiffness-shear=8e11 coupling-cohesion-shear=20e3
coupling-friction-shear=30 ...
            coupling-stiffness-normal=8e11 coupling-cohesion-normal=30e3 coupling-friction-normal=30
coupling-gap-normal=off
; =====================================================
; Specify and apply velocity to pile tip.
struct node fix velocity-x                   range position-z 21
struct node initialize velocity-x 2e-7 local range position-z 21
; =====================================================
; Set up histories for monitoring model behavior
struct node history name='disp'  displacement-z position (5,5,21)
struct pile history name='force' force-x position (5,5,21)
; =====================================================
struct damping combined-local
model save 'Initial-state of stress'
; =====================================================
; Apply velocity to achieve total displacement of 10mm
model cycle 50000
model save 'shaft resistance'
; =====================================================
; Include end-bearing effect
```

```
model restore 'Initial-state of stress'
struct link delete range position-z 10
struct link create target zone group 'End' range position-z 10
struct link attach x=normal-yield y=free z=free                            range group 'End'
struct link attach rotation-x=free rotation-y=free rotation-z=free        range group 'End'
struct link property x area=0.7854 stiffness=5.27e11 yield-compression=5.75e6 range group 'End'
model cycle 50000
model save 'Shaft + end bearing'
```

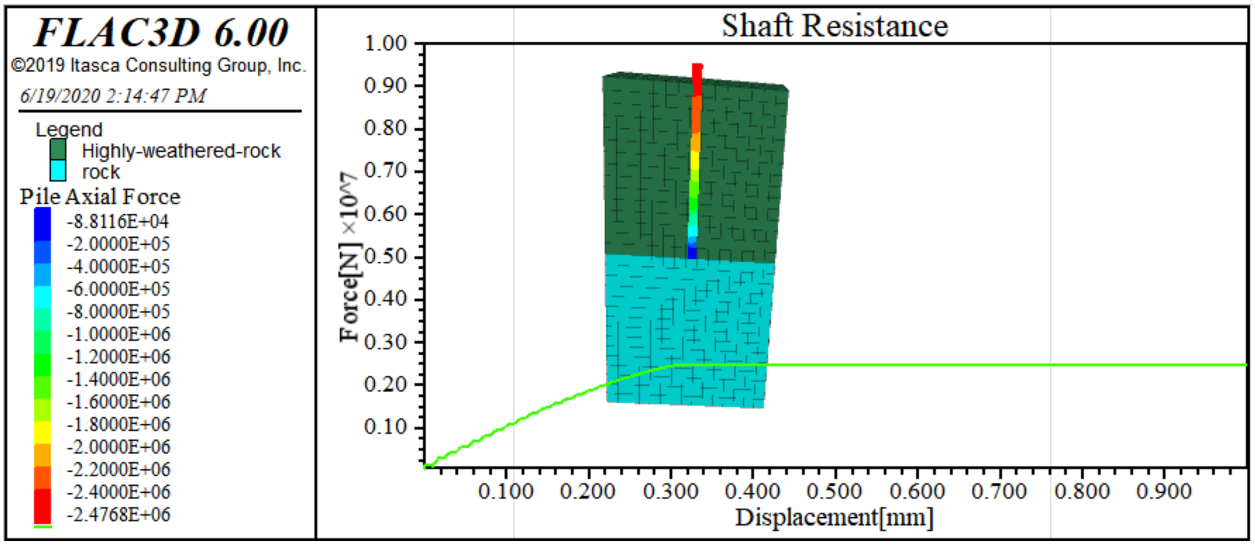

APPENDIX 4A

In this appendix the sensitivity analysis code for a boundary size of 20m is include but the rest are not provided due to space limitation.

```
model new
zone creat radial-tunnel point 0 (0 0 0) ...
                         point 1 (0 40 0) ...
                         point 2 (0 0 22) ...
                         point 3 (40 0 0) dimension 21 21 fill size 14 15 14 11 ratio 1 1 1 1.1
;the size here is (x y z and then around the tinnel)
zone creat radial-tunnel point 0 (0 0 22) ...
                       point 1 (0 40 22) ...
                      point 2 (0 0 60) ...
                      point 3 (40 0 22) dimension 21 21 fill size 14 22 14 11 ratio 1 1.005 1 1.1
;the size here is (x y z and then around the tunnel)
zone attach by-face range position-z 22
model save 'geometry for 40m'
;========================================================
;===========Assign Group for each material=============
;========================================================
zone group "exc1" range position-z 0 6.5
zone group "exc2" range position-z 6.5 16.5
zone group "exc3" range position-z 16.5 22
zone group "Highly-weathered-rock" range position-z 22 32
zone group "Rock" range position-z 32 38
zone group "weak-to-strong silty clay" range position-z 38 47
zone group "Durable rock" range position-z 47 60
;========================================================
;===========Assigning a Constitutive Model=============
;========================================================
; layer 1
zone cmodel assign mohr-coulomb range group "exc1"
zone property density 1524 bulk 15.56e6 shear 6.36e6 friction 19.5 ...
cohesion 25.3e3 range group "exc1"
; layer 2-1
zone cmodel assign mohr-coulomb range group "exc2"
zone property density 1743 bulk 36.44e6 shear 12.15e6 friction 21.3 ...
cohesion 210e3 range group "exc2"
; layer 2-2
zone cmodel assign mohr-coulomb range group "exc3"
zone property density 1743 bulk 36.44e6 shear 12.15e6 friction 21.3 ...
cohesion 210e3 range group "exc3"
; layer 3
zone cmodel assign mohr-coulomb range group "Highly-weathered-rock"
zone property density 2359 bulk 88e6 shear 40.62e6 friction 31.4 ...
cohesion 28e3 range group "Highly-weathered-rock"
; layer 4
zone cmodel assign elastic range group "Rock"
zone property density 2626 young 1027e6 poisson 0.25 bulk 684.10e6 ...
shear 410.8e6  range group "Rock"
; layer 5
zone cmodel assign mohr-coulomb range group "weak-to-strong silty clay"
zone property density 1871 bulk 245.83e6 shear 100.510e6 friction 35 ...
cohesion 25e3 range group "weak-to-strong silty clay"
; layer 6
zone cmodel assign elastic range group "Durable rock"
zone property density 2887 young 1680e6 Poisson 0.25 bulk 684.10e6 ...
shear 410.8e6  range group "Durable rock"
;========================================================
;=================Apply boundary condition=============
;========================================================
zone face apply velocity-normal 0 range position-x 0
zone face apply velocity-normal 0 range position-x 40
zone face apply velocity-normal 0 range position-y 0
zone face apply velocity-normal 0 range position-y 40
zone face apply velocity (0 0 0) range position-z 60

;========================================================
;=================Initialize Stress=============
```

```
;=======================================================
model gravity (0,0,10)
zone initialize-stresses ratio 0.610 range  position-z 0 6.5
zone initialize-stresses ratio 0.64 range   position-z 6.5 22
zone initialize-stresses ratio 0.39 range  position-z 22 32
zone initialize-stresses ratio 0.36 range position-z 32 38
zone initialize-stresses ratio 0.43 range position-z 38 47
zone initialize-stresses ratio 0.29 range  position-z 47 60
;=======================================================
;=================Step to equilibrium====================
;=======================================================
;zone geometry-tolerance 0
model largestrain on
model history mechanical ratio
model solve ;default value of convergence will be used
model save "initial-stress-state 40m"
;=======================================================
;=================Excavation to -21m===================
;=======================================================
;the first 7m
model restore "initial-stress-state 40m"
zone relax excavate range position-z 0 7.5
model solve ratio-local 1e-4
model save 'stage1'
;2nd 7m
model restore 'stage1'
zone relax excavate range position-z 0 15
model solve ratio-local 1e-4
model save 'stage2'
;3rd 7m
model restore 'stage2'
zone relax excavate range position-z 0 22
model solve ratio-local 1e-4
model save 'End of excavation 40'
model restore 'End of excavation 40'
zone gridpoint initialize displacement (0 0 0)
zone gridpoint initialize velocity (0 0 0)
;=========================================================
;=================Installation of Pile====================
;=========================================================
; will consist of 36 piles(6*6) with outer edge of 3m
;=========================================================
struct pile create by-line (1.5, 1.5, 21.9021) (1.5, 1.5, 32) segments=20 id 1
struct pile create by-line (1.5, 4.5,  21.9021) (1.5, 4.5, 32) segments=20 id 2
struct pile create by-line (1.5, 7.5,  21.9021) (1.5, 7.5, 32) segments=20 id 3
struct pile create by-line (1.5, 10.5,  21.9021) (1.5, 10.5, 32) segments=20 id 4
struct pile create by-line (1.5, 13.5,  21.9021) (1.5, 13.5, 32) segments=20 id 5
struct pile create by-line (1.5, 16.5,  21.9021) (1.5, 16.5, 32) segments=20 id 6

struct pile create by-line (4.5, 1.5,  21.9021) (4.5, 1.5, 32) segments=20 id 7
struct pile create by-line (4.5, 4.5,  21.9021) (4.5, 4.5, 32) segments=20 id 8
struct pile create by-line (4.5, 7.5,  21.9021) (4.5, 7.5, 32) segments=20 id 9
struct pile create by-line (4.5, 10.5,  21.9021) (4.5, 10.5, 32) segments=20 id 10
struct pile create by-line (4.5, 13.5,  21.9021) (4.5, 13.5, 32) segments=20 id 11
struct pile create by-line (4.5, 16.5,  21.9021) (4.5, 16.5, 32) segments=20 id 12

struct pile create by-line (7.5, 1.5,  21.9021) (7.5, 1.5, 32) segments=20 id 13
struct pile create by-line (7.5, 4.5,  21.9021) (7.5, 4.5, 32) segments=20 id 14
struct pile create by-line (7.5, 7.5,  21.9021) (7.5, 7.5, 32) segments=20 id 15
struct pile create by-line (7.5, 10.5,  21.9021) (7.5, 10.5, 32) segments=20 id 16
struct pile create by-line (7.5, 13.5,  21.9021) (7.5, 13.5, 32) segments=20 id 17
struct pile create by-line (7.5, 16.5,  21.9021) (7.5, 16.5, 32) segments=20 id 18

struct pile create by-line (10.5, 1.5,  21.9021) (10.5, 1.5, 32) segments=20 id 19
struct pile create by-line (10.5, 4.5,  21.9021) (10.5, 4.5, 32) segments=20 id 20
struct pile create by-line (10.5, 7.5,  21.9021) (10.5, 7.5, 32) segments=20 id 21
struct pile create by-line (10.5, 10.5,  21.9021) (10.5, 10.5, 32) segments=20 id 22
```

```
struct pile create by-line (10.5, 13.5,  21.9021) (10.5, 13.5, 32) segments=20 id 23
struct pile create by-line (10.5, 16.5,  21.9021) (10.5, 16.5, 32) segments=20 id 24

struct pile create by-line (13.5, 1.5,  21.9021) (13.5, 1.5, 32) segments=20 id 25
struct pile create by-line (13.5, 4.5,  21.9021) (13.5, 4.5, 32) segments=20 id 26
struct pile create by-line (13.5, 7.5,  21.9021) (13.5, 7.5, 32) segments=20 id 27
struct pile create by-line (13.5, 10.5,  21.9021) (13.5, 10.5, 32) segments=20 id 28
struct pile create by-line (13.5, 13.5,  21.9021) (13.5, 13.5, 32) segments=20 id 29
struct pile create by-line (13.5, 16.5,  21.9021) (13.5, 16.5, 32) segments=20 id 30

struct pile create by-line (16.5, 1.5,  21.9021) (16.5, 1.5, 32) segments=20 id 31
struct pile create by-line (16.5, 4.5,  21.9021) (16.5, 4.5, 32) segments=20 id 32
struct pile create by-line (16.5, 7.5,  21.9021) (16.5, 7.5, 32) segments=20 id 33
struct pile create by-line (16.5, 10.5,  21.9021) (16.5, 10.5, 32) segments=20 id 34
struct pile create by-line (16.5, 13.5,  21.9021) (16.5, 13.5, 32) segments=20 id 35
struct pile create by-line (16.5, 16.5,  21.9021) (16.5, 16.5, 32) segments=20 id 36
model save 'pile installed'
;========================================================
;================ Assign property for pile===============
;========================================================


struct pile property young=31.37e9 poisson=0.15 cross-sectional-area=3.14 moi-polar=1.57 moi-y=0.7854
 moi-z=0.7854 ...
            perimeter=6.28 coupling-stiffness-shear=8e11 coupling-cohesion-shear=20e3
coupling-friction-shear=30 ...
            coupling-stiffness-normal=8e11 coupling-cohesion-normal=30e3 coupling-friction-normal=30
coupling-gap-normal=on


;========================================================
;=========== Include end bearing  for the pile ==========
;========================================================
struct link delete range position-z 32
struct link create target zone group 'End' range position-z 32
struct link attach x=normal-yield y=free z=free                        range group 'End'
struct link attach rotation-x=free rotation-y=free rotation-z=free        range group 'End'
struct link property  x stiffness 1.44e11 yield-compression 24.3e6  area 3.14 range position-z 32
;yield compression or end bearing
structure link slide on range position-z 32
;========================================================
;=================Creat raft============================
;========================================================
struct shell create by-quadrilateral (0,0,21.9021) (19.5,0,21.9021) (19.5,19.5,21.9021) (0,19.5,
21.9021) ...
size (13,13) id 37    ...
element-type dkt-csth cross-diagonal ;constant strain trianlge hybride
struct shell property density 2500 isotropic (31.4e9, 0.15) thick 3 ;isotropic (E, v)
;structure link tolerance-slide 0.1  range position-z 21.9021
;structure link slide on range position-z 21.9021
;========================================================
;=============Connection Raft and Soil ==================
;========================================================
struct link delete range position-z 21.9021
struct link create target zone group 'raft_with_soil' range position-z 21.9021
struct link attach x rigid y rigid  z rigid                       range group 'raft_with_soil'
struct link attach rotation-x=free rotation-y=free rotation-z=free        range group 'raft_with_soil'
structure link slide on range group 'raft_with_soil'

;========================================================
;=============Connection B/N Pile and Raft===============
;========================================================
structure node join range id 37

;structure link slide on range id 37 not

;===========================================================================
```

```
;=========Apply Uniform distributed Load from the S,structure================
;============================================================================
struct shell apply 926690 range  position-x 0 19.5 position-y 0 19.5
; Set large strain on, creating coupling between bending and membrane
model largestrain on
;==========================================================
;=============History points to analyse the model=========
;==========================================================
model history mechanical ratio-local
zone history displacement-z position (0,0,21.9021)
zone history displacement-z position (1.5,3,21.9021)
zone history displacement-z position (19.5 19.5 21.9021)
;for the central pile
struct pile history name='Force(x) @ (1.5 1.5)' force-x position (1.5 ,1.5, 21.9021)
struct pile history name='Force(y) @ (1.5 1.5)' force-y position (1.5 ,1.5, 21.9021)
struct pile history name='Force (z) @ (1.5 1.5)' force-z position (1.5 ,1.5, 21.9021)
struct pile history name='Moment (y) @ (1.5 1.5)' moment-Y position (1.5 ,1.5, 21.9021)
struct pile history name='Moment (z) @ (1.5 1.5)' moment-z position (1.5 ,1.5, 21.9021)
struct node history name='Disp(y) @ (1.5 1.5)'displacement-y position (1.5,1.5,21.9021)
struct node history name='Disp(z) @ (1.5 1.5)'displacement-z position (1.5,1.5,21.9021)
;for the pile at the edge of the group
struct pile history name='Force @ (x) (16.5 16.5)' force-x position (16.5 ,16.5, 21.9021)
struct pile history name='Force @ (y)(16.5 16.5)' force-y position (16.5 ,16.5, 21.9021)
struct pile history name='Force @ (z) (16.5 16.5)'force-z position (16.5 ,16.5, 21.9021)
struct pile history name='Moment @ (y) (16.5 16.5)' moment-Y position (16.5 ,16.5, 21.9021)
struct pile history name='Moment @ (z) (16.5 16.5)' moment-z position (16.5 ,16.5, 21.9021)
struct node history name='Disp(y) @ (16.5 16.5)'displacement-y position (16.5,16.5,21.9021)
struct node history name='Disp(z) @ (16.5 16.5)'displacement-z position (16.5,16.5,21.9021)

;==========================================================
;=============Solving the model==========================
;==========================================================
model solve ratio-local=1e-4
;==========================================================
;=============Save the model============================
;==========================================================
model save 'for 40m piled raft'
```

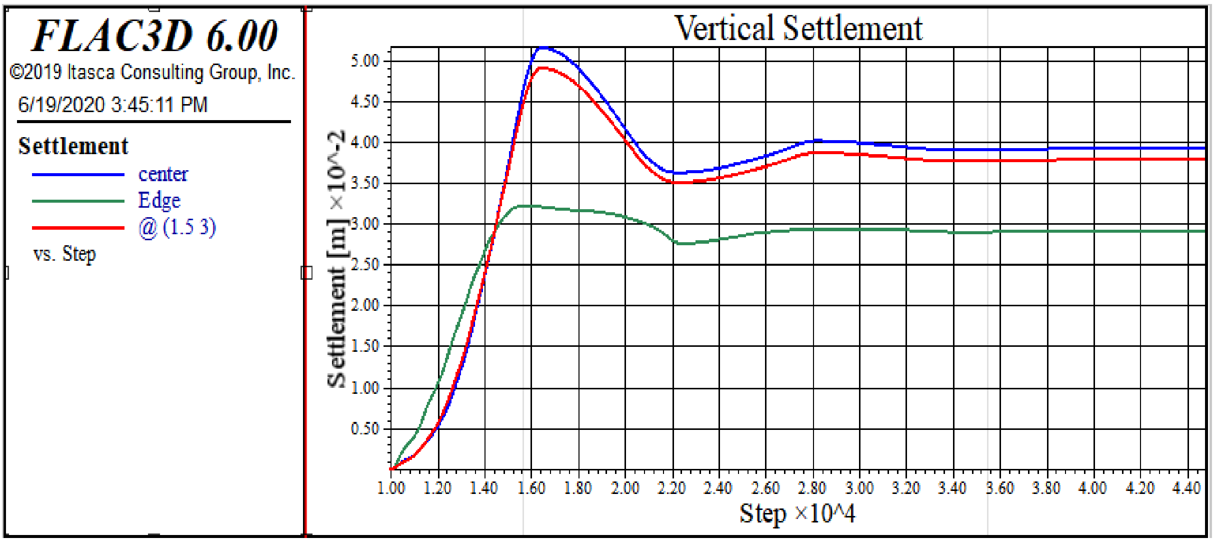
FLAC3D 6.00
©2019 Itasca Consulting Group, Inc.
6/19/2020 3:45:11 PM
Settlement
center
Edge
@ (1.5 3)
vs. Step
Vertical Settlement
Settlement [m] ×10^-2
Step ×10^4

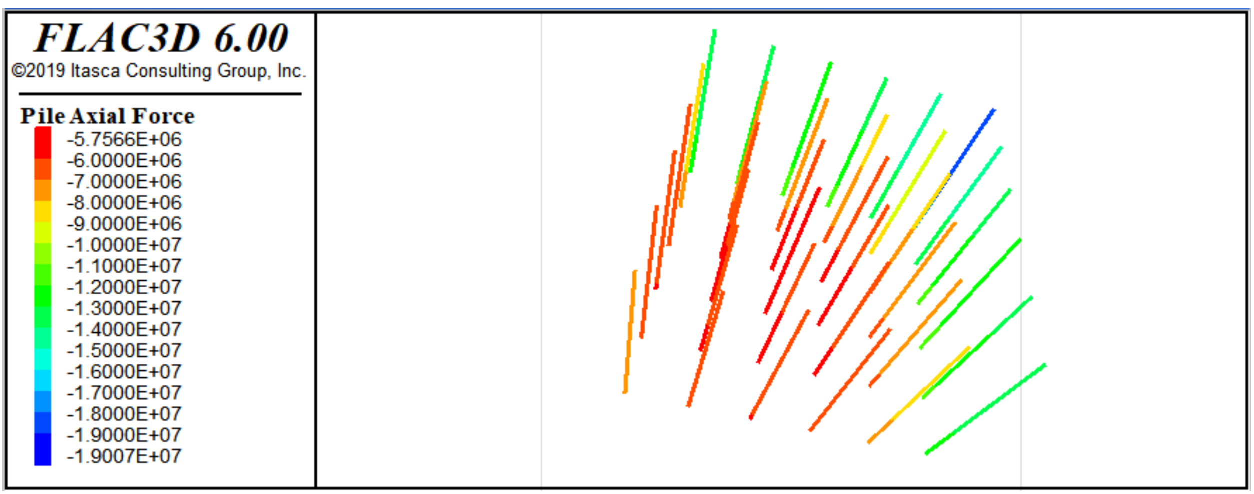
FLAC3D 6.00
©2019 Itasca Consulting Group, Inc.
Pile Axial Force
-5.7566E+06
-6.0000E+06
-7.0000E+06
-8.0000E+06
-9.0000E+06
-1.0000E+07
-1.1000E+07
-1.2000E+07
-1.3000E+07
-1.4000E+07
-1.5000E+07
-1.6000E+07
-1.7000E+07
-1.8000E+07
-1.9000E+07
-1.9007E+07

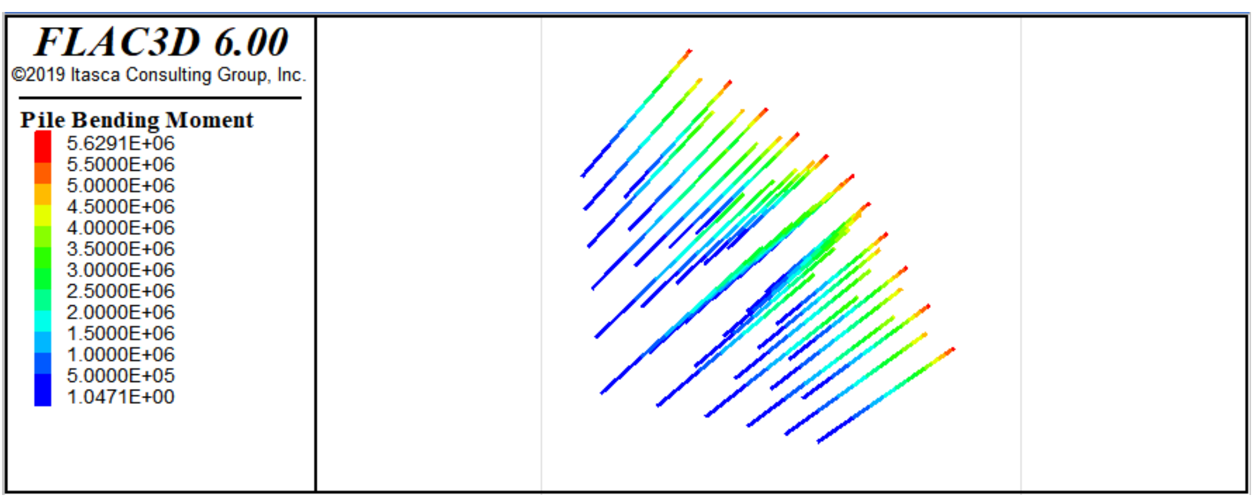
FLAC3D 6.00
©2019 Itasca Consulting Group, Inc.
Pile Bending Moment
5.6291E+06
5.5000E+06
5.0000E+06
4.5000E+06
4.0000E+06
3.5000E+06
3.0000E+06
2.5000E+06
2.0000E+06
1.5000E+06
1.0000E+06
5.0000E+05
1.0471E+00

APPENDIX 4B

In this appendix it is only displaced the code for a pile raft of 10m length, 1m diameter and 3d spacing. Other 27 codes are not displayed due to limitation of space.

```
model new
model title "PRF-1-3D"
zone creat radial-tunnel point 0 (0 0 0) ...
                         point 1 (0 50 0) ...
                         point 2 (0 0 22) ...
                         point 3 (50 0 0) dimension 21 21 fill size 28 30 28 20 ratio 1 1 1 1.1
;the size here is (x y z and then around the tunnel)
zone creat radial-tunnel point 0 (0 0 22) ...
                       point 1 (0 50 22) ...
                      point 2 (0 0 60) ...
                      point 3 (50 0 22) dimension 21 21 fill size 28 45 28 20 ratio 1 1.005 1 1.1
;the size here is (x y z and then around the tunnel)
zone attach by-face range position-z 22
;=======================================================
;===========Assign Group for each material=============
;=======================================================
zone group "exc1" range position-z 0 6.5
zone group "exc2" range position-z 6.5 16.5
zone group "exc3" range position-z 16.5 22
zone group "Highly-weathered-rock" range position-z 22 32
zone group "Rock" range position-z 32 38
zone group "weak-to-strong silty clay" range position-z 38 47
zone group "Durable rock" range position-z 47 60
;=======================================================
;===========Assigning a Constitutive Model=============
;=======================================================
; layer 1
zone cmodel assign mohr-coulomb range group "exc1"
zone cmodel assign mohr-coulomb range group "exc2"
zone cmodel assign mohr-coulomb range group "exc3"
zone cmodel assign mohr-coulomb range group "Highly-weathered-rock"
zone cmodel assign elastic range group "Rock"
zone cmodel assign mohr-coulomb range group "weak-to-strong silty clay"
zone cmodel assign elastic range group "Durable rock"
; layer 1
zone cmodel assign mohr-coulomb range group "exc1"
zone property density 1524 bulk 15.56e6 shear 6.36e6 friction 19.5 ...
cohesion 25.3e3 range group "exc1"
; layer 2-1
zone cmodel assign mohr-coulomb range group "exc2"
zone property density 1743 bulk 36.44e6 shear 12.15e6 friction 21.3 ...
cohesion 210e3 range group "exc2"
; layer 2-2
zone cmodel assign mohr-coulomb range group "exc3"
zone property density 1743 bulk 36.44e6 shear 12.15e6 friction 21.3 ...
cohesion 210e3 range group "exc3"
; layer 3
zone cmodel assign mohr-coulomb range group "Highly-weathered-rock"
zone property density 2359 bulk 88e6 shear 40.62e6 friction 31.4 ...
cohesion 28e3 range group "Highly-weathered-rock"
; layer 4
zone cmodel assign elastic range group "Rock"
zone property density 2626 young 1027e6 poisson 0.25 bulk 684.10e6 ...
shear 410.8e6  range group "Rock"
; layer 5
zone cmodel assign mohr-coulomb range group "weak-to-strong silty clay"
zone property density 1871 bulk 245.83e6 shear 100.510e6 friction 35 ...
cohesion 25e3 range group "weak-to-strong silty clay"
; layer 6
zone cmodel assign elastic range group "Durable rock"
zone property density 2887 young 1680e6 Poisson 0.25 bulk 684.10e6 ...
shear 410.8e6  range group "Durable rock"
;=======================================================
;================Apply boundary condition=============
;=======================================================
```

```
zone face apply velocity-normal 0 range position-x 0
zone face apply velocity-normal 0 range position-x 50
zone face apply velocity-normal 0 range position-y 0
zone face apply velocity-normal 0 range position-y 50
zone face apply velocity (0 0 0) range position-z 60

;=======================================================
;=================Initialize Stress=============
;=======================================================
model gravity (0,0,10)
zone initialize-stresses ratio 0.610 range  position-z 0 6.5
zone initialize-stresses ratio 0.64 range   position-z 6.5 22
zone initialize-stresses ratio 0.39 range  position-z 22 32
zone initialize-stresses ratio 0.36 range position-z 32 38
zone initialize-stresses ratio 0.43 range position-z 38 47
zone initialize-stresses ratio 0.29 range  position-z 47 60
;=======================================================
;=================Step to equilibrium===================
;=======================================================
;zone geometry-tolerance 0
model largestrain on
model history mechanical ratio
model solve ;default value of convergence will be used
model save "initial-stress-state 10-1-3D"
;=======================================================
;=================Excavation to -21m==================
;=======================================================
;the first 7m
model restore "initial-stress-state 10-1-3D"
zone relax excavate range position-z 0 7.5
model solve ratio-local 1e-3
model save 'stage1 10-1-3D'
;2nd 7m
model restore 'stage1 10-1-3D'
zone relax excavate range position-z 0 15
model solve ratio-local 1e-3
model save 'stage2 10-1-3D'
;3rd 7m
model restore 'stage2 10-1-3D'
zone relax excavate range position-z 0 22
model solve ratio-local 1e-3
model save 'End of excavation 10-1-3D'
model restore 'End of excavation 10-1-3D'
zone gridpoint initialize displacement (0 0 0)
zone gridpoint initialize velocity (0 0 0)
;=========================================================
;=================Installation of Pile===================
;=========================================================
; will consist of 36 piles(6*6) with outer edge of 3m
;=========================================================
struct pile create by-line (1.5, 1.5, 21.8922) (1.5, 1.5, 32) segments=20 id 1
struct pile create by-line (1.5, 4.5,  21.8922) (1.5, 4.5, 32) segments=20 id 2
struct pile create by-line (1.5, 7.5,  21.8922) (1.5, 7.5, 32) segments=20 id 3
struct pile create by-line (1.5, 10.5,  21.8922) (1.5, 10.5, 32) segments=20 id 4
struct pile create by-line (1.5, 13.5,  21.8922) (1.5, 13.5, 32) segments=20 id 5
struct pile create by-line (1.5, 16.5,  21.8922) (1.5, 16.5, 32) segments=20 id 6

struct pile create by-line (4.5, 1.5,  21.8922) (4.5, 1.5, 32) segments=20 id 7
struct pile create by-line (4.5, 4.5,  21.8922) (4.5, 4.5, 32) segments=20 id 8
struct pile create by-line (4.5, 7.5,  21.8922) (4.5, 7.5, 32) segments=20 id 9
struct pile create by-line (4.5, 10.5,  21.8922) (4.5, 10.5, 32) segments=20 id 10
struct pile create by-line (4.5, 13.5,  21.8922) (4.5, 13.5, 32) segments=20 id 11
struct pile create by-line (4.5, 16.5,  21.8922) (4.5, 16.5, 32) segments=20 id 12

struct pile create by-line (7.5, 1.5,  21.8922) (7.5, 1.5, 32) segments=20 id 13
struct pile create by-line (7.5, 4.5,  21.8922) (7.5, 4.5, 32) segments=20 id 14
struct pile create by-line (7.5, 7.5,  21.8922) (7.5, 7.5, 32) segments=20 id 15
```

```
struct pile create by-line (7.5, 10.5,  21.8922) (7.5, 10.5, 32) segments=20 id 16
struct pile create by-line (7.5, 13.5,  21.8922) (7.5, 13.5, 32) segments=20 id 17
struct pile create by-line (7.5, 16.5,  21.8922) (7.5, 16.5, 32) segments=20 id 18

struct pile create by-line (10.5, 1.5,  21.8922) (10.5, 1.5, 32) segments=20 id 19
struct pile create by-line (10.5, 4.5,  21.8922) (10.5, 4.5, 32) segments=20 id 20
struct pile create by-line (10.5, 7.5,  21.8922) (10.5, 7.5, 32) segments=20 id 21
struct pile create by-line (10.5, 10.5,  21.8922) (10.5, 10.5, 32) segments=20 id 22
struct pile create by-line (10.5, 13.5,  21.8922) (10.5, 13.5, 32) segments=20 id 23
struct pile create by-line (10.5, 16.5,  21.8922) (10.5, 16.5, 32) segments=20 id 24

struct pile create by-line (13.5, 1.5,  21.8922) (13.5, 1.5, 32) segments=20 id 25
struct pile create by-line (13.5, 4.5,  21.8922) (13.5, 4.5, 32) segments=20 id 26
struct pile create by-line (13.5, 7.5,  21.8922) (13.5, 7.5, 32) segments=20 id 27
struct pile create by-line (13.5, 10.5,  21.8922) (13.5, 10.5, 32) segments=20 id 28
struct pile create by-line (13.5, 13.5,  21.8922) (13.5, 13.5, 32) segments=20 id 29
struct pile create by-line (13.5, 16.5,  21.8922) (13.5, 16.5, 32) segments=20 id 30

struct pile create by-line (16.5, 1.5,  21.8922) (16.5, 1.5, 32) segments=20 id 31
struct pile create by-line (16.5, 4.5,  21.8922) (16.5, 4.5, 32) segments=20 id 32
struct pile create by-line (16.5, 7.5,  21.8922) (16.5, 7.5, 32) segments=20 id 33
struct pile create by-line (16.5, 10.5,  21.8922) (16.5, 10.5, 32) segments=20 id 34
struct pile create by-line (16.5, 13.5,  21.8922) (16.5, 13.5, 32) segments=20 id 35
struct pile create by-line (16.5, 16.5,  21.8922) (16.5, 16.5, 32) segments=20 id 36
model save "pile installed 10-1-3D"
;=========================================================
;================ Assign property for pile================
;=========================================================


struct pile property young=31.32e9 poisson=0.15 cross-sectional-area=0.7854 moi-polar=0.098 moi-y=
0.0491 moi-z=0.0491 ...
            perimeter=3.14 coupling-stiffness-shear=8e11 coupling-cohesion-shear=20e3
coupling-friction-shear=30 ...
            coupling-stiffness-normal=8e11 coupling-cohesion-normal=30e3 coupling-friction-normal=30
coupling-gap-normal=on


;=========================================================
;=========== Include end bearing  for the pile ===========
;=========================================================
struct link delete range position-z 32
struct link create target zone group 'End' range position-z 32
struct link attach x=normal-yield y=free z=free                        range group 'End'
struct link attach rotation-x=free rotation-y=free rotation-z=free        range group 'End'
struct link property  x stiffness 5.27e11 yield-compression 5.75e6  area 0.7854 range position-z 32
structure link slide on range position-z 32
;=========================================================
;=================Creat raft============================
;=========================================================
struct shell create by-quadrilateral (0,0,21.8922) (19.5,0,21.8922) (19.5,19.5,21.8922) (0,19.5,
21.8922) ...
size (26,26) id 37    ...
element-type dkt-csth cross-diagonal ;constant strain trianlge hybride
struct shell property density 2500 isotropic (31.4e9, 0.15) thick 3 ;isotropic (E, v)
;structure link tolerance-slide 0.1  range position-z 21.8922
;structure link slide on range position-z 21.8922
;=========================================================
;============Connection Raft and Soil ==================
;=========================================================
struct link delete range position-z 21.8922
struct link create target zone group 'raft_with_soil' range position-z 21.8922
struct link attach x rigid y rigid  z rigid                        range group 'raft_with_soil'
struct link attach rotation-x=free rotation-y=free rotation-z=free        range group 'raft_with_soil'
structure link slide on range group 'raft_with_soil'
```

```
;=============Connection B/N Pile and Raft================
;========================================================
structure node join range id 37

;structure link slide on range id 37 not

;=============================================================================
;=========Apply Uniform distributed Load from the S,structure================
;=============================================================================
struct shell apply 926690 range  position-x 0 19.5 position-y 0 19.5
; Set large strain on, creating coupling between bending and membrane
model largestrain on
;========================================================
;============History points to analyse the model========
;========================================================
model history mechanical ratio-local
zone history displacement-z position (0,0,21.8922)
zone history displacement-z position (1.5,3,21.8922)
zone history displacement-z position (19.5 19.5 21.8922)
;for the central pile
struct pile history name='Force(x) @ (1.5 1.5)' force-x position (1.5 ,1.5, 21.8922)
struct pile history name='Force(y) @ (1.5 1.5)' force-y position (1.5 ,1.5, 21.8922)
struct pile history name='Force (z) @ (1.5 1.5)' force-z position (1.5 ,1.5, 21.8922)
;y-axis moment
struct pile history name='Moment 1(y) @ (1.5 1.5)' moment-Y position (1.5 ,1.5, 21.8922)
struct pile history name='Moment 2(y) @ (1.5 1.5)' moment-Y position (1.5 ,1.5, 23.8922)
struct pile history name='Moment 3(y) @ (1.5 1.5)' moment-Y position (1.5 ,1.5, 25.8922)
struct pile history name='Moment 4(y) @ (1.5 1.5)' moment-Y position (1.5 ,1.5, 27.8922)
struct pile history name='Moment 5(y) @ (1.5 1.5)' moment-Y position (1.5 ,1.5, 29.8922)
struct pile history name='Moment 8(y) @ (1.5 1.5)' moment-Y position (1.5 ,1.5, 32)

;z-axis moment
struct pile history name='Moment 1(z) @ (1.5 1.5)' moment-z position (1.5 ,1.5, 21.8922)
struct pile history name='Moment 2(z) @ (1.5 1.5)' moment-z position (1.5 ,1.5, 23.8922)
struct pile history name='Moment 3(z) @ (1.5 1.5)' moment-z position (1.5 ,1.5, 25.8922)
struct pile history name='Moment 4(z) @ (1.5 1.5)' moment-z position (1.5 ,1.5, 27.8922)
struct pile history name='Moment 5(z) @ (1.5 1.5)' moment-z position (1.5 ,1.5, 29.8922)
struct pile history name='Moment 6(z) @ (1.5 1.5)' moment-z position (1.5 ,1.5, 32)

struct node history name='Disp(y) @ (1.5 1.5)'displacement-y position (1.5,1.5,21.8922)
struct node history name='Disp(z) @ (1.5 1.5)'displacement-z position (1.5,1.5,21.8922)
;for the pile at the edge of the group
struct pile history name='Force @ (x) (16.5 16.5)' force-x position (16.5 ,16.5, 21.8922)
struct pile history name='Force @ (y)(16.5 16.5)' force-y position (16.5 ,16.5, 21.8922)
struct pile history name='Force @ (z) (16.5 16.5)'force-z position (16.5 ,16.5, 21.8922)
; y-axis moment
struct pile history name='Moment @ 1(y) (16.5 16.5)' moment-Y position (16.5 ,16.5, 21.8922)
struct pile history name='Moment @ 2(y) (16.5 16.5)' moment-Y position (16.5 ,16.5, 23.8922)
struct pile history name='Moment @ 3(y) (16.5 16.5)' moment-Y position (16.5 ,16.5, 25.8922)
struct pile history name='Moment @ 4(y) (16.5 16.5)' moment-Y position (16.5 ,16.5, 27.8922)
struct pile history name='Moment @ 5(y) (16.5 16.5)' moment-Y position (16.5 ,16.5, 29.8922)
struct pile history name='Moment @ 6(y) (16.5 16.5)' moment-Y position (16.5 ,16.5, 32)
; z-axis moment
struct pile history name='Moment @ 1(z) (16.5 16.5)' moment-z position (16.5 ,16.5, 21.8922)
struct pile history name='Moment @ 2(z) (16.5 16.5)' moment-z position (16.5 ,16.5, 23.8922)
struct pile history name='Moment @ 3(z) (16.5 16.5)' moment-z position (16.5 ,16.5, 25.8922)
struct pile history name='Moment @ 4(z) (16.5 16.5)' moment-z position (16.5 ,16.5, 27.8922)
struct pile history name='Moment @ 5(z) (16.5 16.5)' moment-z position (16.5 ,16.5, 29.8922)
struct pile history name='Moment @ 6(z) (16.5 16.5)' moment-z position (16.5 ,16.5, 32)

struct node history name='Disp(y) @ (16.5 16.5)'displacement-y position (16.5,16.5,21.8922)
struct node history name='Disp(z) @ (16.5 16.5)'displacement-z position (16.5,16.5,21.8922)

;========================================================
;============Solving the model==========================
;========================================================
model solve ratio-local=1e-3
```

```
;=============Save the model===============================
;==========================================================
model save 'PRF-10-1-3D'
```

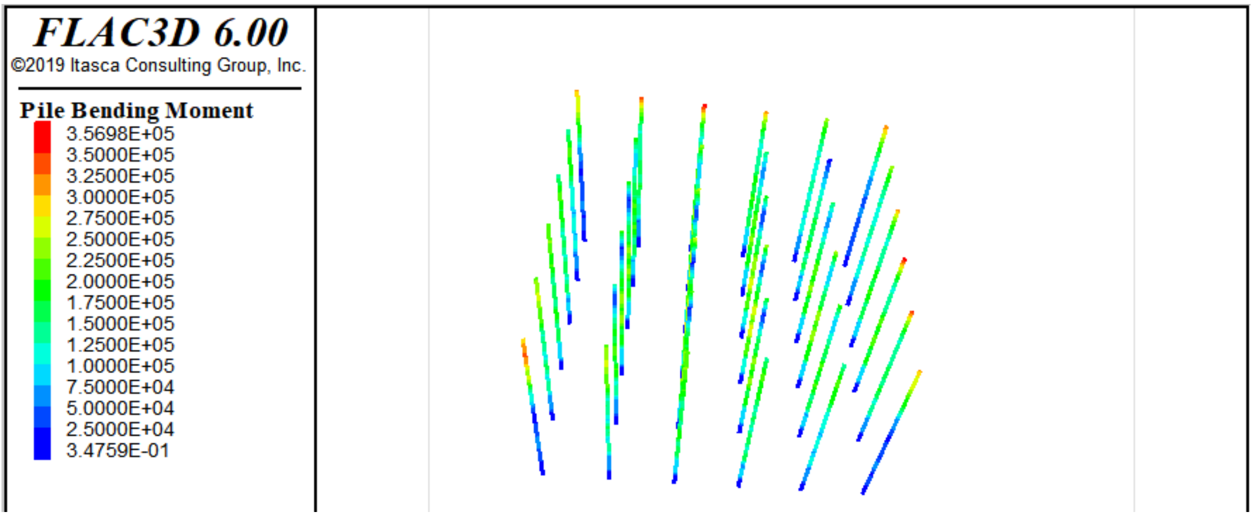

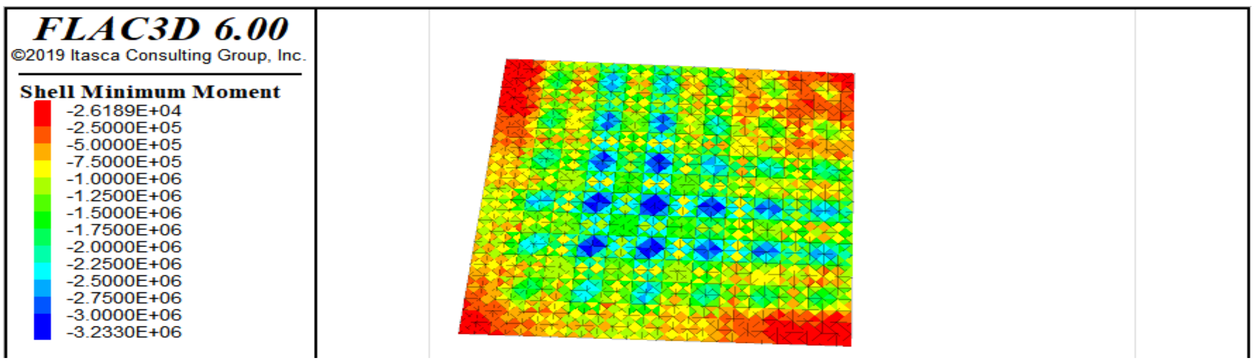

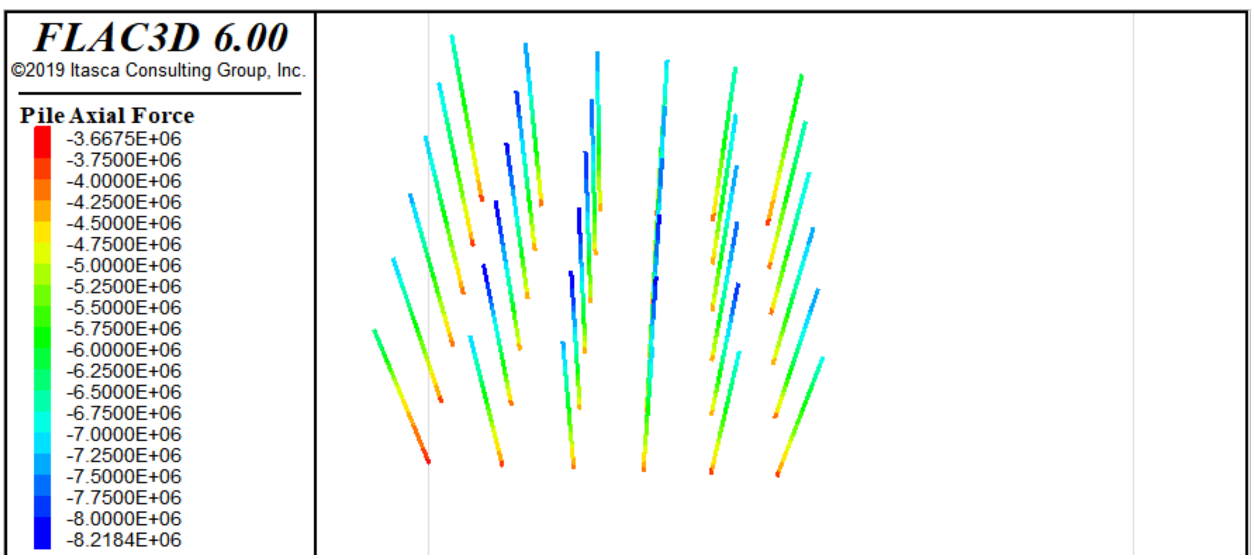

APPENDIX 4C

Coding sequence for optimized design of piled raft foundation.

```
model new
model title "PRF-1-3D"
zone creat radial-tunnel point 0 (0 0 0) ...
                         point 1 (0 50 0) ...
                         point 2 (0 0 22) ...
                         point 3 (50 0 0) dimension 21 21 fill size 28 30 28 20 ratio 1 1 1 1.1
;the size here is (x y z and then around the tunnel)
zone creat radial-tunnel point 0 (0 0 22) ...
                       point 1 (0 50 22) ...
                      point 2 (0 0 60) ...
                      point 3 (50 0 22) dimension 21 21 fill size 28 45 28 20 ratio 1 1.005 1 1.1
;the size here is (x y z and then around the tunnel)
zone attach by-face range position-z 22
model save 'geometry for 10-1-3D'
;=======================================================
;===========Assign Group for each material=============
;=======================================================
zone group "exc1" range position-z 0 6.5
zone group "exc2" range position-z 6.5 16.5
zone group "exc3" range position-z 16.5 22
zone group "Highly-weathered-rock" range position-z 22 32
zone group "Rock" range position-z 32 38
zone group "weak-to-strong silty clay" range position-z 38 47
zone group "Durable rock" range position-z 47 60
;=======================================================
;===========Assigning a Constitutive Model=============
;=======================================================
; layer 1
zone cmodel assign mohr-coulomb range group "exc1"
zone property density 1524 bulk 15.56e6 shear 6.36e6 friction 19.5 ...
cohesion 25.3e3 range group "exc1"
; layer 2-1
zone cmodel assign mohr-coulomb range group "exc2"
zone property density 1743 bulk 36.44e6 shear 12.15e6 friction 21.3 ...
cohesion 210e3 range group "exc2"
; layer 2-2
zone cmodel assign mohr-coulomb range group "exc3"
zone property density 1743 bulk 36.44e6 shear 12.15e6 friction 21.3 ...
cohesion 210e3 range group "exc3"
; layer 3
zone cmodel assign mohr-coulomb range group "Highly-weathered-rock"
zone property density 2359 bulk 88e6 shear 40.62e6 friction 31.4 ...
cohesion 28e3 range group "Highly-weathered-rock"
; layer 4
zone cmodel assign elastic range group "Rock"
zone property density 2626 young 1027e6 poisson 0.25 bulk 684.10e6 ...
shear 410.8e6  range group "Rock"
; layer 5
zone cmodel assign mohr-coulomb range group "weak-to-strong silty clay"
zone property density 1871 bulk 245.83e6 shear 100.510e6 friction 35 ...
cohesion 25e3 range group "weak-to-strong silty clay"
; layer 6
zone cmodel assign elastic range group "Durable rock"
zone property density 2887 young 1680e6 Poisson 0.25 bulk 684.10e6 ...
shear 410.8e6  range group "Durable rock"
;=======================================================
;=================Apply boundary condition=============
;=======================================================
zone face apply velocity-normal 0 range position-x 0
zone face apply velocity-normal 0 range position-x 50
zone face apply velocity-normal 0 range position-y 0
zone face apply velocity-normal 0 range position-y 50
zone face apply velocity (0 0 0) range position-z 60
```

```
;=================Initialize Stress==============
;=======================================================
model gravity (0,0,10)
zone initialize-stresses ratio 0.610 range  position-z 0 6.5
zone initialize-stresses ratio 0.64 range   position-z 6.5 22
zone initialize-stresses ratio 0.39 range  position-z 22 32
zone initialize-stresses ratio 0.36 range position-z 32 38
zone initialize-stresses ratio 0.43 range position-z 38 47
zone initialize-stresses ratio 0.29 range  position-z 47 60
;=======================================================
;=================Step to equilibrium====================
;=======================================================
;zone geometry-tolerance 0
model largestrain on
model history mechanical ratio
model solve ;default value of convergence will be used
model save "initial-stress-state 10-1-3D"
;=======================================================
;=================Excavation to -21m===================
;=======================================================
;the first 7m
model restore "initial-stress-state 10-1-3D"
zone relax excavate range position-z 0 7.5
model solve ratio-local 1e-3
model save 'stage1 10-1-3D'
;2nd 7m
model restore 'stage1 10-1-3D'
zone relax excavate range position-z 0 15
model solve ratio-local 1e-3
model save 'stage2 10-1-3D'
;3rd 7m
model restore 'stage2 10-1-3D'
zone relax excavate range position-z 0 22
model solve ratio-local 1e-3
model save 'End of excavation 10-1-3D'
model restore 'End of excavation 10-1-3D'
zone gridpoint initialize displacement (0 0 0)
zone gridpoint initialize velocity (0 0 0)
;=========================================================
;=================Installation of Pile====================
;=========================================================
; will consist of 36 piles(6*6) with outer edge of 3m
;=========================================================
struct pile create by-line (1.5, 1.5, 21.8922) (1.5, 1.5, 32) segments=20 id 1
struct pile create by-line (1.5, 4.5,  21.8922) (1.5, 4.5, 32) segments=20 id 2
struct pile create by-line (1.5, 7.5,  21.8922) (1.5, 7.5, 32) segments=20 id 3

struct pile create by-line (4.5, 1.5,  21.8922) (4.5, 1.5, 32) segments=20 id 7
struct pile create by-line (4.5, 4.5,  21.8922) (4.5, 4.5, 32) segments=20 id 8
struct pile create by-line (4.5, 7.5,  21.8922) (4.5, 7.5, 32) segments=20 id 9

struct pile create by-line (7.5, 1.5,  21.8922) (7.5, 1.5, 32) segments=20 id 13
struct pile create by-line (7.5, 4.5,  21.8922) (7.5, 4.5, 32) segments=20 id 14
struct pile create by-line (7.5, 7.5,  21.8922) (7.5, 7.5, 32) segments=20 id 15

;outer round
struct pile create by-line (18.75,18.75,  21.8922) (18.75,18.75, 32) segments=20

struct pile create by-line (18.75,12.75,  21.8922) (18.75,12.75, 32) segments=20

struct pile create by-line (18.75,6.75,  21.8922) (18.75,6.75, 32) segments=20

struct pile create by-line (18.75,0.75,  21.8922) (18.75,0.75, 32) segments=20

struct pile create by-line (12.75,18.75,  21.8922) (12.75,18.75, 32) segments=20

struct pile create by-line (6.75,18.75,  21.8922) (6.75,18.75, 32) segments=20
```

```
struct pile create by-line (0.75,18.75,  21.8922) (0.75,18.75, 32) segments=20
;inner round
;struct pile create by-line (15.75,15.75,  21.8922) (15.75,15.75, 32) segments=20

struct pile create by-line (15.75,12.75,  21.8922) (15.75,12.75, 32) segments=20

struct pile create by-line (15.75,6.75,  21.8922) (15.75,6.75, 32) segments=20

struct pile create by-line (15.75,0.75,  21.8922) (15.75,0.75, 32) segments=20

struct pile create by-line (12.75,15.75,  21.8922) (12.75,15.75, 32) segments=20

struct pile create by-line (6.75,15.75,  21.8922) (6.75,15.75, 32) segments=20

struct pile create by-line (0.75,15.75,  21.8922) (0.75,15.75, 32) segments=20

model save "pile installed second-Opt-10-1-3D"
;==========================================================
;================ Assign property for pile================
;==========================================================


struct pile property young=31.32e9 poisson=0.15 cross-sectional-area=0.7854 moi-polar=0.098 moi-y=
0.0491 moi-z=0.0491 ...
            perimeter=3.14 coupling-stiffness-shear=8e11 coupling-cohesion-shear=20e3
coupling-friction-shear=30 ...
            coupling-stiffness-normal=8e11 coupling-cohesion-normal=30e3 coupling-friction-normal=30
coupling-gap-normal=on


;==========================================================
;=========== Include end bearing  for the pile ===========
;==========================================================
struct link delete range position-z 32
struct link create target zone group 'End' range position-z 32
struct link attach x=normal-yield y=free z=free                           range group 'End'
struct link attach rotation-x=free rotation-y=free rotation-z=free        range group 'End'
struct link property  x stiffness 5.27e11 yield-compression 5.75e6  area 0.7854 range position-z 32
structure link slide on range position-z 32
;==========================================================
;=================Creat raft==============================
;==========================================================
struct shell create by-quadrilateral (0,0,21.8922) (19.5,0,21.8922) (19.5,19.5,21.8922) (0,19.5,
21.8922) ...
size (26,26) id 37    ...
element-type dkt-csth cross-diagonal ;constant strain trianlge hybride
struct shell property density 2500 isotropic (31.4e9, 0.15) thick 3 ;isotropic (E, v)
;structure link tolerance-slide 0.1  range position-z 21.8922
;structure link slide on range position-z 21.8922
;==========================================================
;=============Connection Raft and Soil ==================
;==========================================================
struct link delete range position-z 21.8922
struct link create target zone group 'raft_with_soil' range position-z 21.8922
struct link attach x rigid y rigid  z rigid                          range group 'raft_with_soil'
struct link attach rotation-x=free rotation-y=free rotation-z=free        range group 'raft_with_soil'
structure link slide on range group 'raft_with_soil'

;==========================================================
;=============Connection B/N Pile and Raft===============
;==========================================================
structure node join range id 37

;structure link slide on range id 37 not

;============================================================================
```

```
;=========Apply Uniform distributed Load from the S,structure===============
;==========================================================================
struct shell apply 926690 range  position-x 0 19.5 position-y 0 19.5
; Set large strain on, creating coupling between bending and membrane
model largestrain on
;=========================================================
;=============History points to analyse the model========
;=========================================================
model history mechanical ratio-local
zone history displacement-z position (0,0,21.8922)
zone history displacement-z position (1.5,3,21.8922)
zone history displacement-z position (19.5 19.5 21.8922)
zone history displacement-z position (9.75 9.75 21.8922)
zone history displacement-z position (15.75 15.75 21.8922)

;for the central pile
struct pile history name='Force(x) @ (1.5 1.5)' force-x position (1.5 ,1.5, 21.8922)
struct pile history name='Force(y) @ (1.5 1.5)' force-y position (1.5 ,1.5, 21.8922)
struct pile history name='Force (z) @ (1.5 1.5)' force-z position (1.5 ,1.5, 21.8922)
;y-axis moment
struct pile history name='Moment 1(y) @ (1.5 1.5)' moment-Y position (1.5 ,1.5, 21.8922)
struct pile history name='Moment 2(y) @ (1.5 1.5)' moment-Y position (1.5 ,1.5, 23.8922)
struct pile history name='Moment 3(y) @ (1.5 1.5)' moment-Y position (1.5 ,1.5, 25.8922)
struct pile history name='Moment 4(y) @ (1.5 1.5)' moment-Y position (1.5 ,1.5, 27.8922)
struct pile history name='Moment 5(y) @ (1.5 1.5)' moment-Y position (1.5 ,1.5, 29.8922)
struct pile history name='Moment 8(y) @ (1.5 1.5)' moment-Y position (1.5 ,1.5, 32)

;z-axis moment
struct pile history name='Moment 1(z) @ (1.5 1.5)' moment-z position (1.5 ,1.5, 21.8922)
struct pile history name='Moment 2(z) @ (1.5 1.5)' moment-z position (1.5 ,1.5, 23.8922)
struct pile history name='Moment 3(z) @ (1.5 1.5)' moment-z position (1.5 ,1.5, 25.8922)
struct pile history name='Moment 4(z) @ (1.5 1.5)' moment-z position (1.5 ,1.5, 27.8922)
struct pile history name='Moment 5(z) @ (1.5 1.5)' moment-z position (1.5 ,1.5, 29.8922)
struct pile history name='Moment 6(z) @ (1.5 1.5)' moment-z position (1.5 ,1.5, 32)

struct node history name='Disp(y) @ (1.5 1.5)'displacement-y position (1.5,1.5,21.8922)
struct node history name='Disp(z) @ (1.5 1.5)'displacement-z position (1.5,1.5,21.8922)
;=========================================================
;=============Solving the model==========================
;=========================================================
model solve ratio-local=1e-3
;=========================================================
;=============Save the model=============================
;=========================================================
model save 'second-OPT-PRF-10-1-3D'

=====================================================
=====================================================
=====================================================
```

APPENDIX 4D

Friction piled raft under the 1940 El Centro earthquake with 3 m/sec^2 excitation is shown here.

```
;=================================================================
;======= Creat the geometric grid for the pile raft==============
;=================================================================
model new
model config dynamic
model dynamic active off
;creating raft
zone create radial-cylinder point 0 (3,11,30)  point 1 (3,12.5,30) ...
                           point 2 (3,11,30.5) point 3 (4.5,11,30) ...
                           group 'raft' size 2 1 2 2 dim 0.6 0.6 0.6 0.6 ratio 1.05 1.15 1 1.15 fill
;=========================
zone create radial-cylinder point 0 (3,11,23.5)   point 1 (3,12.5,23.5)   ...
                              point 2 (3,11,30)  point 3 (4.5,11,23.5)   ...
                              group 'layer 1 above' size 2 7 2 2 dim 0.6 0.6 0.6 0.6  ratio 1.05 1 1
1.15 fill group 'pile'
zone create radial-cylinder point 0 (3,11,20)   point 1 (3,12.5,20)   ...
                              point 2 (3,11,23.5)  point 3 (4.5,11,20)   ...
                              group 'layer 1 below' size 2 3 2 2 dim 0.6 0.6 0.6 0.6  ratio 1.05 0.95
 1 1.15 fill group 'pile'
;creating underlaying soil below the pile
zone create radial-cylinder point 0 (3,11,0)   point 1 (3,12.5,0)   ...
                              point 2 (3,11,20)  point 3 (4.5,11,0)   ...
                              size 2 13 2 2 dim 0.6 0.6 0.6 0.6  ratio 1.05 0.95 1 1.15 fill

zone reflect dip 90 dip-direction 90 origin (3,11,0)
zone reflect dip 90 origin (3,11,0)
zone copy 0 3 0 range position-x 1.5 4.5 position-y 9.5 12.5 position-z 0 30.5
zone copy 0 6 0 range position-x 1.5 4.5 position-y 9.5 12.5 position-z 0 30.5
zone copy 3 0 0 range position-x 1.5 4.5 position-y 9.5 12.5 position-z 0 30.5
zone copy 6 0 0 range position-x 1.5 4.5 position-y 9.5 12.5 position-z 0 30.5
zone copy 3 3 0 range position-x 1.5 4.5 position-y 9.5 12.5 position-z 0 30.5
zone copy 6 3 0 range position-x 1.5 4.5 position-y 9.5 12.5 position-z 0 30.5
zone copy 3 6 0 range position-x 1.5 4.5 position-y 9.5 12.5 position-z 0 30.5
zone copy 6 6 0 range position-x 1.5 4.5 position-y 9.5 12.5 position-z 0 30.5
;front brick
zone creat brick point 0 0 .5 23.5 point 1 0 9.5 23.5 ...
                 point 2 0 0.5 30 point 3 12 0.5 23.5 size 6 7 8 ratio 1 1 1 group 'layer 1 above'
zone creat brick point 0 0 0.5 20 point 1 0 9.5 20 ...
                point 2 0 0.5 23.5 point 3 12 0.5 20 size 6 3 8 ratio 1 0.95 1 group 'layer 1 below'
zone creat brick point 0 0 0.5 0 point 1 0 9.5 0 ...
                 point 2 0 0.5 20 point 3 12 0.5 0 size 6 13 8 ratio 1 0.95 1
;last brick on the other end
zone creat brick point 0 0 18.5 23.5 point 1 0 30.5 23.5 ...
                 point 2 0 18.5 30 point 3 12 18.5 23.5 size 8 7 8 ratio 1 1 1 group 'layer 1 above'
zone creat brick point 0 0 18.5 20 point 1 0 30.5 20 ...
                 point 2 0 18.5 23.5 point 3 12 18.5 20 size 8 3 8 ratio 1 0.95 1 group 'layer 1
below'
zone creat brick point 0 0 18.5 0 point 1 0 30.5 0 ...
                 point 2 0 18.5 20 point 3 12 18.5 0 size 8 13 8 ratio 1 0.95 1
;sides having only one by eight (2*10) dimension
;front side
zone creat brick point 0 0 9.5 23.5 point 1 0 18.5 23.5 ...
                 point 2 0 9.5 30 point 3 1.5 9.5 23.5 size 6 7 1 ratio 1 1 1 group 'layer 1 above'
zone creat brick point 0 0 9.5 20 point 1 0 18.5 20 ...
                  point 2 0 9.5 23.5 point 3 1.5 9.5 20 size 6 3 1 ratio 1 0.95 1 group 'layer 1
below'
zone creat brick point 0 0 9.5 0 point 1 0 18.5 0 ...
                 point 2 0 9.5 20 point 3 1.5 9.5 0 size 6 13 1 ratio 1 0.95 1
; the back side
zone creat brick point 0 10.5 9.5 23.5 point 1 10.5 18.5 23.5 ...
                 point 2 10.5 9.5 30 point 3 12 9.5 23.5 size 6 7 1 ratio 1 1 1 group 'layer 1 above'
zone creat brick point 0 10.5 9.5 20 point 1 10.5 18.5 20 ...
                 point 2 10.5 9.5 23.5 point 3 12 9.5 20 size 6 3 1 ratio 1 0.95 1 group 'layer 1
below'
zone creat brick point 0 10.5 9.5 0 point 1 10.5 18.5 0 ...
```

```
                    point 2 10.5 9.5 20 point 3 12 9.5 0 size 6 13 1 ratio 1 0.95 1
   zone face skin

;===============================================
;=========assign group for each layer==========
;==================================================
zone group "layer 2" range position-z 8 20
zone group "layer 3" range position-z 0 8
;========================================================
;==========Assigning a Constitutive Model=============
;========================================================
; layer 1
zone cmodel assign mohr-coulomb range group "layer 1 above"
zone cmodel assign mohr-coulomb range group "layer 1 below"
zone cmodel assign mohr-coulomb range group "layer 2"
zone cmodel assign mohr-coulomb range group "layer 3"
zone cmodel assign elastic range group "pile" or "raft"
;raft
;zone cmodel assign elastic range union group "raft" or "pile"
;zone property density 2500 bulk 14.94e7 shear 13.64e7 range union group "raft" or "pile"
;layer 3
fish define layer3(y_zero3)
    loop foreach pnt zone.list
        z_depth = -(zone.pos.z(pnt)-30)
        if zone.pos.z(pnt)  <= 8 then
          y_mod3 = y_zero3 + 2.54e6 * (z_depth) - 0.02638e6 * (z_depth) * (z_depth)
          zone.prop(pnt,'young') = y_mod3
        else
        end_if
    end_loop
end
@layer3(77.54e6)

;layer 1 and 2
fish define exc1(y_zero1)
    loop foreach pnt zone.list
        z_depth = -(zone.pos.z(pnt)-30)
        if zone.pos.z(pnt) > 8 and <= 30 then
         y_mod1 = y_zero1 + 3.6344e6 * (z_depth) - 0.1532e6 * (z_depth)^2 + 0.0022e6 * (z_depth)^3
         zone.prop(pnt,'young') = y_mod1
        else
        end_if
    end_loop
end
@exc1(6.1505e6)
;raft and pile
zone cmodel assign elastic range union group "raft" or "pile"
zone property density 2500 poissn 0.15 bulk 14.94e9 shear 13.64e9 range union group "raft" or "pile"

zone property poisson 0.32 density 1524 friction 19.5 cohesion 25.3e3 range group "layer 1 above"
zone property poisson 0.35 density 1743 friction 21.3 cohesion 27e3 range group "layer 1 below" or
"layer 2"
zone property poisson 0.3 density 2359 friction 31.4 cohesion 28e3 range group "layer 3"


;separate automatic connection for interface mdeling
zone separate by-face range group  "layer 1 above" group "pile"
zone separate by-face range group  "layer 1 below" group "pile"
zone separate by-face range group  "layer 2" group "pile"
zone separate by-face range group  "raft" group "layer 1 above"
;interface mdeling
zone interface 'pile-skin' create by-face range group 'pile'
zone interface 'pile-skin' node property stiffness-normal 1651.6e9 ...
                                     stiffness-shear 1651.6e9 ...
                                     tension 0
```

```
zone interface "raft-soil" create by-face range  group "raft" position-z 30
zone interface "raft-soil" node property stiffness-normal 330.3e9 ...
                                     stiffness-shear 330.3e9 ...
                                     tension 0
;=========================================================
;=============Connection Raft and pile ===================
;=========================================================
zone attach by-face range union group "raft" or "pile"
zone face skin
 ;==========================================================
;=========Apply Uniform distributed Load on the raft =======
;==========================================================
zone face apply stress-zz -101000 range position-z 30.5

;=======================================================
;=================Apply boundary condition=============
;=======================================================
zone face apply velocity-normal 0 range position-x 0
zone face apply velocity-normal 0 range position-x 12
zone face apply velocity-normal 0 range position-y 0.5
zone face apply velocity-normal 0 range position-y 30.5
zone face apply velocity (0 0 0) range position-z 0
;=======================================================
;=================Initialize Stress====================
;=======================================================
model gravity (0 0 -9.81)
zone initialize-stresses ratio 0.39 range position-z 0 8
zone initialize-stresses ratio 0.64 range position-z 8 20
zone initialize-stresses ratio 0.61 range position-z 20 30
;=============================================
;===========water table======================
;=============================================
zone water plane origin (0,0,23.5) normal (0,0,-1)
zone water density 1000
;=========================================================
;=================Step to equilibrium====================
;=========================================================
model history mechanical ratio
model solve ratio-local 1e-3
model save "initial static PRF floating 0.3g"


;===============================
;==============================================================
;=== Dynamic excitation of PRF - coupled simulation=============
;==============================================================
model restore "initial static PRF floating 0.3g"
model dynamic active=on
model largestrain on
; Apply free field/source from external
zone dynamic free-field on
; Apply dynamic boundary conditions
table 'El Centro' import '1940 El Centro f.TAB'
zone face apply velocity (0 0.67 0) table 'El Centro' range position-z=0 ; scaled to 0.2g/0.3g
; Reset velocities and displacements
zone gridpoint initialize velocity (0,0,0)
zone gridpoint initialize displacement (0,0,0)

;
model history name='time' dynamic time-total
zone history name='acc-base' acceleration-y position (0,0.5,0)
zone history name='acc-top' acceleration-y position (0,0.5, 30)
zone history name='velo-base' velocity-y position (12,30,0)
zone history name='velo-top' velocity-y position (12,30, 30)

zone history name='acc-top-raft' acceleration-y position (6,15, 30.25)
```

```
zone history name='pile head 3-3/30' displacement-y position (9,19,30)
zone history name='pile head 3-3/27.5' displacement-y position (9,19,27.5)
zone history name='pile head 3-3/25' displacement-y position (9,19,25)
zone history name='pile head 3-3/22.5' displacement-y position (9,19,22.5)
zone history name='pile head 3-3/20' displacement-y position (9,19,20)


zone history name='pp3' pore-pressure position (6,15,23.5)
zone history name='pp4' pore-pressure position (6,15,15)
; Set rayliegh damping 5% for zones
zone dynamic damping rayleigh 0.05 2 range position-z 0 30.5
zone dynamic multi-step on
model solve time-total 5
model save 'Dynamic PRF float el centro 0.3g 1'
model restore 'Dynamic PRF float el centro 0.3g 1'
model solve time-total 10
model save 'Dynamic PRF float el centro 0.3g 2'
model restore 'Dynamic PRF float el centro 0.3g 2'
model solve time-total 15
model save 'Dynamic PRF float el centro 0.3g 3'
model restore 'Dynamic PRF float el centro 0.3g 3'
model solve time-total 20
model save 'Dynamic PRF float el centro 0.3g 4'
model restore 'Dynamic PRF float el centro 0.3g 4'
model solve time-total 25
model save 'Dynamic PRF float el centro 0.3g 5'
model restore 'Dynamic PRF float el centro 0.3g 5'
model solve time-total 30
model save 'Dynamic PRF float el centro 0.3g 6'
model restore 'Dynamic PRF float el centro 0.3g 6'
model solve time-total 35
model save 'Dynamic PRF float el centro 0.3g 7'
model restore 'Dynamic PRF float el centro 0.3g 7'
model solve time-total 40
model save 'Dynamic PRF float el centro 0.3g 8'
model restore 'Dynamic PRF float el centro 0.3g 8'
model solve time-total 45
model save 'Dynamic PRF float el centro 0.3g 9'
model restore 'Dynamic PRF float el centro 0.3g 9'
model solve time-total 50
model save 'Dynamic PRF float el centro 0.3g 10'
model restore 'Dynamic PRF float el centro 0.3g 10'
model solve time-total 54
model save 'Dynamic PRF float el centro 0.3g 11'
```

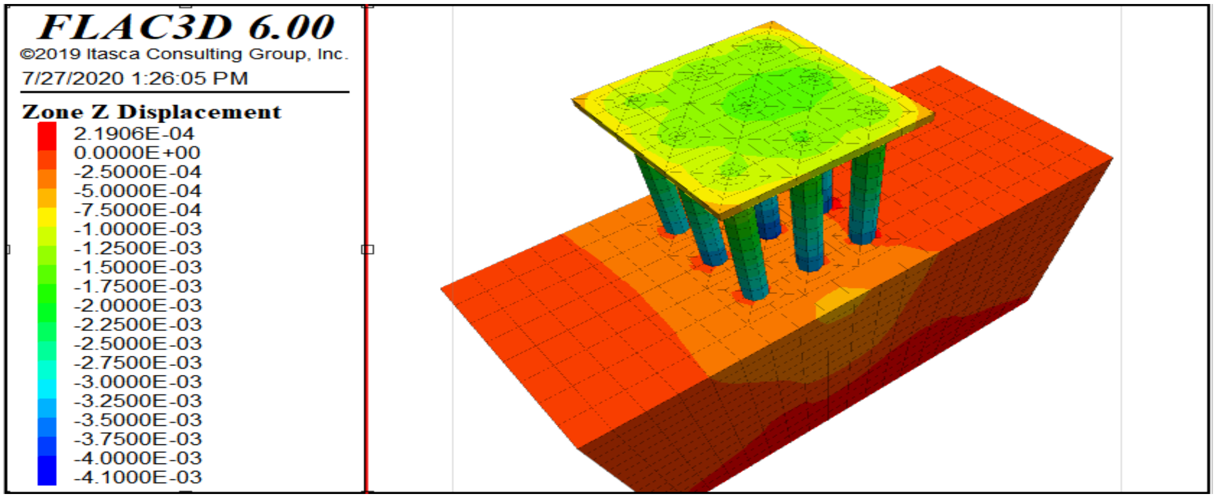
FLAC3D 6.00
©2019 Itasca Consulting Group, Inc.
7/27/2020 1:26:05 PM
Zone Z Displacement
2.1906E-04
0.0000E+00
-2.5000E-04
-5.0000E-04
-7.5000E-04
-1.0000E-03
-1.2500E-03
-1.5000E-03
-1.7500E-03
-2.0000E-03
-2.2500E-03
-2.5000E-03
-2.7500E-03
-3.0000E-03
-3.2500E-03
-3.5000E-03
-3.7500E-03
-4.0000E-03
-4.1000E-03

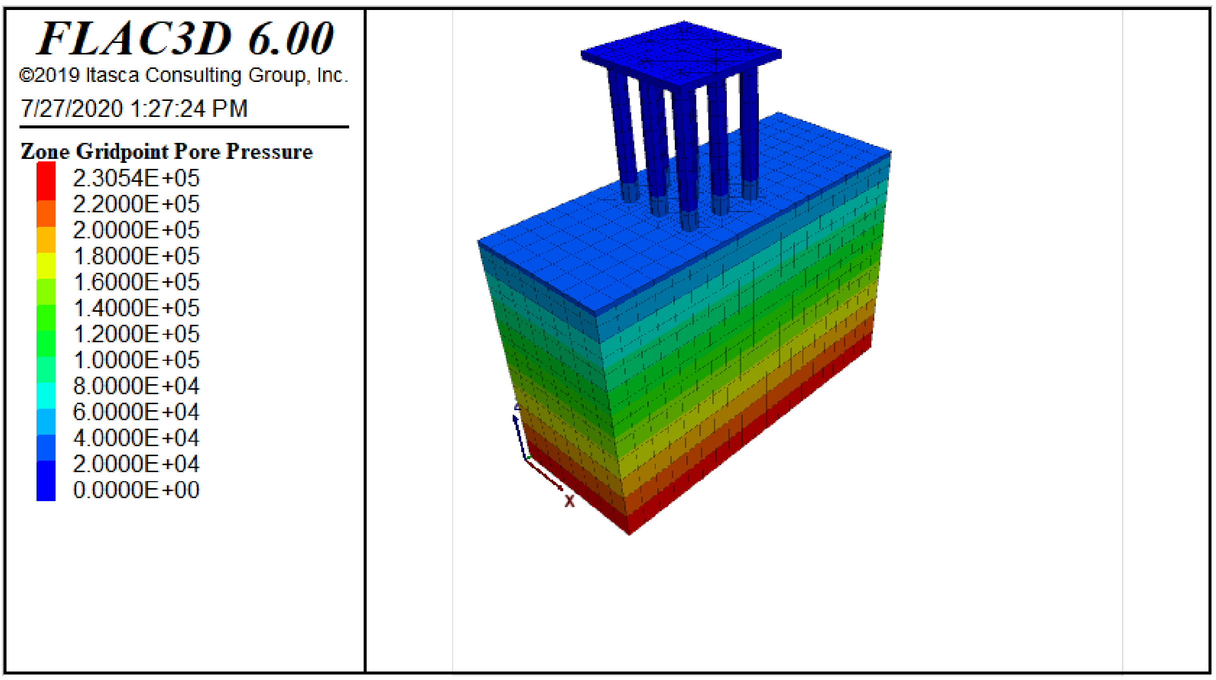
FLAC3D 6.00
©2019 Itasca Consulting Group, Inc.
7/27/2020 1:27:24 PM
Zone Gridpoint Pore Pressure
2.3054E+05
2.2000E+05
2.0000E+05
1.8000E+05
1.6000E+05
1.4000E+05
1.2000E+05
1.0000E+05
8.0000E+04
6.0000E+04
4.0000E+04
2.0000E+04
0.0000E+00
X

APPENDIX 4E

The code for validation of static numerical studies is presented here with settlement at the center for three different static vertical loads on the raft.

```
FILE: validation.f3dat, DATE: Wed Jul 1 22:07:58 2020
----------------------------------------------------
model new
zone creat radial-tunnel point 0 (0 0 0) ...
                         point 1 (0 10 0) ...
                         point 2 (0 0 20) ...
                         point 3 (10 0 0) dimension 5 3 fill size 20 30 12 10 ratio 1 1.05 1 1.1
zone creat brick  point 0 (0 0 -0.5) ...
                         point 1 (0 5 -0.5) ...
                         point 2 (0 0 0) ...
                         point 3 (3 0 -0.5)  size 20 2 12 ratio 1 1.05 1
zone face skin
;=======================================================
;==========Assign Group for each material=============
;=======================================================
zone group "soil" range position-z 0 20
zone group "pile" range  position-x 0.75 1.25 position-y 1.75 2.25 position-z 0 10
zone group "pile" range  position-y  0 0.25 position-x 0 0.25  position-z 0 10
zone group "pile" range position-y 1.75 2.25 position-x 0 0.25 position-z 0 10
zone group "pile" range position-y 0 0.25  position-x 0.75 1.25  position-z 0 10
zone group "raft" range position-z -0.5 0
;=======================================================
;==========Assigning a Constitutive Model=============
;=======================================================
; layer 1
zone cmodel assign elastic range group "soil"
zone property density 1700 bulk 16.6e6 shear 6.7e6 range group "soil"
zone cmodel assign elastic range union group "pile" group "raft"
zone property density 2500 bulk 16.6e9 shear 12.5e9 range union group "pile" group "raft"

;=======================================================
;================Apply boundary condition=============
;=======================================================
zone face apply velocity-normal 0 range position-x 0
zone face apply velocity-normal 0 range position-x 10
zone face apply velocity-normal 0 range position-y 0
zone face apply velocity-normal 0 range position-y 10
zone face apply velocity (0 0 0) range position-z 20
;=======================================================
;================Initialize Stress=============
;=======================================================
model gravity (0,0,10)
;=======================================================
;================Step to equilibrium===================
;=======================================================
;zone geometry-tolerance 0
model largestrain on
model history mechanical ratio
model solve ratio-local 1e-4 ;default value of convergence will be used
model save "validation"
;=======================================================
;======validation for 5MN LOAD========================
;=======================================================
model restore "validation"
zone gridpoint  initialize velocity (0 0 0)
zone gridpoint  initialize displacement (0 0 0)

zone history name 'center' displacement-z position (0 0 -0.379755)

zone face apply stress-normal -0.3e6 range group "Bottom1"  position-y 0 5 position-x 0 0.5 ;5MN
zone face apply stress-normal -0.015e6 range group "Bottom1"  position-y 0 5 position-x 0.50 5;5MN

model solve ratio-local 1e-4
model save "validation 1"
;=======================================================
;============validation for 10MN LOAD================
;=======================================================
```

```
;the first 7m
model restore "validation"
zone gridpoint  initialize velocity (0 0 0)
zone gridpoint  initialize displacement (0 0 0)

zone history name 'center' displacement-z position (0 0 -0.379755)

zone face apply stress-normal -0.6e6 range group "Bottom1"  position-y 0 5 position-x 0 0.5 ;10MN
zone face apply stress-normal -0.03e6 range group "Bottom1"  position-y 0 5 position-x 0.50 5;10MN

model solve ratio-local 1e-4
model save "validation 2"

;========================================================
;=======validation for 15MN LOAD========================
;========================================================
model restore "validation"
zone gridpoint  initialize velocity (0 0 0)
zone gridpoint  initialize displacement (0 0 0)

zone history name 'center' displacement-z position (0 0 -0.379755)

zone face apply stress-normal -0.9e6 range group "Bottom1"  position-y 0 5 position-x 0 0.5 ;15MN
zone face apply stress-normal -0.045e6 range group "Bottom1"  position-y 0 5 position-x 0.50 5;15MN

model solve ratio-local 1e-4
model save "validation 3"
```

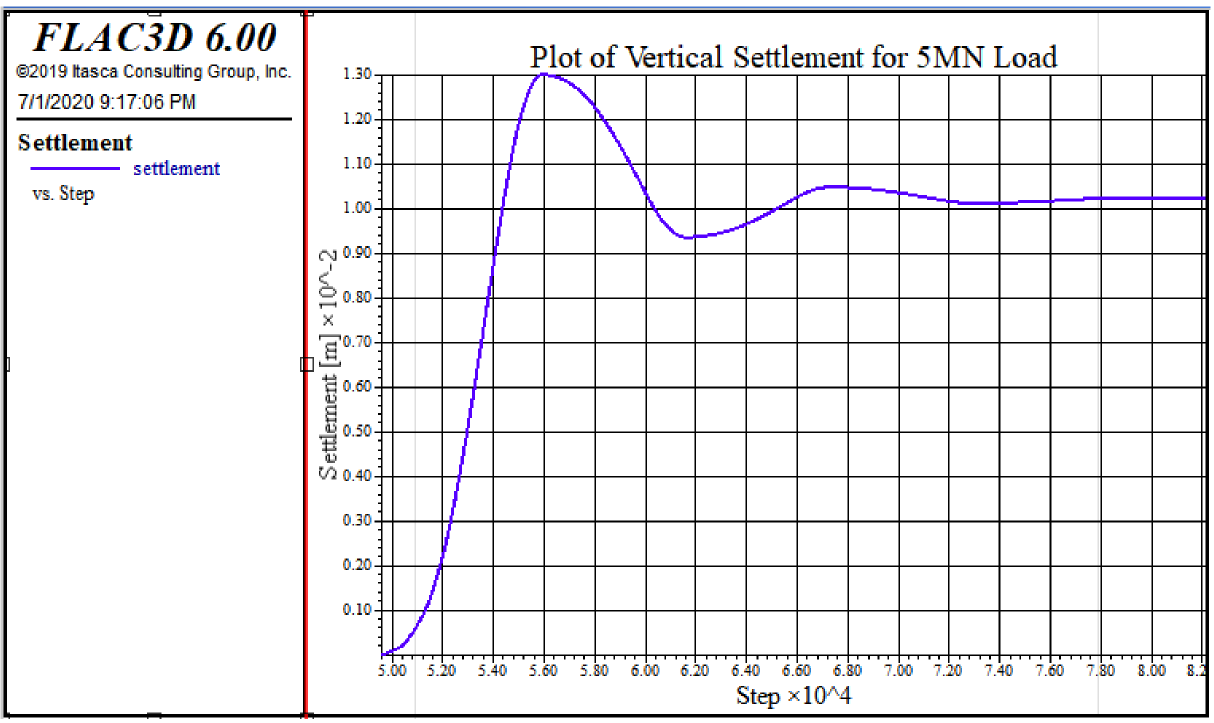

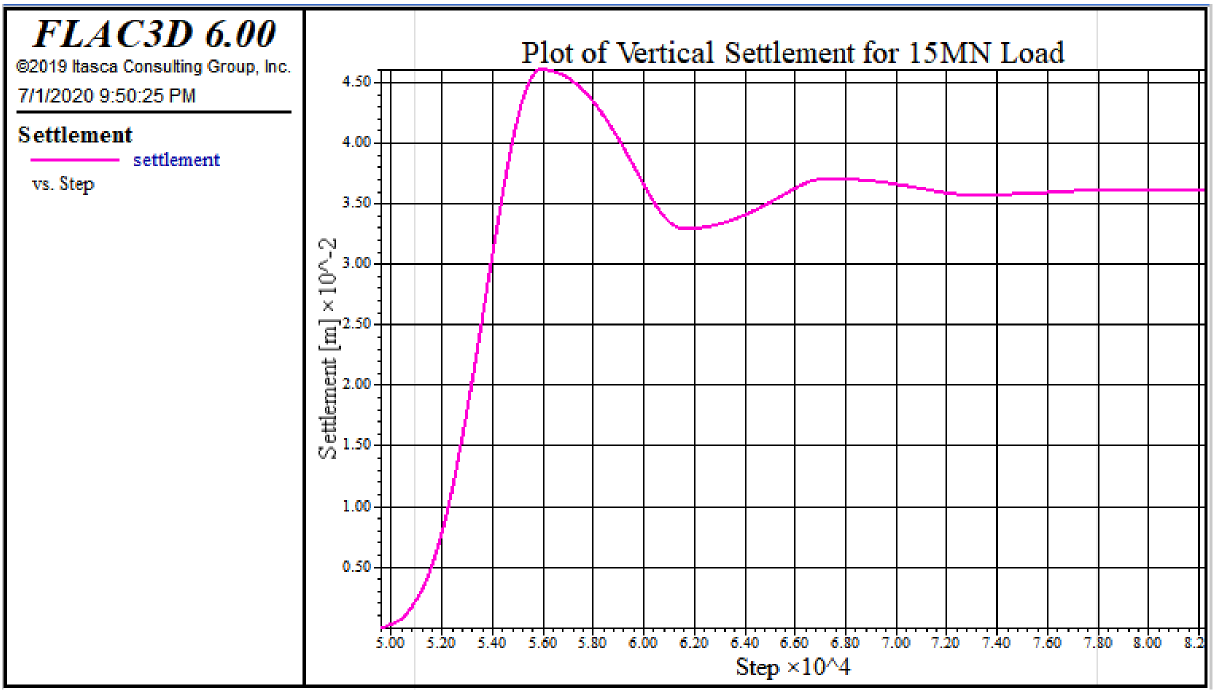
FLAC3D 6.00
©2019 Itasca Consulting Group, Inc.
7/1/2020 9:50:25 PM
Settlement
settlement
vs. Step
Plot of Vertical Settlement for 15MN Load
Settlement [m] ×10^-2
Step ×10^4

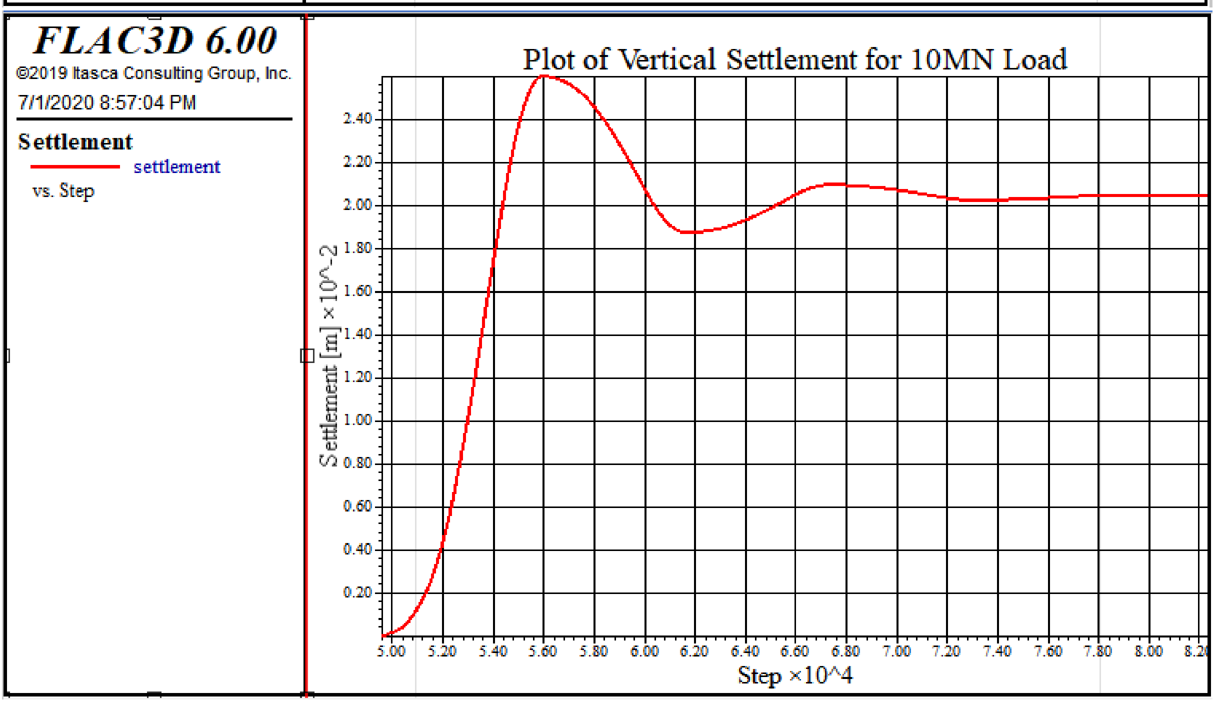
FLAC3D 6.00
©2019 Itasca Consulting Group, Inc.
7/1/2020 8:57:04 PM
Settlement
settlement
vs. Step
Plot of Vertical Settlement for 10MN Load
Settlement [m] ×10^-2
Step ×10^4